A STUDY OF THE REACTIONS OF HYDROGEN ATOMS IN THE GASEOUS PHASE

by

Nicholas Demchuk

A thesis

submitted to

the Faculty of Graduate Studies and Research

of the University of Manitoba

in partial fulfillment

of the requirements for the degree of

Doctor of Philosophy

From the Parker Chemistry Laboratory of the

University of Manitoba

under the supervision of Professor H. D. Gesser

September, 1967

ACKNOWLEDGEMENTS

A sincere word of thanks to the following:

1) Professor H. D. Gesser for his patience with me as a director and advisor in all aspects of this work; but above all, for having someone to blame during moments of despair, and someone to share the joy and excitement with during moments of victory.

2) Mr. J. J. Czubryt to whom I am indebted for many practical ideas on electronics and equipment, and whom I admire as a fine competitor.

3) Mr. B. Garbutt, Mr. T. Blain, Mr. D. Grey, and the many other students of Dr. Funt's and Dr. Gesser's laboratories for some of the "lighter" moments during the time of this study.

4) Mr. G. Epp and Mr. R. Luptak for some fine glass blowing and photography; the construction of a difficult piece of apparatus was always looked upon by them as a challenge.

5) Mr. G. Trider and the workers in the technical laboratory whose contributions are so often overlooked.

6) The workers in the storeroom department for help with numerous small jobs and for ordering some of the equipment and

supplies.

7) Imperial Oil Limited, for the award of a Graduate Fellowship for part of this study.

8) The University of Manitoba for the award of two summer assistantships.

9) St. John's College for the opportunity to teach Chemistry there for three years; to the many fine students there whose excellent work has been an inspiration to me; and in particular, to Dr. J.W.S. Jamieson, formerly the head of the Chemistry Department of this College for getting me started on lecturing in Chemistry, and for many practical hints on apparatus and technique.

"God is everywhere, all the time, showing us the right way to go." (M.L.L. age 17)

To Marcia, Ron and Roseanne, Mrs. Betty E.-F. and other Christian friends whose testimony, prayers, love and concern have inspired me and who are living witnesses to the greatest Truth - that God is not dead, but is risen and lives.

ABSTRACT

This thesis is a continuation of the study of hydrogen atom reactions begun earlier for the candidate's M.Sc. degree. Further work has been done on the reaction of hydrogen atoms with ketene to clarify some of the steps in the proposed mechanism. A similar study of the hydrogen atom - carbon suboxide system was initiated and preliminary experiments on the iso-electronic HNCO molecule were conducted. Photolysis of carbon suboxide in the presence of hydrogen at low pressures was also investigated. Most of these studies tend to support the original postulate that the primary reaction step is the addition of a hydrogen atom to the carbonyl carbon of the molecule.

Excited (^2P) hydrogen atoms, produced by irradiation of ground-state hydrogen atoms with a Lyman-α lamp, were reacted with nitrogen at low temperatures to form ammonia. Thermal hydrogen atoms were also found to react rapidly with carbon tetrachloride at -78° C. Further development of the adsorption - desorption technique led to the collection of hydrogen and its isotopes from a fast-flowing helium system on "saran" charcoal at low pressures.

An improved method for the determination of the hydrogen atom concentration in the reaction vessel prior to each experiment was developed, and this along with a water-cooled dissociator, a low temperature reaction vessel and the novel hydrogen adsorption technique were applied to the study of the $H + D_2$ reaction from -78° C to 170° C in a helium flowing system. Interpreting the results in the normal Arrhenius law fashion and taking the high temperature values of other workers gives a value of 8.01 kcal/mole as the activation energy; on the other hand, making use of the low temperature values and taking quantum mechanical tunnelling and zero point energies into consideration gives a value of E_c = 12.46 kcal/mole and a parabolic energy barrier width (2a) of 0.582 $\mathring{A}$.

TABLE OF CONTENTS

LIST OF FIGURES

TABLE OF CONTENTS CONT'D

TABLE OF CONTENTS CONT'D

TABLE OF CONTENTS CONT'D

LIST OF TABLES

LIST OF TABLES CONT'D

LIST OF FIGURES CONT'D

LIST OF FIGURES CONT'D

LIST OF FIGURES CONT'D

INTRODUCTION

The candidate's M.Sc. thesis was a study of hydrogen atoms and the role that they play during the photolysis of simple molecules in the gaseous phase[1]. Since a literature survey of the methods of production, detection and pertinent reactions of hydrogen atoms and free radicals has already been given in that study it will only be up-dated where necessary in this thesis. In particular, the reaction of hydrogen atoms with ketene was investigated because it had been postulated previously[2,3] that during the photolysis of ketene in the presence of hydrogen the reaction

$$H + CH_2CO = CH_3 + CO \qquad (1)$$

along with

$$CH_2 + H_2 = CH_3 + H \qquad (2)$$

could be the cause of a chain mechanism observed at high temperatures. It was thought that if reaction (1) was correct, then at low temperatures hydrogen atoms should be scavenged to form CO and C_2H_6 as major products.

During the study, however, it was found that above room

temperature the ketene was destroyed very rapidly at all flow rates by means of a chain mechanism which presumably was carried by HCO radicals with the formation of CO (1:1 mole ratio with ketene), CH_4, and significant amounts of C_2H_6 particularly at high ketene flows. The C_2H_6 production increased as the temperature was raised, but CH_4 formation decreased.

At -130° C the chain reaction did not occur, and CO and CH_4 (in roughly equal amounts) being the main products whose production levelled off at a value approximately equal to the H-atom concentration (estimated at high temperatures). At -78° C the results were similar to the above at low ketene flows, but a chain was initiated when the ketene flow rate increased beyond the value of the H-atom concentration.

The surface reaction at -196° C indicated glyoxal formation, and it is for this reason that HCO radicals were postulated to be present in the system, giving rise to the chain mechanism at -78° C. A series of reactions that would best explain the results was set forth as follows:

$$H + CH_2{=}CO = CH_2\text{-}\overset{H}{\underset{|}{C}}O^* \qquad (3a)$$

$$H + CH_2{=}CO = CH_3\text{-}CO^* \qquad (3b)$$

$$CH_2\text{-}\overset{H}{C}O^* + H_2 = CH_4 + HCO \quad (4)$$

$$2\ HCO = (HCO)_2 \quad (5)$$

$$2\ HCO = H_2 + 2\ CO \quad (6)$$

$$HCO + CH_2{=}CO = CH_2\text{-}\overset{H}{C}O^* + CO \quad (7)$$

$$2\ CH_3\text{-}CO^* = C_2H_6 + 2\ CO \quad (8)$$

$$CH_2\text{-}\overset{H}{C}O^* = CH_2 + HCO \quad (9)$$

$$HCO = H + CO \quad (10)$$

$$CH_2 + H_2 = CH_3 + H \quad (2)$$

$$CH_3 + H + W = CH_4 + W \quad (11)$$

$$CH_3 + HCO + W = CH_4 + CO + W \quad (12)$$

$$CH_3 + CH_3 = C_2H_6 \quad (13)$$

From the experimental data, reaction (3a) was favored over reaction (3b). Further work on the above system is described in section A.

As a test of the above mechanism it was thought that the study of the reaction of H-atoms with photochemically similar molecules, OCCCO, and HNCO in particular may prove valuable.

These studies are described in Sections B and C.

Recently, a study of the reaction of hydrogen atoms with acetaldehyde in which the products were analyzed directly by mass spectrometry, has shown that a long-lived radical with m/e = 43 is produced in large proportions[4]. It is believed to be the $CH_2\overset{H}{\overset{|}{C}}O$ radical, and the following reaction scheme is postulated:

$$H + CH_3CHO = CH_4 + CHO \quad (14)$$

$$CHO + CH_3CHO = CO + H_2 + CH_2CHO \quad (15)$$

where reaction (14) is a novel Walden-inversion process in which the hydrogen atom enters the acetaldehyde molecule from one side and displaces the larger HCO radical. The CH_2CHO radical formed by reaction (15) is found to be long-lived probably due to the fact that it is resonance stabilized by electron delocalization as follows:

$$\dot{C}H_2-\overset{H}{\overset{|}{C}}=O \longleftrightarrow CH_2=\overset{H}{\overset{|}{\dot{C}}}-\dot{O}$$

The above free radical is similar to the one that has been postulated in the candidate's M.Sc. study except that here it is formed by addition instead of hydrogen abstraction and

would be expected to have 15-40 kcal/mole excess energy which would enable it to undergo reactions such as

$$CH_2\overset{H}{\underset{|}{C}}O^* + H_2 = CH_4 + HCO \qquad (4)$$

quite readily.

With the recent advances in outer space technology, there has been a great deal of interest in the composition of the earth's atmosphere and in some of the reactions that take place within it at higher altitudes. (See ref. 5 for example). Using the adsorption of the solar Lyman-α line it has been possible to identify and monitor the concentrations of hydrogen atoms in the earth's atmosphere. A value of 2-4 x 10^{12} atoms/$cm.^3$ has been estimated above 120 Km[6]. Ground state hydrogen atoms are quite unreactive toward N_2, O_2, and CO_2 and most other atmospheric gases at low temperatures. However, it is relatively easy for an H-atom to absorb the 1216 Lyman-α resonance line and be excited to the $H(^2P)$ state[7], 10.20 ev. above the ground state H (^2S). Since this is a larger energy than any known chemical bond (except CO), the excited hydrogen atom could at least in theory become quite reactive even with respect to the inert atmospheric gases, and consequently be a species of considerable chemical interest. It could either

transfer this energy to other molecules by collision, or react directly by abstracting other atoms from normally stable molecules.

In 1962 Tanaka and McNesby[8] reported the formation of H (^2P) atoms in a laboratory vacuum system and observed their reactions with N_2 to form NH_3. Since the 1216 Å Lyman-α line is not transmitted by many materials, problems unknown to ordinary photochemistry are involved. The above experimenters have used LiF as the window material and the intensity of the lamp was estimated by the photoionization of butene-1. It has been shown, however, that this window tends to become inefficient after a few hours of use. Another solution to the problem has been the use of a windowless hydrogen discharge as the Lyman-α source in a flow system. Our attempt to study reactions of H (^2P) atoms is described in Section D.

A second development during the M.Sc. study has been the use of a thin film of SiO_2 gel for the collection of non-condensable gases such as CH_4, CO, and N_2 from a fast-flow low-pressure system[9]. This has enabled us to study the H + CH_2CO, H + OCCCO, and H + HNCO reactions where these gases are produced as primary products. Jamieson and Brown have since applied this method to the re-examination of the H + CH_4

reaction[10] and to the study of H-atoms with nitrogen containing compounds in a Wood-Bonhoeffer apparatus[11]. During the course of the present studies, this technique has been improved upon and attempts have been made to extend it to the manipulation and quantitative estimation of non-condensable gases in a vacuum system. Section E is a description of this study.*

As this research progressed it became evident that an absolute method of determining the hydrogen atom concentration in a fast flow system prior to each experiment would be of great value (see Discussion section for reason). A short summary of the methods of detecting H-atoms has already been given[1]. A lengthy report in which this problem is re-examined has recently appeared[12]. The author concludes that the Wrede-Harteck gauge normally used for H-atom determination may not be absolute. Also, it is very sensitive to impurities in the hydrogen stream, and cannot discriminate between H-atoms and other atomic species. Some of the other main findings about the H-atom concentration in a fast flow system are as follows:

1) Trace amounts of water do not influence the yield of atoms from a microwave or electrodeless discharge at 0.075 cm

---

*I am indebted to Mr. J. J. Czubryt (Ph.D. candidate of this laboratory) with whom some of these studies have been conducted.

Hg.

2) Small amounts of O_2 and N_2, however, increase the yield of atoms by a factor of two atoms per molecule of oxygen and less for nitrogen.

3) The intensity of the Balmer line is not a reliable indication of the concentration of atoms.

4) The presence of a catalytic probe in the atom stream affects the concentration of the atoms throughout the flow tube at low pressures.

5) An isothermal calorimeter is a good method for determining the absolute atom concentration providing the following conditions hold:

a) All atoms are scavenged on the calorimeter surface.

b) The diffusive and convective flux of the atoms is known.

c) The presence of atoms does not alter the rate of heat loss from the calorimeter.

d) The thermal accommodation coefficient of the recombination energy must be equal to unity; i.e. all the energy given up in the formation of the molecule in its ground state must be absorbed by the calorimeter.

Section F is a description of our attempts at estimating the atom concentration prior to a set of experiments in a fast flow system.

By this time we had accumulated some valuable experience and techniques for the study of H-atoms and it was thought that one of the most elementary reactions known, $H + D_2$ in a helium flowing stream would be a good test of the applicability of the re-modelled apparatus to H-atom studies. This would not only enable the candidate to examine the reaction at low temperatures, but would also allow him to consider some of the more interesting theoretical and quantum mechanical aspects of chemical kinetics which have been predicted at least thirty years ago but which are only now beginning to be observed as a result of improved techniques and development of low temperature technology. The major previous attempts at this study are summarized in Table I.

The final column of the table gives the values of the activation energy for the reaction as estimated by a log.k vs. 1/T Arrhenius law plot. The activation energies obtained by Geib and Harteck are calculated on the basis of two assumptions:

A) streamlined flow - poor mixing of reactants and a non-uniform distribution of reactants in the vessel,

B) turbulent flow - rapid mixing and a uniform concentration of reactants throughout the reaction vessel. An asterisk indicates that quantum mechanical tunnelling has been taken into account. The two values obtained for H + p-H_2 by Schulz and LeRoy are estimated using transition state theory along with parabolic and Eckart barriers respectively. E_o is the "threshold energy" or the minimum amount of energy a D atom must have to react with H_2 at room temperature as estimated from a products versus energy plot in the "hot atom" experiments (see Appendix IX).

TABLE I

Summary of the experimental data for the reaction

Researchers	Reaction Studied	Temperature
Farkas (1930)[13]	H + p-H_2 from n-H_2 + p-H_2 eq^m	873-1023° K
Farkas & Farkas (1935)[14]	H + D_2 from H_2 + D_2 eq^m	900-980° K
Geib & Harteck (1931)[15]	H + p-H_2	10° C - 100° C
Melville & Robb (1949)[16]	H + p-H_2	ambient
M. van Meersche (1951)[17]	H + p-H_2	720° K - 880° K
B.C.C.M.V. (1955)[18]	H + D_2 homog. exchange	916°K - 1010° K

TABLE I (CONT'D)

Researchers	Reaction Studied	Temperature	Other Conditions	Analysis method	ΔE_o (kcal/mole)
Schulz & LeRoy (1964)[19]	$H + D_2$	368-468° K	Flow system with probe	Gas Chrom.	7.30
Schulz & LeRoy (1965)[20]	$H + p\text{-}H_2$	300-444° K	Flow system with probe	Thermal conductivity	9.70* and 14.0*
Ridley, Schulz & LeRoy (1966)[21]	$D + H_2$	274-468° K	Flow system with probe	Thermal conductivity	9.21*
Kuppermann & White (1966)[22]	$D + H_2$	ambient	Hot H-atoms produced by photolysis	Mass Spectro.	$E_o = 7.6$

DETAILED DESCRIPTION OF EACH PROJECT

A. Reaction of Hydrogen Atoms with Ketene

Introduction

In an attempt to clarify some aspects of the reaction mechanism between hydrogen atoms and ketene as put forward in the M.Sc. thesis two other types of experiments were conducted as follows:

1) The reaction of hydrogen atoms with ketene at -96° C, and
2) The reaction of hydrogen atoms with ketene in the presence of helium at 232° C and at -196° C (surface).

Apparatus and materials.

The apparatus and materials in these cases were exactly the same as those used in the previous experiments[1]. The reaction vessel was cylindrical as described previously but the poisoning material was dri-film (G.E. SC 77)[23] rather than $Na_2HPO_4 \cdot 10\ H_2O$. The atom concentration was estimated at 235° C by the use of CCl_4 as a scavenger and found to be 47 micromoles/min. The refrigerant for the -96° C experiments was solid acetone. In the helium dilution experiments, the helium

which was obtained from the Linde Company, was purified in the same manner as the hydrogen and was introduced into the system by means of flow valves and manometers at a rate of 694 micromoles per minute. The molecular hydrogen flow was reduced to 129 micromoles per minute and the operating pressure was maintained at 1.05 mm Hg. Under these conditions the hydrogen atom concentration was estimated to be approximately 13 micromoles per minute. The temperature of these latter helium dilution experiments was 232 $\pm$ 2° C and one experiment was conducted at -196° C in which the ketene was condensed onto the surface of the reaction vessel.

Results

The results obtained are listed in Table II and plotted in Fig. I for the -96° C experiments. The values obtained for the helium dilution experiments are summarized in Table III.

Discussion

The results of experiments at -96° C show that hydrogen atoms are scavenged at moderate ketene flow rates but at high ketene flow rates a chain reaction is initiated. This is believed to be due to the presence of HCO radicals (as postulated in the M.Sc. work) which act as chain carriers in a

FIGURE I

Yields of products versus flow rates of ketene in the reaction of hydrogen atoms with ketene at $-96 \pm 2^{\circ}$ C.

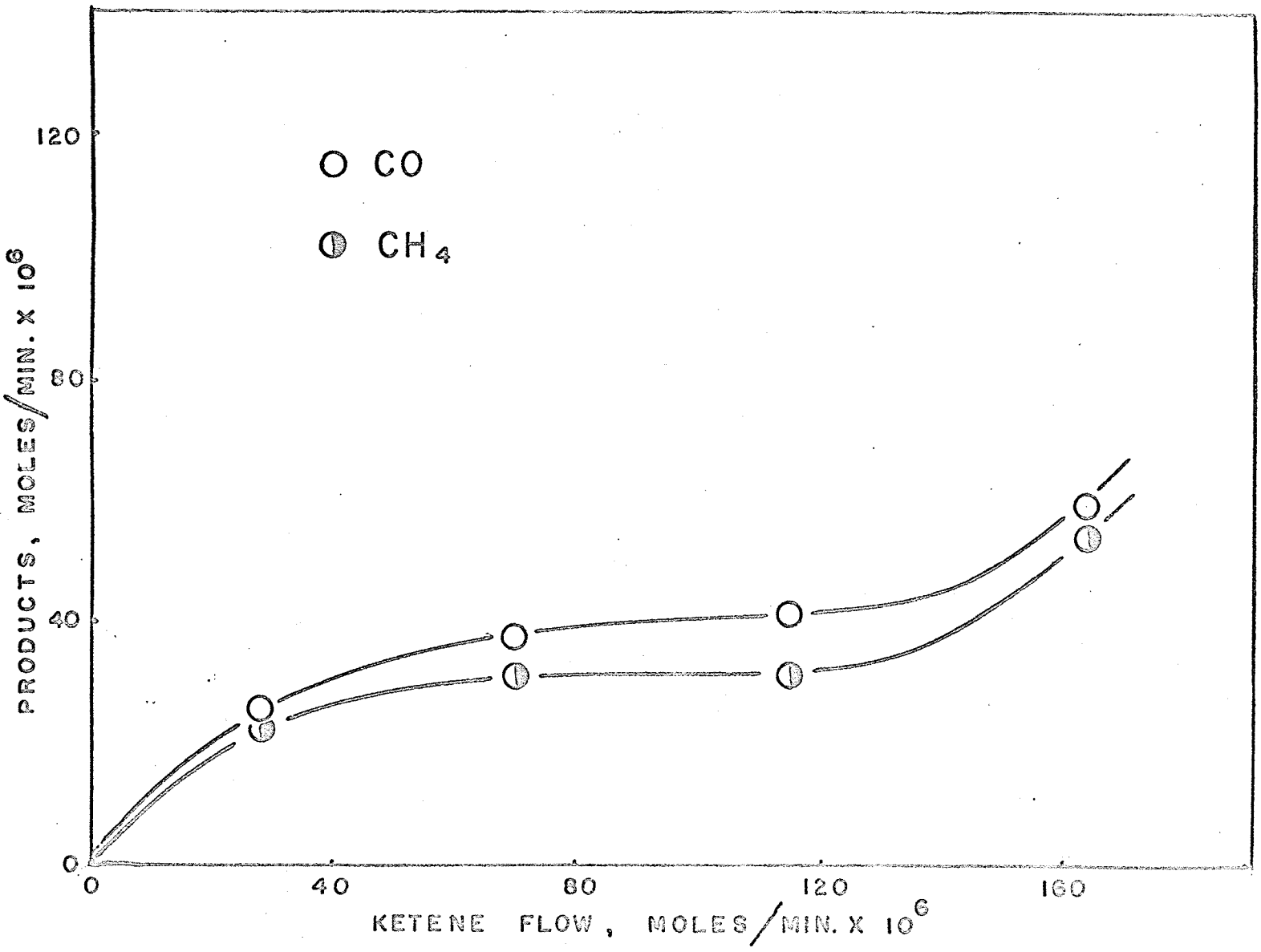
O CO
CH4
PRODUCTS, MOLES/MIN. X 10^6
120
80
40
0
0
40
80
120
160
KETENE FLOW, MOLES/MIN. X 10^6

TABLE II

Yields of products in the reaction of hydrogen atoms with ketene at -96 ± 2° C in a poisoned, cylindrical reaction vessel.

Duration of experiment (min)	Ketene flow (moles x 10^6/min)	Products (moles x 10^6/min)			$\frac{2\,C_2H_6 + CH_4}{CO}$
		CO	CH_4	C_2H_6	
2.0	28.1	26.0	23.9	--	0.92
2.0	70.1	37.6	31.0	trace	0.83
1.5	115.5	41.4	30.2	1.9	0.82
1.0	163.4	58.9	54.9	3.3	1.04

Note: (1) -- signifies that the product was analyzed for but not detected.

(2) A blank indicates that the product was not analyzed.

TABLE III

Yields of products in the reaction of hydrogen atoms with ketene in the presence of helium

Conditions (temp)	Duration of experiment	Ketene flow (μmoles/min)	Products (moles x 10^6/min)		
			CO	CH_4	C_2H_6
232 ± 2° C	3.0	65.0	16.8	--	--
	3.0	104.0	11.4	--	--
	1.0	140.0	25.6	--	3.7
	1.0	206.0	21.5	--	
-196° C	5.0	110.0 (ads.)	5.1	--	--

Note: (1) See Note for Table II.

(2) Summary of conditions:

He flow-rate : 694 moles x 10^6/min.

H_2 flow-rate : 129 moles x 10^6/min.

H atom flow : 13 moles x 10^6/min.

Pressure in R.V. : 1.05 mm Hg.

Type of R.V. : cylindrical, poisoned.

way which is similar to that of the -78° experiments.

In the experiments at 232° C using He as a diluent (with only 18.5% H_2) it is seen that the chain reaction is quenched. Very little methane was detected and only small amounts of ethane were observed along with trace amounts of glyoxal. In the -196° C experiment the methane was completely eliminated and carbon monoxide became the major product along with some glyoxal. This series of experiments indicates that molecular hydrogen is indeed necessary for the formation of methane and the propagation of the chain processes which were observed in the pure hydrogen system. The complete mechanism as put forward at that time appears in the Overall Discussion Section of this thesis (see page 140).

Conclusion

It was concluded that the primary H-atom attack was on the carbonyl carbon of the ketene molecule and it was thought that a similar study of the reaction of hydrogen atoms with carbon suboxide might prove valuable. This study is described in the next section.

B. Studies on Carbon Suboxide

Introduction

Within the past decade a great deal of interest has arisen in the rather unfamiliar compound, C_3O_2, chiefly due to its formation as a product in the radiolysis of CO and CO_2[24,25]. Harteck and co-workers[26] have reacted C_3O_2 with oxygen atoms in a fast-flowing system and found CO as the main product with minor amounts of C_2O and CO_2. The short-lived C_2O species was postulated to react with O-atoms in two ways:

$$O + C_2O = C + CO_2 \quad \text{fast} \qquad (16)$$

$$O + C_2O = CO + CO \quad \text{slow} \qquad (17)$$

A similar study of the reaction with O_3 was found to be extremely slow. The authors conclude that C_3O_2 as a kinetic entity ought to be examined in detail due to its importance in combustion processes and, also, due to its role in the photochemistry of planetary atmospheres containing substantial amounts of CO and CO_2.

In 1961 Kyle Bayes[27,28,29] undertook the study of the photochemical decomposition of C_3O_2 in the presence of free radical scavengers. He found that the most probable primary step is

$$C_3O_2 + h\nu = CO + CCO \quad (18)$$

The CCO intermediate was found to be very reactive and apparently underwent rapid reactions as follows:

$$CCO + C_2H_4 = C_3H_4 + CO \quad (19)$$

$$CCO + C_3O_2 \text{ excess} = \text{Polymer} + nCO \quad (20)$$

where C_3H_4 represents a mixture of allene and methylacetylene isomers. When O_2 was added to the above system it was shown that at short wavelengths it had little effect on the production of allene, but at longer wavelengths it quenched allene formation quite efficiently. He thus concluded that the CCO could exist in two forms, a triplet ground state (formed at long wave-lengths), and a low-lying singlet (formed at short wave-lengths) similar to the methylene (CH_2) case. Later studies[30,31] have indicated that an excited C_3O_2 molecule is probably formed in the primary step.

Thermal decomposition studies by Palmer and Hirt[32] showed that the reaction

$$C_3O_2 = C_2O + CO \quad (21)$$

is 54 kcal endothermic.

A great deal of interest has also arisen in the polymer associated with the thermal and photolytic studies[33,34]. The thermal polymer is thought to consist of approximately six suboxide units fused into a heterocyclic structure with five carbon atoms and one oxygen in the ring, and a carbonyl group adjacent to the hetero atom as follows:

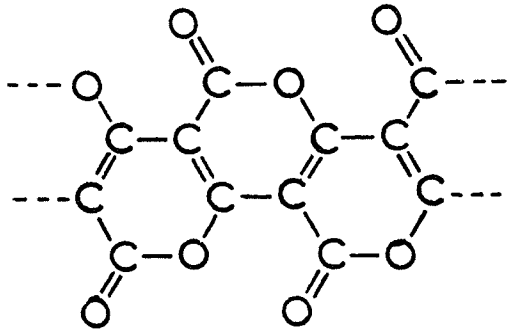

The photopolymer is similar except that ketenyl groups were also found to be present with the basic unit being

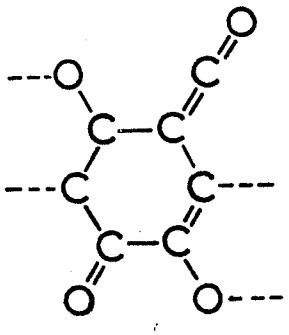

rather than

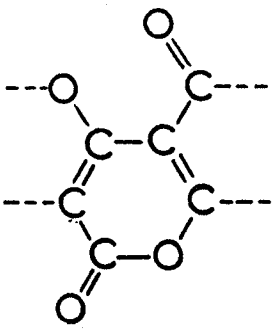

for the thermal case.

Recently Blake and Hodgson[25] have shown that the polymer formed by γ-radiolysis of C_3O_2 is similar to the thermal

one and is formed by ionic mechanisms such as:

$$C_3O_2^+ + n\,C_3O_2 + e = \text{polymer} + m\,CO \quad (22)$$

$$C_2O^+ + n\,C_3O_2 + e = \text{polymer} + m\,CO \quad (23)$$

Harteck[35] has implied that this polymer (which could also be produced by the radiolysis of CO) may be an important intermediate in the formation of organic compounds from CO as follows:

$$CO \rightsquigarrow C_3O_2 \rightsquigarrow \text{polymer} \quad (24)$$

$$\text{polymer} + H_2O = \text{organic compounds} \quad (25)$$

Due to this surge of interest in C_3O_2 and also due to its similarity to the ketene molecule (see u.v. absorption spectrum)[36] we have studied its reaction with hydrogen atoms and have also performed a few photolytic experiments on C_3O_2 in the presence of hydrogen.

a) Reaction of C_3O_2 with hydrogen atoms

Apparatus and materials

The apparatus was modified from that of the previous studies in three ways:

a Wood-Bonhoeffer tube (with aluminum electrodes) with the hope of obtaining a more constant hydrogen atom source.

2) The reaction vessel was altered to prevent back diffusion of reactants into the discharge zone and to prevent a direct light path from the discharge to the reaction region[37].

3) A toepler pump - gas burette - gas chromatograph was installed at the reaction side of the apparatus whereby the non-condensable products adsorbed on the Si O_2 gel trap[9] could be collected and analyzed immediately by gas chromatography.

The molecular hydrogen flow was increased to 2698 micromoles/min but the reaction pressure was maintained at 1.05 $\pm$ 0.01 mm Hg. The reaction vessel was not poisoned and the hydrogen atom concentration under these conditions was found to be about 45 micromoles/min (using C_2H_5Cl as a titrant) but once again it was difficult to keep this value constant.

Carbon suboxide was prepared by the dehydration of malonic acid (Matheson, Coleman and Bell) with P_2O_5 (Baker, reagent grade) according to Stock and Stoltzenburg[38] and was fractionated by bulb-to-bulb distillation. The final product contained less than 3% CO_2 as determined by vapour pressure analysis in a LeRoy still.

FIGURE II

Diagram of discharge tube, reaction vessel, and D.C. circuit diagram for the study of the H + C_3O_2 reaction.

H_2 : hydrogen inlet

P : to product traps and pump

R : reactant inlet

T : thermocouple well

d : high voltage wires to electrodes

g : spark gap (with radioactive source)

c : 8 μf condensor

r_1 : 10,000 Ω power resistors (water cooled)

t_1 : step-down transformers

t_2 : neon sign step-up transformer (5000 v. at 220 input)

r_2 : variac

s^2 : dp dt switches

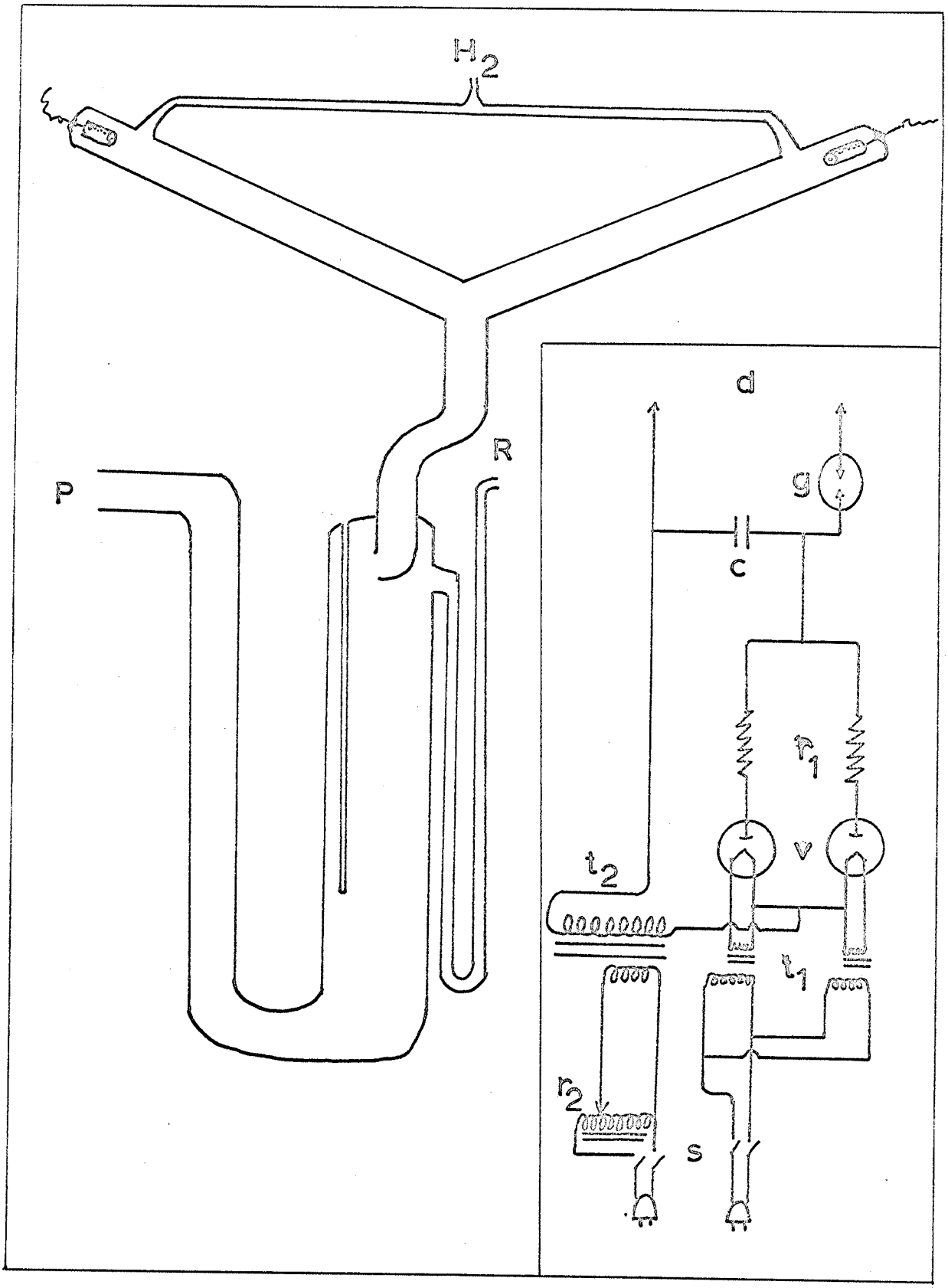
H2
P
R
d
g
c
r1
v
t2
t1
r2
s

FIGURE III

Toepler pump-gas burette - gas chromatograph system for analysis of products.

a,b : flow stopcocks (closed after reaction)

c : small stopcock opened when products are pumped into gas burette

f : capillary stopcock for placing sample into loop

d,e : two way stopcocks for carrier gas by-pass

h : carrier gas inlet

g : thermal conductivity cell

i : column

j : bubble meter

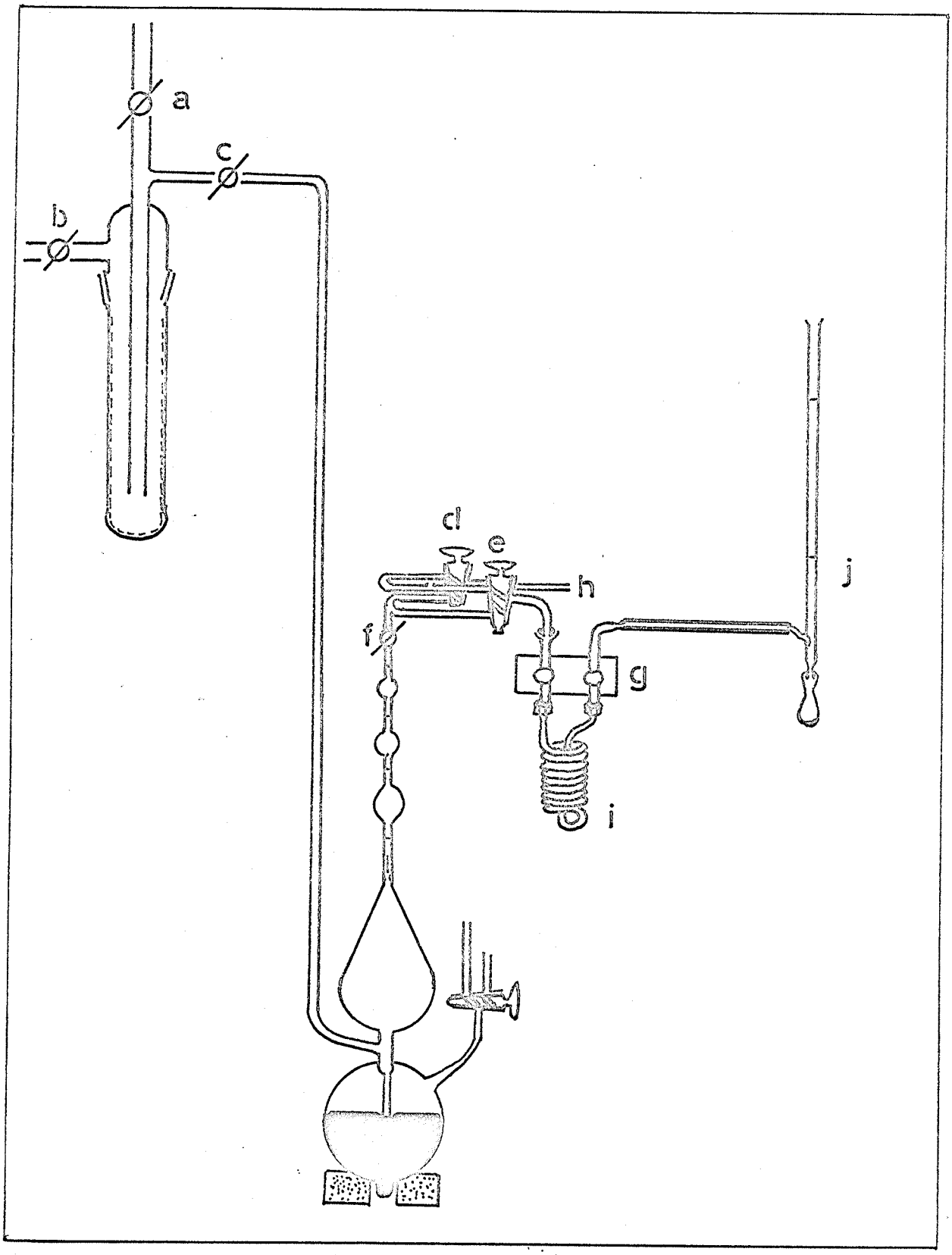
a
b
c
d
e
f
g
h
i
j

The non-condensable products CO, and CH_4 were trapped on SiO_2 gel, pumped into the gas burette, and quantitatively determined by gas chromatography under the following conditions:

1) Column: six foot, 1/8" SiO_2 gel (60-80 mesh) at ambient temperature.

2) Detector: thermal conductivity fabricated in the technical laboratory using glow-plug filaments.

3) Carrier gas: helium at 26 cc/min.

Results

The results obtained are listed in Table IV and are plotted in typical "flow curve" fashion in Figures IV to VII.

Discussion

At all temperatures the main reaction product is carbon monoxide. Especially at the lower temperatures the next most predominant one is CH_4, with increasing amounts of CH_2CO and C_2H_6 as the temperature is raised. Glyoxal was detected at the 77° and the -78° experiments but no attempt was made to estimate it quantitatively. In all experiments a dark residue was left behind in the reaction vessel which may have been carbon or polymer, and which accounts for the lack of mass

TABLE IV

Yields of products in the reaction of hydrogen atoms with carbon suboxide

Durat. of experi.	C_3O_2 flow	C_3O_2 reacted	CO	CH_4	CH_2CO	C_2H_6	carbon balance
			Temperature: -96 ± 2° C				
2.5	46	34	29	8.4	trace	trace	0.36
3.0	72	48	72	21	trace	trace	0.65
2.0	95		90*	30*			
2.5	108	26	24	5.4	trace	trace	0.43
2.0	170	44	49	4.0	trace	trace	0.40
1.0	203	50	47	15	trace	trace	0.43
			Temperature: -78 ± 2° C				
4.0	19	19	29	6.3	trace	trace	0.69
3.0	89	84	158	35	8.8	trace	0.65
2.0	126	93	137	25	7.2	trace	0.64
1.0	203	104	162	26	10	2.6	0.69
			Temperature: 77 ± 2° C				
5.0	33	21	38	7.0	trace	2.1	0.71
4.0	60	46	85	10	4.6	5.7	0.86
3.0	98	63	115	11	7.8	7.4	0.84
2.0	136	71	123	14	8.2	7.9	0.80
1.0	214	148	228	15	15	13	0.68
			Temperature: 235 ± 2° C				
6.0	45	15	36	2.0	3.8	trace	
3.0	77	30	43	2.3	6.1	2.0	
2.0	103	46	55	2.9	6.7	4.5	
1.0	203	58	88	4.6	14	7.5	
			Temperature: -196° C (ads.)				
5.0	139 (ads)	27	13	trace	nil	nil	trace glyoxal

TABLE IV (CONT'D)

Note: (1) A blank indicates that the product was not analyzed for.
(2) "Trace" indicates that the amount of product was less than 2 μmoles/min.
(3) The "carbon balance" was determined by taking the ratio of the total carbon gaseous products and three times the C_3O_2 reacted.
(4) *In this experiment the total CO + CH_4 fraction is known but the absolute values of each are estimated.
(5) Duration of experiment is expressed in minutes, but all other values are micromoles/min.
(6) The atom concentration for these experiments was 45 micromoles/min as estimated by the use of C_2H_5Cl as a titrant at 65° C.

FIGURE IV

Yields of products from the reaction of hydrogen atoms with C_3O_2 at $-96 \pm 2^{\circ}$ C.

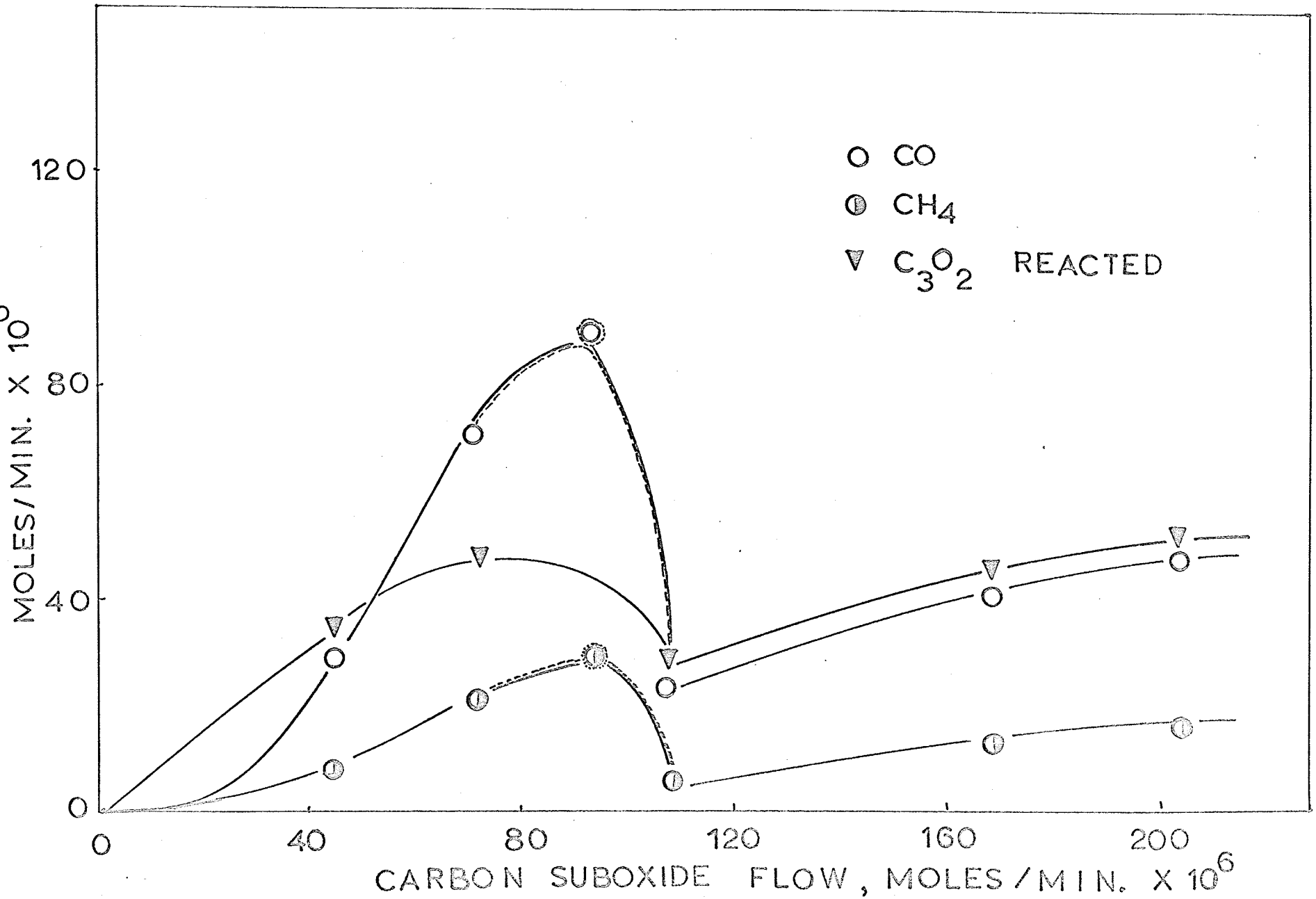
O CO
CH4
C3O2 REACTED
120
80
40
0
MOLES/MIN. X 10^6
0
40
80
120
160
200
CARBON SUBOXIDE FLOW, MOLES/MIN. X 10^6

FIGURE V

Yields of products in the reaction of hydrogen atoms with C_3O_2 at $-78 \pm 2^{\circ}$ C.

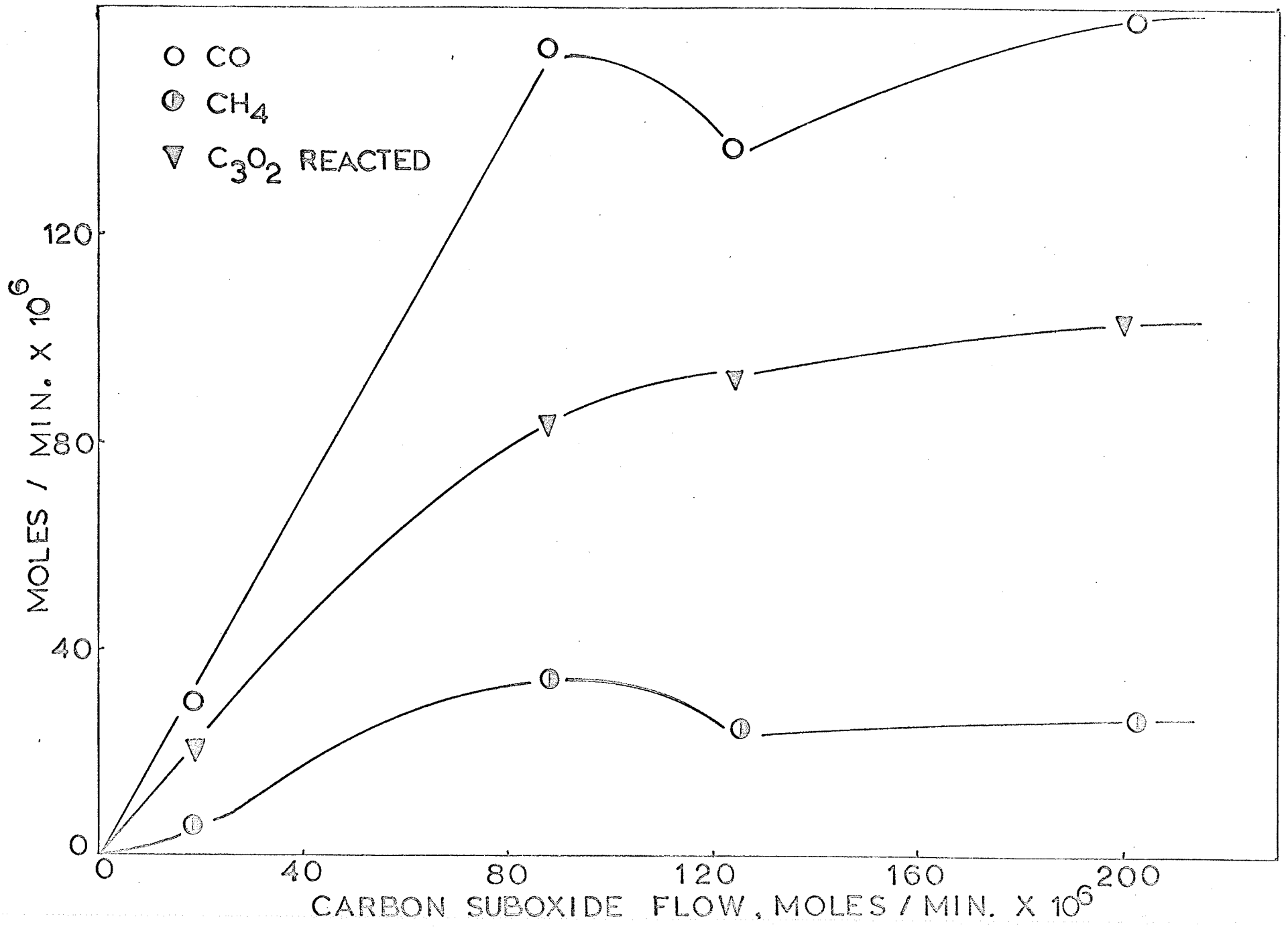
O CO
CH4
C3O2 REACTED
MOLES / MIN. X 10^6
0
40
80
120
0
40
80
120
160
200
CARBON SUBOXIDE FLOW, MOLES / MIN. X 10^6

FIGURE VI

Yields of products in the reaction of hydrogen atoms with C_3O_2 at 77 $\pm$ 2° C.

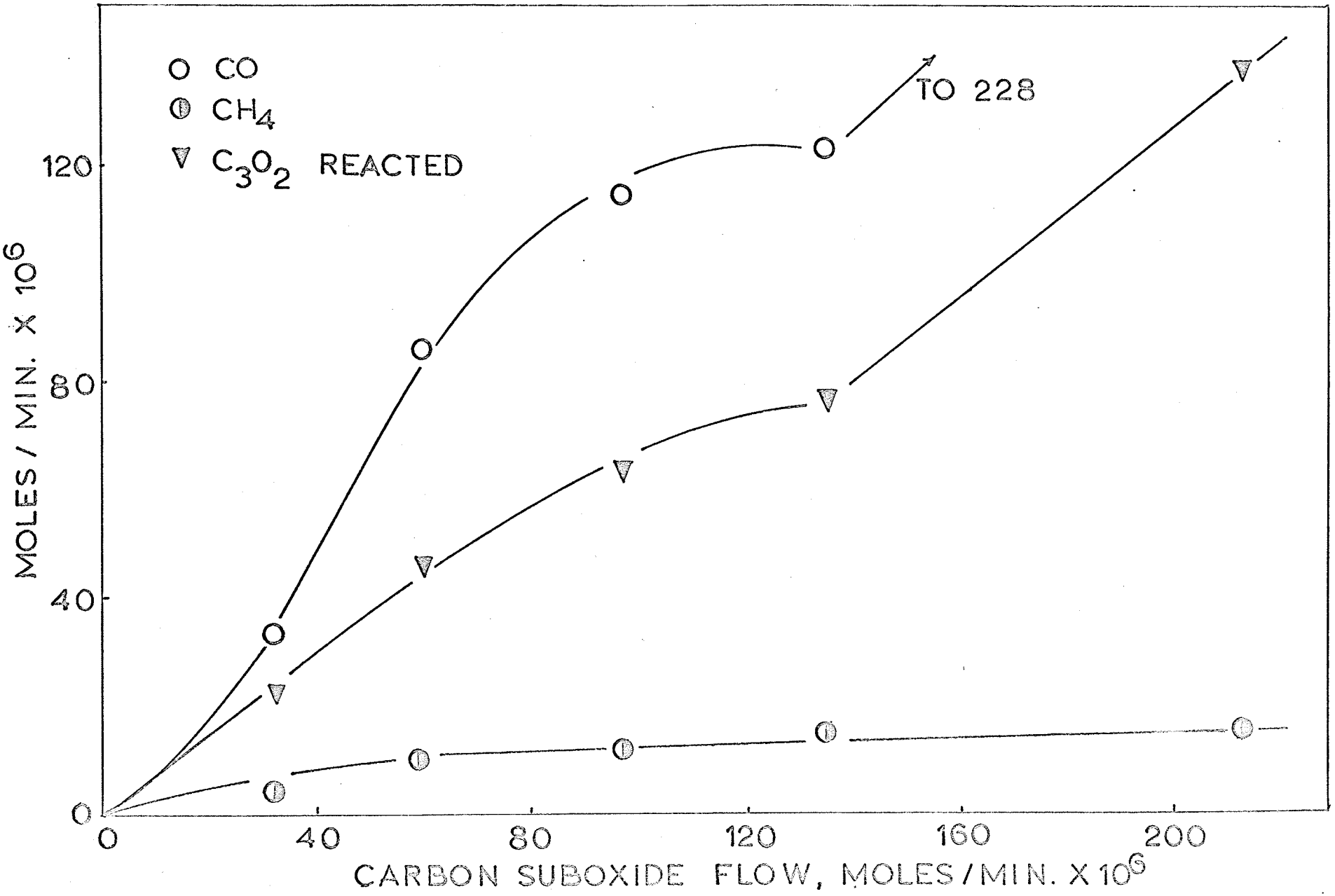
O CO
CH4
C3O2 REACTED
TO 228
MOLES / MIN. X 10^6
0
40
80
120
0
40
80
120
160
200
CARBON SUBOXIDE FLOW, MOLES / MIN. X 10^6

FIGURE VII

Yields of products from the reaction of hydrogen atoms with C_3O_2 at 235 $\pm$ 2° C.

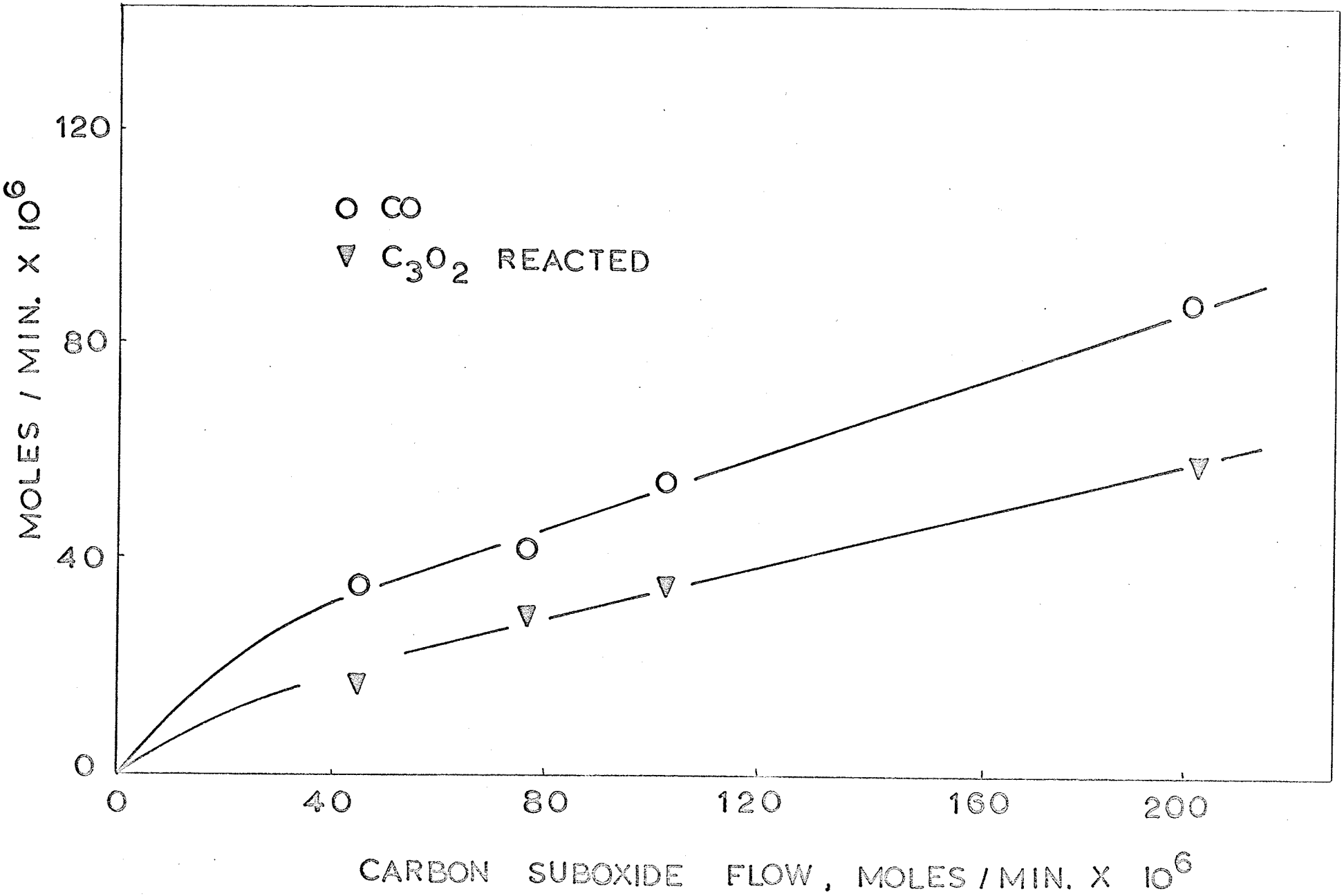
120
80
40
0
MOLES / MIN. X 10^6
O CO
▼ C_3O_2 REACTED
0
40
80
120
160
200
CARBON SUBOXIDE FLOW, MOLES / MIN. X 10^6

balance in the gaseous products. The outstanding difference in the 235° runs was the formation of a large amount of dark brown polymer within the reaction zone near the C_3O_2 inlet. An attempt to characterize the polymer was made by trying to form it on rock-salt window for I.R. analysis but this experiment was unsuccessful. Because of the predominant polymer formation at this temperature, it is believed that a thermal polymerization of C_3O_2 took place, in the presence of hydrogen, and catalyzed by hydrogen atoms. Thus these high temperature results will be discussed separately from the others.

The main feature of the results at -96° C, -78° C, and 77° C is the unusual maximum in the flow curves at low C_3O_2 flow rates. This seems to point to a reactive intermediate possibly C_2O which is only formed when there is an excess of atoms in the reaction vessel, and which no longer becomes prominant when the atoms are completely scavenged by the primary addition step according to reactions such as

			ΔH kcal/mole
$H + OCCCO$	$\rightarrow HOC-C=C=O^*$	(26a)	-34
	$\rightarrow O=C=C(H)-C=O^*$	(26b)	-34

It will be seen below that reaction (26a) is favored. The following mechanism is postulated to account for the products:

At -96° C:

		ΔH (kcal/mole)
$H + OCCCO = OCC\overset{H}{C}O^*$	(26a)	-34
$H + OCC\overset{H}{C}O^* = OCC + CO + H_2$	(26b)	-17
$OCC + H_2 = H_2CCO^* \overset{W}{\rightarrow} CH_2CO$	(27a)	-87
$H_2CCO^* \rightarrow CH_2 + CO$	(27b)	-13
$CH_2 + H_2 \overset{W}{\rightarrow} CH_4$	(2a)	-103
$CH_2 + H_2 \rightarrow CH_3 + H$	(2b)	-1
$CH_3 + CH_3 = C_2H_6$	(13)	-84
$O=C=C-\overset{H}{C}=O + O=C=C-C=O \atop \qquad\qquad\quad H = \begin{matrix} O=C=C \\ \quad\vert \\ O=C=C \end{matrix} + H_2 + 2\,CO$	(28)	-32
$\begin{matrix} O=C=C \\ \quad\vert \\ O=C=C \end{matrix} = OCCCO + C$	(29)	
$C \overset{W}{=} \text{residue}$	(30)	
$C + H_2 = CH_2$	(31)	-86

At low C_3O_2 concentrations there is an excess of H-atoms in the reaction vessel and thus reaction (26b) occurs quite readily. This is followed by (27) and (2) giving rise to a chain mechanism, and hence the maximum in the flow diagram of Fig. IV. Then when the C_3O_2 flow exceeds 90 micromoles/min (or twice the atom concentration) all the H-atoms are scavenged by the primary step, (26a), and the chain reaction is quenched. The most probable secondary reactions now are (28), (29), and (30). Reaction (31) has been postulated to occur previously[39] and is necessary for the minor amounts of CH_4 observed at high C_3O_2 flow rates. Reaction (29) in which a molecule of C_3O_2 is regenerated is necessary for the 1:1 ratio of C_3O_2 reacted to H-atoms consumed as is observed under these conditions.

At -78° C:

					ΔH (kcal/mole)
Reaction	$OCC-\overset{H}{\underset{|}{C}}O^*$	$+ H_2$	$=$	$CH_2CO + HCO^*$ (32)	-23

becomes important followed by (27) and (2) as before. This not only explains the appearance of significant amounts of ketene but also enables the chain to be carried further by

reactions such as:

			ΔH (kcal/mole)
$HCO^* + OCCCO = OCC\overset{H}{C}O^* + CO$	(33)		-10

It eventually terminates, however, due to the fact that the $OCC\overset{H}{C}O^*$ now formed has less excess energy than when it is formed by reaction (26a). Also, some of the HCO* radicals are destroyed by

$HCO^* + HCO^* \rightarrow H_2 + 2\,CO$	(6)		-48
$HCO^* + HCO^* \xrightarrow{W} (HCO)_2$	(5)		-80

At 77° C:

All reactions postulated at -78° C still occur except now the $OCC\overset{H}{C}O^*$ formed by (33) has enough energy to react according to (32) and lengthen the chain at high C_3O_2 flow rates.

At 235° C:

The most prominant reaction is

$$CCO + C_3O_2 = \text{polymer} + 2\,CO \qquad (20)$$

as originally postulated by Bayes in photochemical studies.

It is interesting to note from the flow curves at 235° C

that exactly three molecules of CO are formed for every two C_3O_2 decomposed and the reaction must proceed according to the following stoichiometry:

$$2\ C_3O_2 + nH_2(?) \quad = \quad \text{polymer} + 3\ CO \qquad (34)$$

From this it can be clearly seen that the C/O ratio in the polymer must of necessity be 3/1 and consequently its composition must be slightly different than those postulated by the previous workers in thermal and photolytic systems without H_2. It is probable that the composition of the polymer could be represented by one of the following two structures depending whether or not hydrogen enters into the reaction scheme:

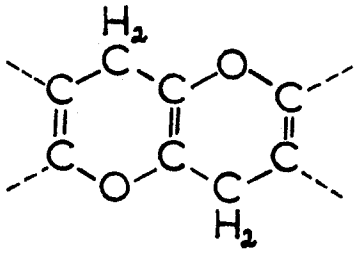

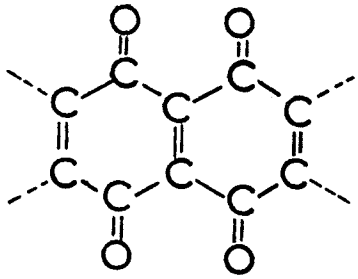

Conclusions

The results of this study require two postulates:

1) That the primary attack of the hydrogen atom is on the

carbonyl carbon atom, as in the ketene case.

2) The CCO biradical is an important reactive intermediate at all temperatures. This is similar to the recent study of $N + C_2H_2$ [40] where a maximum occurs in the flow curves as well, and which is believed to proceed via a CCN intermediate. To test this hypothesis further, the photolysis of C_3O_2 in the presence of H_2 was undertaken.

b) The photolysis of carbon suboxide in the presence of hydrogen

Apparatus

The apparatus was a standard photolysis system employing a quartz low-temperature cell as described by Gesser et al[41] with a volume of 211 cc. A Hanovia S-500 medium pressure arc was used along with a Corning glass #9863 (3 mm) filter as well as a chlorine filter (1 atm., 5 cm) to give an effective radiation of about 2700 Å (see Fig. VIII). In the high pressure closed system the products and reactants were stirred about by means of a glass stirrer. The circuit diagrams of the photocathode tube and lamp circuits are given in Fig. IX. The non-condensable products CO, and CH_4 were collected in a gas burette where their total volume was determined by P.V.T.

FIGURE VIII

Spectra from Hanovia S-500 medium pressure Hg arc using a Hilger medium quartz spectrograph (# $\frac{E\ 498.305}{45438}$) with a slit opening of +7.5μ.

Spectrum #1 : Arc with entire filter combination.

" #2 : Arc with #9638 Corning filter (3 mm)

" #3 : Arc with chlorine filter (1 atm., 5 cm)

" #4 : Arc with Hg filter (1 cm)

" #5 : Unfiltered arc

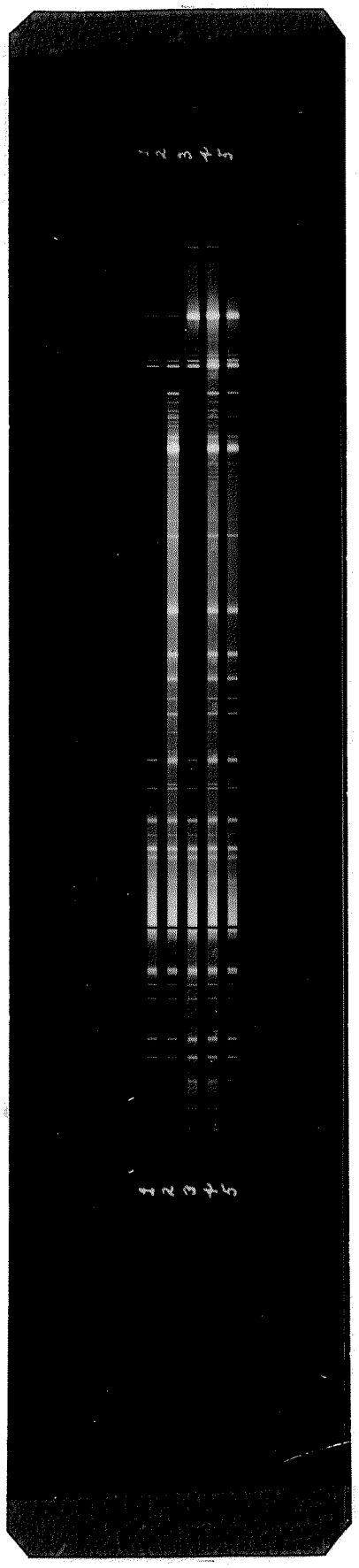

FIGURE IX

a) Photocathode circuit

CDR : Critical damping resistance (802 Ω)

G : Galvanometer

i_G : Galvanometer current

R : Variable resistor

i_R : Current flowing through variable resistor

P.S. : Power supply (193 volts; Heath Kit #EUW-15)

T : Photocathode (RCA 935)

b) Lamp circuit

L : Hanovia S-500 lamp

T : Lamp transformer (250 volts to start, 50 volts to operate)

V : Variac

A : 10 amp. meter (controlled at 9 amps)

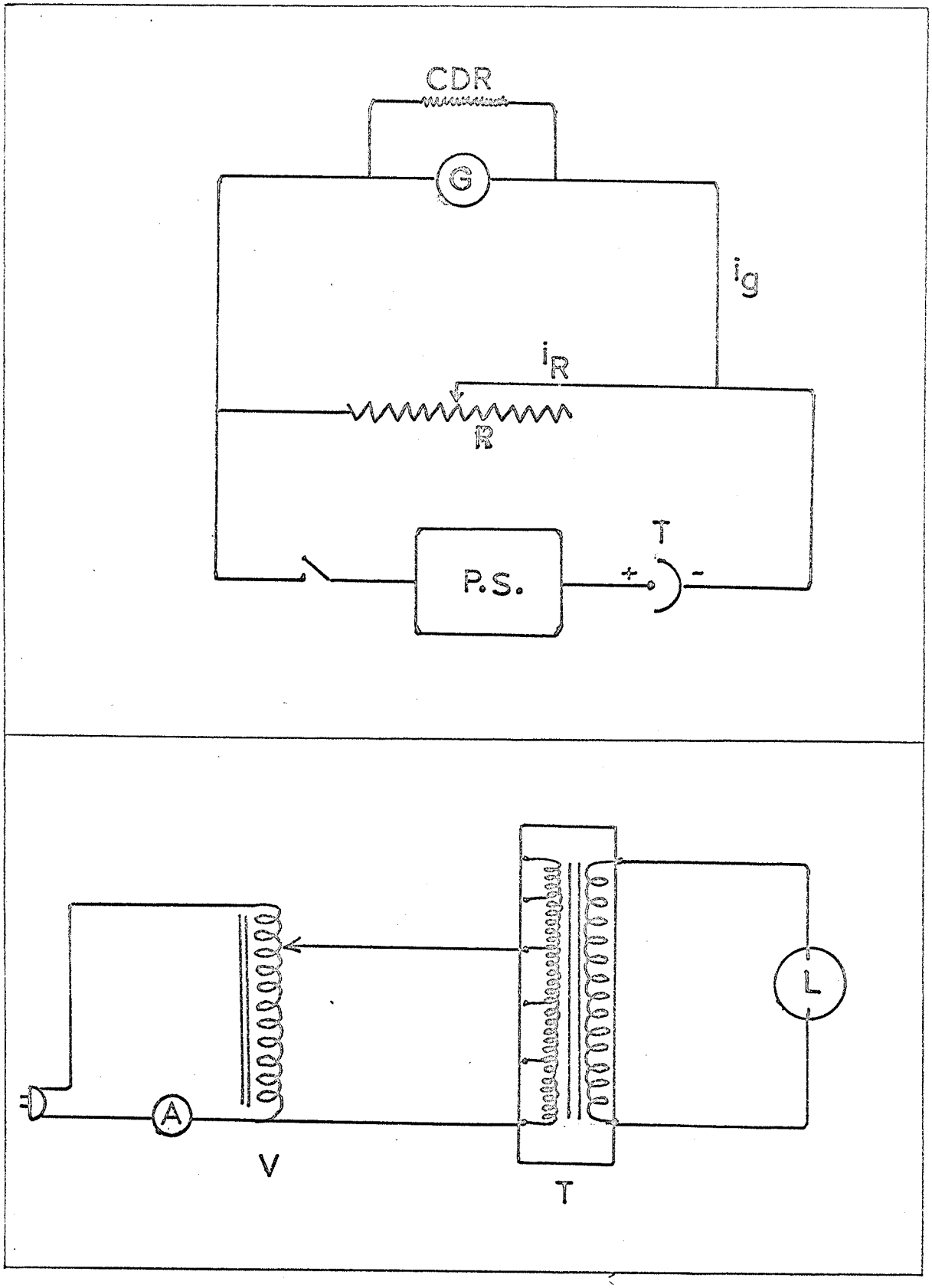
CDR
G
i_g
i_R
R
T
P.S.
+
-
A
V
T
L

measurements. They were then analyzed by combustion in a CuO furnace as described previously in the M.Sc. study.

Results

Three experiments were first conducted with ketene in the presence of hydrogen to establish the galvanometer constants. They are summarized in Table V.

Next, C_3O_2 was placed in the cell along with molecular hydrogen and was photolyzed under the following conditions:

Temp: 25.5° C; C_3O_2 press.: 27.5 mm Hg; H_2 press.: 73.5 mm Hg; Photolysis time: 60 min; Analysis temp: 25.5° C

giving the following results:

V_{CO} : 27.0 cc-cm and thus $\phi_{CO} = 1.3$

V_{CH_4} : 3.04 cc-cm " " $\phi_{CH_4} = 0.17$

$V_{H_2CO(?)}$: 1.51 cc-cm " " $\phi_{H_2CO} = 0.08$

along with a brown polymer which coated the inside of the cell. (It was found that the most effective way to remove the polymer was by filling the cell with HNO_3 vapour and heating). The third gaseous product above was collected in a LeRoy still and had a vapour pressure curve slightly lower (in temperature) than that of ketene. Consequently it was thought to be H_2CO, about the only other possibility. It was not identified in any other way since its amount was too small to be transferred for

TABLE V

Galvanometer constants from the photolysis of ketene at ambient temperatures

Photo. time (min)	Ketene pressure (mm Hg)	Temp. (°C)	% Decomp.	V_{CO} (cc-cm)	$V_{C_2H_4}$ (cc-cm)	R_{CO} (x 10^{-13})	I_a (x 10^{-13})	I_o (x 10^{-13})	i (x 10^6)	β (x 10^{-19})
90	27.7	24.5	0.35	4.43	1.03	0.205	0.11	1.06	2.44	0.45
120	33.7	25.5	0.37	5.18	2.36	0.179	0.09	0.93	1.91	0.49
120	40.7	24.0	1.23	21.5	11.6	0.750	0.38	1.95	4.42	0.44

whence β ave. becomes 0.46 x 10^{19} quanta/cm^3-sec-amp. (See Appendix I for sample calculation)

analysis by other means.

In an attempt to eliminate excessive polymer formation and also duplicate more closely the conditions of the H-atom experiments, the system was altered to include a LeRoy still, a SiO_2 gel trap, and a small Hg diffusion pump for stirring as shown in Fig. X. The C_3O_2 was then condensed into the still upstream from the cell and was maintained at a pressure of about 10 microns Hg. Hydrogen was introduced at a pressure of about 0.4 mm Hg and the system was circulated for eight hours. The results obtained are as follows:

V_{CH_4} : 7.35 cc-cm

V_{CO} : 9.93 cc-cm

$V_{C_2H_6}$: trace

$V_{H_2CO(?)}$: 18.7 cc-cm

Analysis temp: 25.0° C

The absorbance was too low under these conditions for quantum yield studies.

Discussion

The results may be explained by the following mechanisms:

FIGURE X

Apparatus for the low pressure photolysis of C_3O_2 in a flow system.

A : Lamp (Hanovia S-500)

C : Collimating lens

F : Filtering system

Q : Quartz cell with low temperature jacket

P : Photocell

H : High vacuum

T : Liquid N_2 trap

S.T. : Silica gel trap

D : Mercury diffusion pump

L : Low vacuum

S : LeRoy still

G : McLeod Gauge

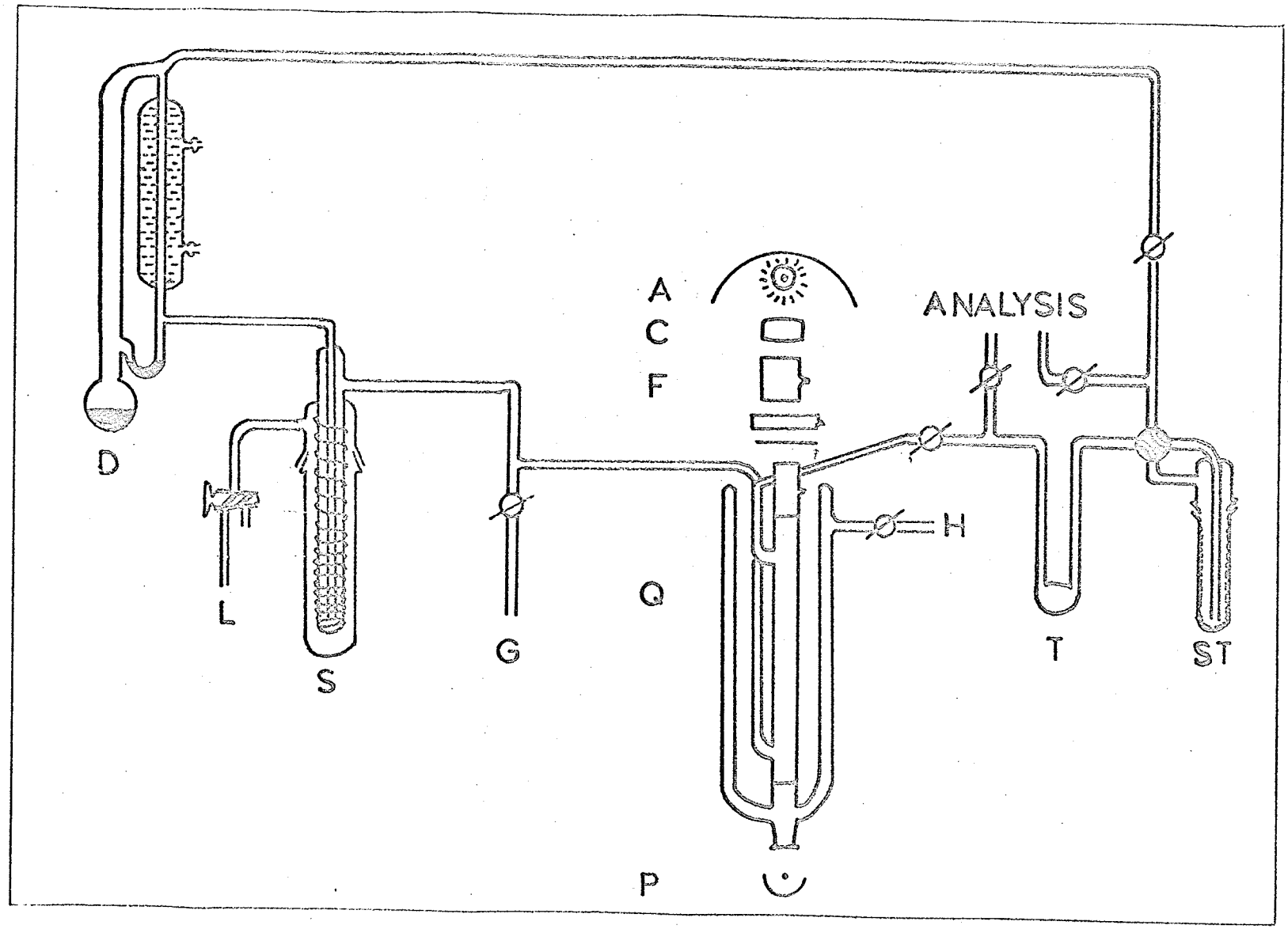
A
C
F
ANALYSIS
D
L
S
G
Q
H
T
ST
P

1) High pressure:

$$OCCCO + h\nu = OCCCO^* \quad (35)$$

$$OCCCO^* + M = OCCCO + M \quad (36a)$$

$$OCCCO^* + H_2 = H_2CO + CCO \quad (36b)$$

$$CCO + H_2 = CH_2 + CO \quad (27b)$$

$$CH_2 + H_2 \overset{W}{=} CH_4 \quad (2a)$$

$$CCO + C_3O_2 = \text{polymer} + n\ CO \quad (20)$$

2) Low pressure flow system:

Reaction (36b) predominates, and also now

$$CH_2 + H_2 = CH_4^* \begin{cases} \xrightarrow{W} CH_4 & (2a) \\ \longrightarrow CH_3 + H & (2b) \end{cases}$$

followed by

$$CH_3 + CH_3 \overset{W}{=} C_2H_6 \quad (13)$$

The formation of a third primary product (most likely H_2CO) in increasing amounts at low pressure necessitates that the primary photolytic process be the formation of an energy rich intermediate (perhaps $C_3O_2^*$) which is de-activated by collisions at

high pressures by reactions such as (36a). This intermediate must possess at least 44 kcal energy above its ground state before reaction (36b) can take place. At low pressures (36b) predominates. Trace amounts of C_2H_6 would also tend to support reactions (12b) and (15).

Conclusions

From this study it may be concluded that CCO indeed does react with hydrogen to form CH_4 and CO as postulated previously but the photolysis reaction is further complicated by the production of another intermediate (perhaps C_3O_2*) in the primary step. This latter conclusion is in agreement with the most recent study of the photolysis of C_3O_2 with olefins[42] where a "two-intermediate" mechanism is put forward as follows:

$$C_3O_2 + h\nu = S \quad (37)$$

$$S + \text{olefin} = I^* \quad (38)$$

$$I^* = \text{allene} + \text{isomers} \quad (39a)$$

$$I^* + M = \text{non-allene products} \quad (39b)$$

in which S is postulated to be C_2O, but not proven to be so. It is suggested from our results that S may also be $C_3O_2^*$.

C. Reaction of Hydrogen Atoms with Isocyanic Acid

Introduction

The photolysis of HNCO has been studied[43] over the temperature range of -31° to 200° C and in the 2 to 200 mm pressure region. The main products CO, N_2, and H_2 were postulated to be formed according to the following mechanism:

$$HNCO + h\nu = NH + CO \quad (40)$$

$$NH + HNCO = NH_2 + NCO \quad (41)$$

$$NH_2 + HNCO = NH_3 + NCO \quad (42)$$

$$2\ NCO = N_2 + 2\ CO \quad (43)$$

$$2\ NH = N_2 + H_2 \quad (44)$$

Since the HNCO molecule is isoelectronic with ketene and since the two structures are similar, it was thought that the study of the reaction of hydrogen atoms with HNCO may prove to be valuable.

Apparatus and materials

The apparatus was again altered from that used in previous experiments. An A.C. discharge with water-cooled

electrodes was used in an attempt to overcome the irregular nature of the D.C. discharge (caused by a troublesome spark-gap). Also, a removeable spherical reaction vessel was employed to make poisoning the system easy (See Fig. XI). The poisoning material was $NaH_2PO_4.H_2O$ (5% by weight) and the scavenger was CCl_4. Under these conditions the atom concentration was still found to be of questionable value but was estimated to be around 45-50 micromoles/min.

Isocyanic acid was prepared by the pyrolysis (700° C) of cyanuric acid (Eastman) in a nitrogen flow system[44,45]. The outgassed product was found to contain approximately 2% CO_2 as estimated by fractional distillation in a LeRoy still.

Results

The results are listed in Table VI below. The non-condensable products are most likely N_2 and CO but were not analyzed due to difficulties with the gas chromatograph.

Discussion

From these preliminary experiments it may be seen that the ratio of ammonia to the other products increases markedly with temperature. This would seem to indicate that it is formed by a reaction such as

FIGURE XI

Diagram of A.C. Dissociator and Spherical removable reaction vessel.

H : Hydrogen inlet

D : Dissociator (with Al electrodes)

P : To pumping system

V : Reaction vessel (200 ml)

T : Thermocouple well

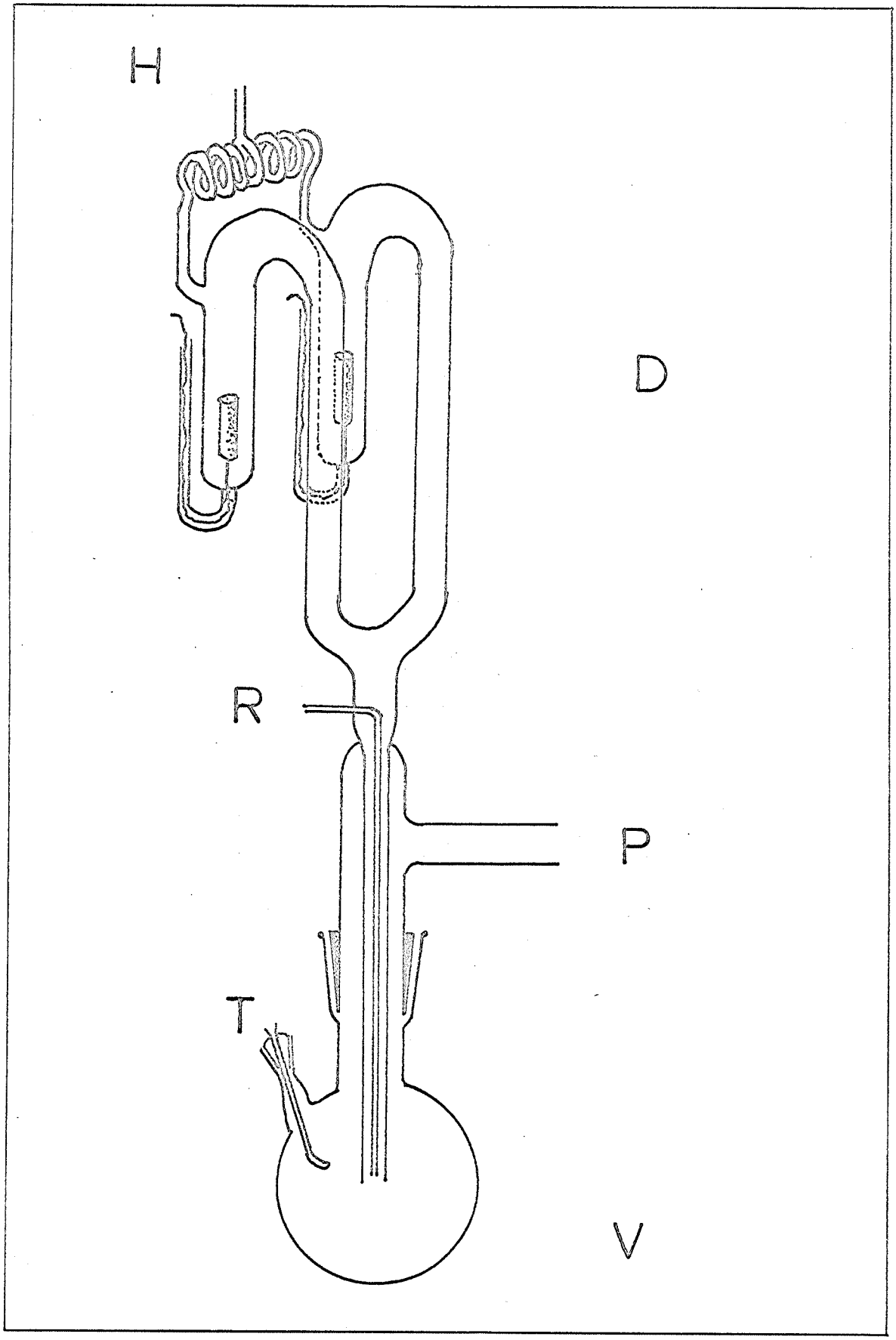
H
D
R
P
T
V

TABLE VI

Yields of products from the reaction of hydrogen atoms with HNCO at various temperatures.

Duration of Experiment (min)	Temp. (°C)	HNCO flow rate (moles x 10^6/min)	$R_{non\text{-}cond.\ products}$ (moles x 10^6/min)	R_{NH_3} (moles x 10^6/min)
5.0	252	33	14	15
2.0	170	137	193	32
3.0	-76	54	57	3.7

$$NH + H_2 = NH_3 \qquad (45)$$

and would necessitate the presence of singlet NH radicals in the system, although it is conceivable that the ammonia may be formed by

$$H_2 + HN\text{-}\overset{H}{\overset{|}{C}}\text{=}O^* = NH_3 + HCO \qquad (46)$$

analogous to CH_4 in the ketene experiments. The formation of the NH_2CO free radical has been postulated in the mercury photosensitized reaction

$$Hg\ (^3P_1) + H_2 + HNCO$$

in a static system at pressures above 1-2 mm Hg[46].

D. Excited Hydrogen Atoms

Introduction

Excited hydrogen atoms (H^2P) were first prepared for reaction purposes by Tanaka and McNesby[8] who produced them by the irradiation of ground-state H (^2S) atoms with the Lyman-α (1216 Å) line. The authors report that NH_3 is the only major product when $H(^2P)$ are reacted with N_2. Two alternative mechanisms of the primary reaction are proposed:

a) Energy transfer

$$H(^2P) + N_2 = H(^2S) + N_2^* \quad (47)$$

$$\text{Then} \quad N_2^* = 2\,N(^4S) \quad (48)$$

b) Atom transfer

$$H(^2P) + N_2 = NH + N(^4S) \quad (49)$$

Ammonia was then thought to be formed either by the reaction of N-atoms with H-atoms or by NH with H or H_2.

In a subsequent paper Koyano and Tanaka[47] report $D(^2P)$ and $H(^2P)$ production and their respective reactions with N_2 using different lamps. The results may be summarized as follows:

$$H + N_2 + H\ \text{Lyman-}\alpha = NH_3 \quad (50)$$

$$H + N_2 + D\ \text{Lyman-}\alpha = \text{no product} \quad (51)$$

$$D + N_2 + H\ \text{Lyman-}\alpha = \text{no product} \quad (52)$$

$$D + N_2 + D\ \text{Lyman-}\alpha = ND_3 \quad (53)$$

indicating that the wave length shift due to isotopic influence

was enough to prevent the absorption of the resonance radiation by atoms.

It was thought that a study of $H(^2P)$ in our system might prove to be interesting and would indicate whether such species are of any importance in ordinary H-atom experiments.

Apparatus and materials

A D.C. discharge was used to produce $H(^2S)$ as described previously (approximately 2% of the total pure H_2 flow). At the entrance of the reaction vessel they were irradiated by a Lyman-α source as shown in Fig. XII. The lamp was first constructed as follows:

An A.C. discharge across molybdenum electrodes in a Hg free mixture of H_2 (0.0062 mm Hg) and Ne (0.30 mm Hg) was used. Both LiF and CaF_2 were tested as window materials. The window was waxed on to the end of the lamp. The output was determined by irradiation of CO_2 (40 cm Hg) in a static system and was found to be about 1.3×10^{16} quanta/sec. See Table VII for results.

Discussion

The experiments show that although there was some back diffusion of N_2 into the discharge zone, a greater amount of NH_3 is formed with the lamp on than without the Lyman-α line, and

FIGURE XII

Diagram of reaction vessel and Lyman-α lamp for H (^2P) studies.

L : Lyman-α lamp

D : to dissociator

M : to McLeod Gauge

P : to traps and pump

R : reactant inlet

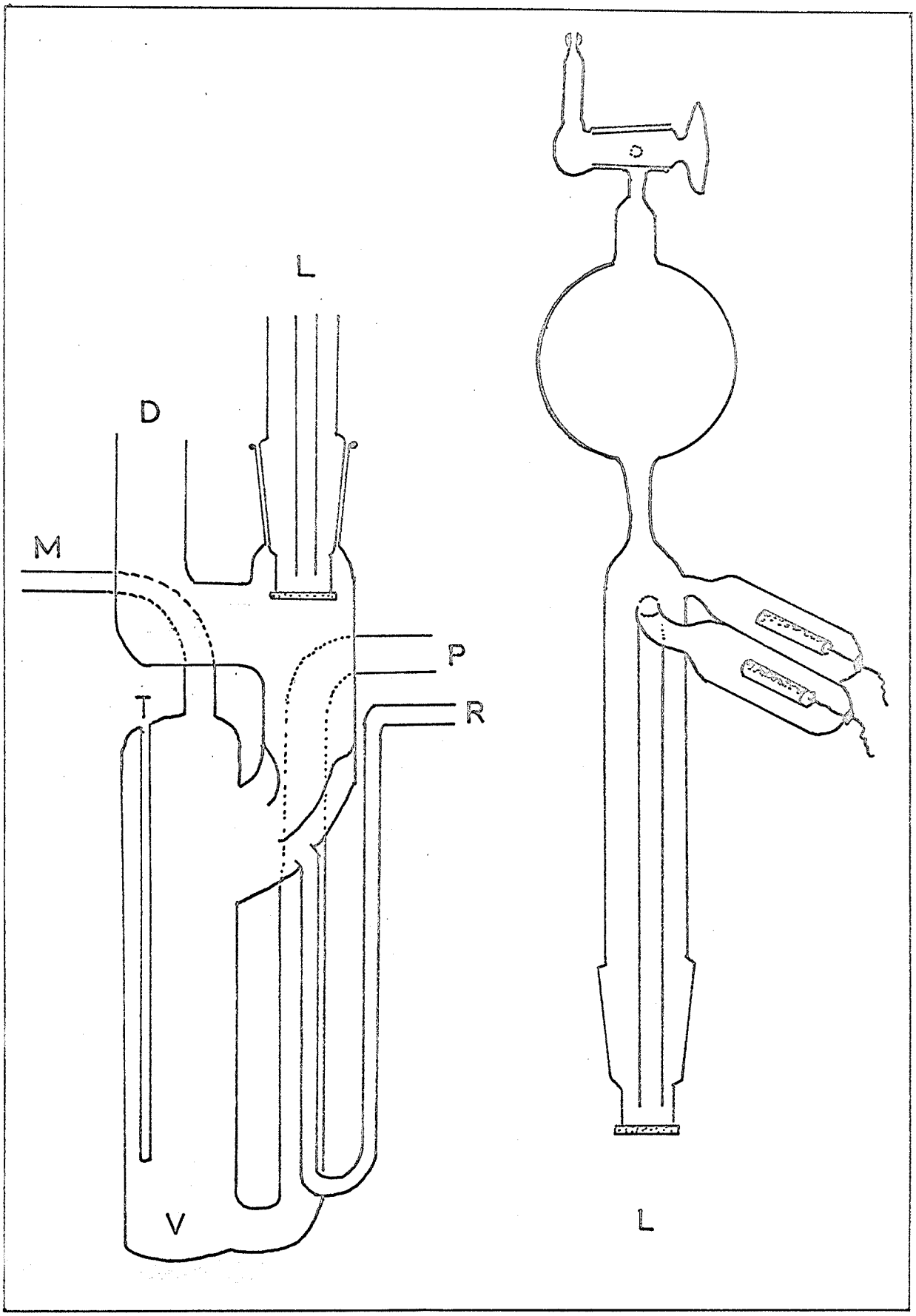
L
D
M
P
T
R
V
L

TABLE VII

Yields of NH_3 from the reaction of $H(^2P)$ with N_2

Duration of experiment (min)	N_2 flow (moles x 10^6/min)	H-atom flow (moles x 10^6/min)	Reaction temp. (°C)	NH_3 formed (moles x 10^6/min) Lamp on	Lamp off
3.0	39	45	37		0.092
21.0	31	45	28	0.198	
30.0	51	45	-196		0.47
30.0	51	45	-196	0.65	

FIGURE XIII

Diagram of Lyman-α lamp with water-cooled window.

B : 250 ml bulb

E : electrodes

W : window

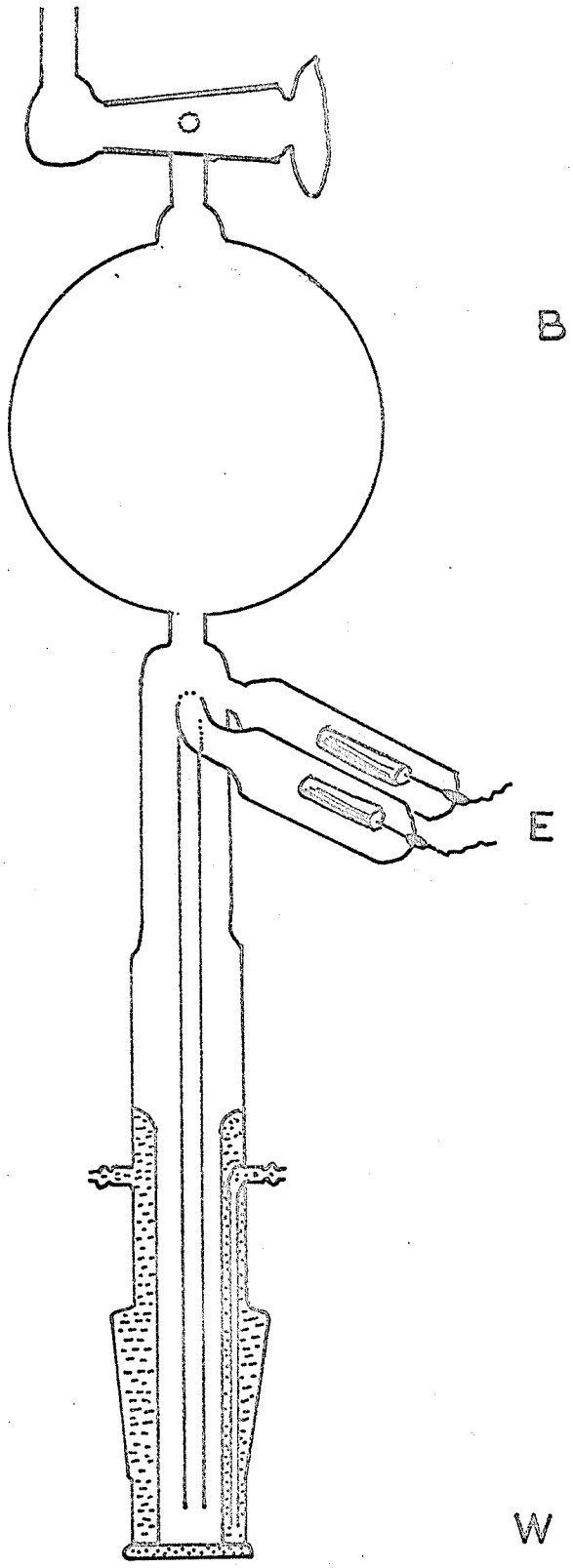
B
E
W

thus indicates the presence of $H(^2P)$. The amounts, however, are negligible when compared with the quantities of products normally formed in hydrogen atom reactions, and thus it may be concluded that this species is of little importance in ordinary studies of thermal hydrogen atoms.

Further work on $H(^2P)$ + CO, $H(^2P)$ + CH_4, and $H(^2P)$ + NO was planned but was later abandoned due to difficulties encountered with the heating of the lamp window. A water-cooled lamp was then designed and constructed (see Fig. XIII), but no experiments were conducted with it.

E. Desorption Studies and Trapping

Although adsorption of gases on SiO_2 gel and charcoal is well-known, the use of these media for the trapping and separation of gases in a fast-flow, low-pressure system is rather unfamiliar. The trapping of CH_4, CO, and N_2 in a fast flow system has previously been described by the author[9], but later it was found that the Dow Corning Vacuum Silicone grease used for adhering the gel to the glass caused a problem in that after repeated warming of the trap, the gel became ineffective as an adsorbing agent, probably due to the filling of the pores of the gel by the grease. It has now been found that water-

glass (reagent grade sodium silicate) is much better for this purpose. The inside of the trap is coated with water-glass and the gel is sprinkled into the trap where it adhers to the walls. The trap is then "cured" at 100° C for a few hours, after which it is heated in vacuo to about 200° C overnight. The resulting gel coating becomes permanent after such a treatment.

Also, an attempt was made to separate non-condensable gases by adsorption-desorption techniques in a LeRoy still. A diagram of the apparatus is shown in Fig. XIV. The desorption curves for CO, CH_4, and N_2 were determined on SiO_2 and porous glass adsorbents. From these it may be seen that CO ought to be separated from CH_4 or N_2 on SiO_2 gel but an attempt to accomplish this failed since the desorption process was found to be much slower than distillation for which the still is so well-known.

Another variation of the previous experiment was as follows: SiO_2 gel (28-60 mesh) was stuck onto the inner walls of the stem of a liquid N_2 trap by means of water glass. The outside was then coated with Sauereisen and a heating coil was wound over it as shown in Fig. XVII.

Trace amounts of CO, CH_4, C_2H_6, and C_2H_4 were then

FIGURE XIV

Diagram of modified LeRoy still for adsorption-desorption studies of non-condensable gases.

I : inlet

G : to McLeod Gauge

L : to low vacuum

T : taper

R_1: 13 ohm resistance

R_2: 9 ohm resistance

t : thermocouples

P : porous glass tubing

A : Al collar

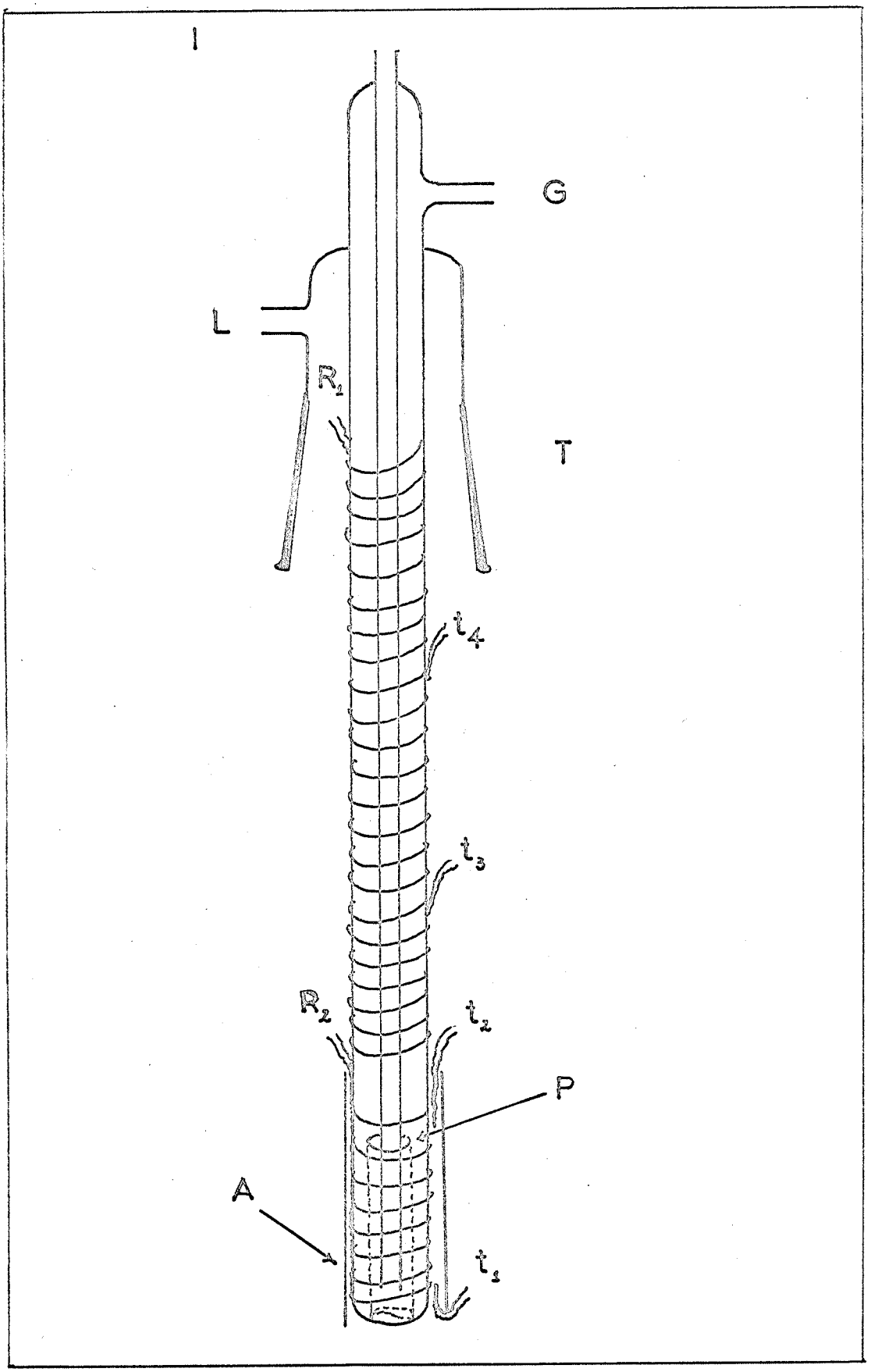
I
G
L
R1
T
t4
t3
R2
t2
P
A
t1

TABLE VIII

Desorption of N_2, CO, and CH_4 from:

a) SiO_2 gel

N_2		CO		CH_4	
Temp.(°C)	Pressure	Temp.(°C)	Pressure	Temp.(°C)	Pressure
-196	0	-194	0	-196	0
-190	2.0	-188	0	-190	1.0
-186	4.5	-175	0	-186	5.0
-182	7.5	-157	10	-180	15
-174	20	-147	25	-176	30
-168	85	-135	90	-168	100

b) Porous glass (Corning #7930)

-196	0.5	-196	0.25	-196	0
-192	5.0	-193	0.40	-192	0.5
-188	11	-189	0.50	-188	1.0
-182	18	-183	1.0	-183	3.5
-176	37	-177	2.0	-178	8.0
-168	75	-170	14	-169	28.0
		-163	65	-163	59.0
		-154	135	-124	120

Note: (1) Amount of gas used: ~100 micromoles
(2) Porous glass used: 3 cm length of 12 mm O.D. tubing
(3) SiO_2 gel: Approximately 0.5 g of 28-200 mesh
(4) Pressure units: microns

FIGURE XV

Desorption curves for CH_4, N_2, and CO from SiO_2 gel

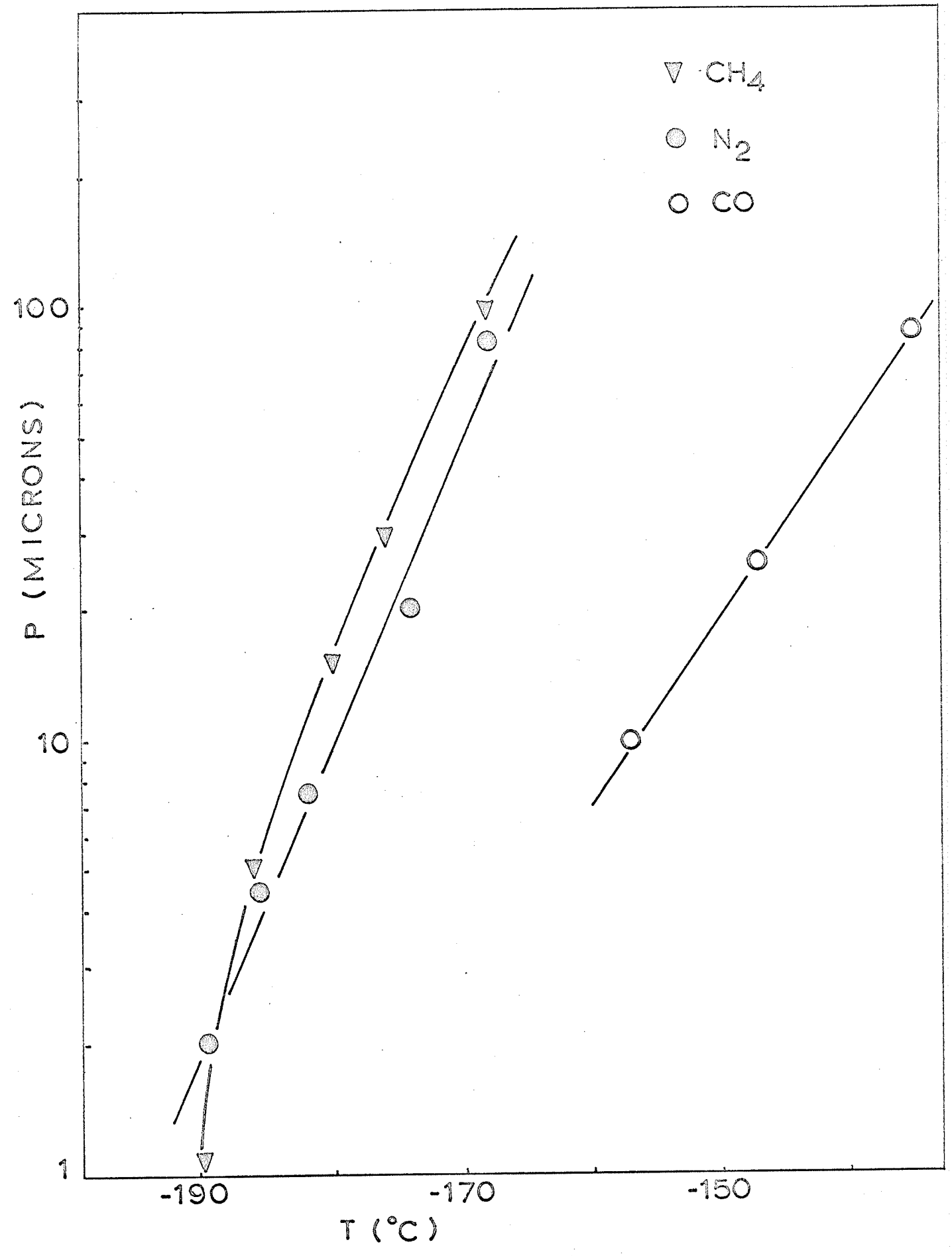
CH4
N2
CO
100
10
1
P (MICRONS)
-190
-170
-150
T (°C)

FIGURE XVI

Desorption curves for CH_4, N_2, and CO from porous glass

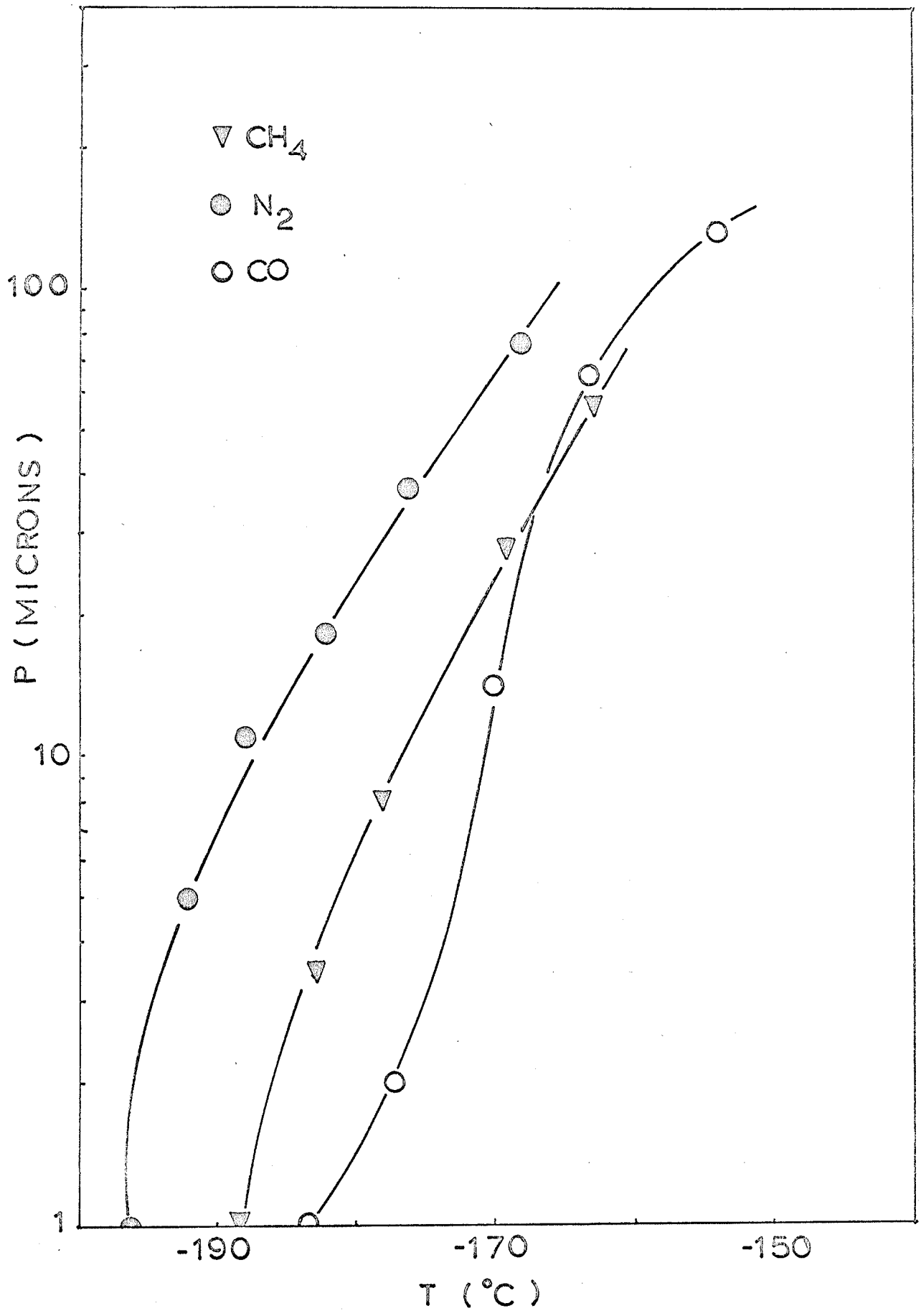
CH4
N2
CO
100
10
1
P (MICRONS)
-190
-170
-150
T (°C)

FIGURE XVII

Diagram of apparatus used for the trap desorption experiment

V : to variac

S : sampling system

C : SiO_2 gel coating on inner stem of trap

I : Sauereisen insulation

H : Heating coil

p : Pirani gauge leads

r_L : variable resistor

r_2, r_3 : matched resistors

z : zero adjust

b : six volt battery

c : variable resistor for current control

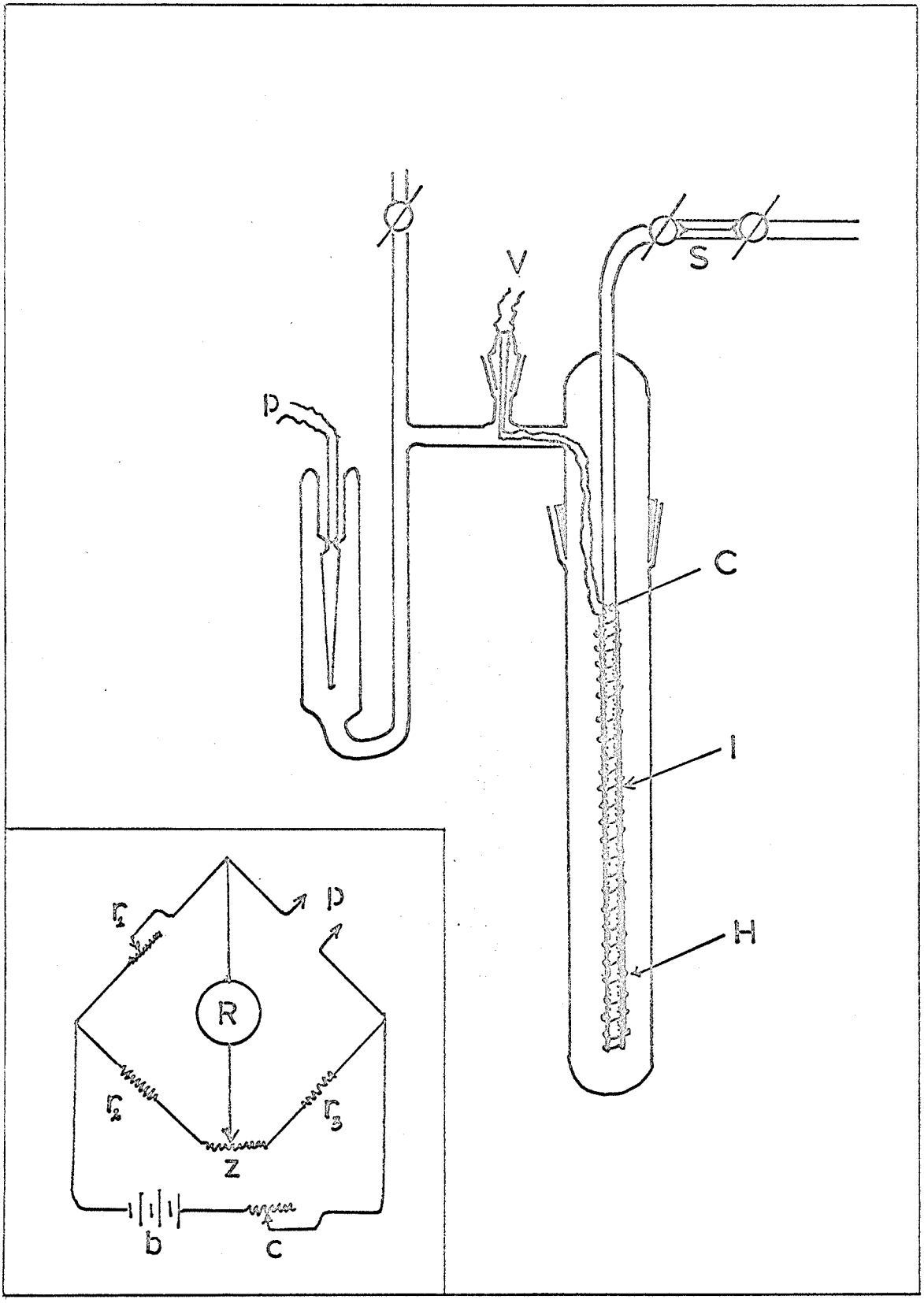
V
S
P
C
I
H
P
R
Z
b
c

adsorbed on the inner part of the trap at -196° C, and then the temperature of the inner stem was slowly raised by means of the heating coil. The pressure was continuously followed by means of a Pirani gauge connected to a strip chart recorder.

As could be seen from the "desorptigram" four broad peaks were obtained. Unfortunately, similar studies using only CH_4 gave two to three peaks probably due to different adsorption sites or multi-layer adsorption. Consequently the experiments were abandoned. However, it is believed by the author that further refinement of this technique may prove useful in the direct quantitative determination of non-condensable and condensable gases from a single trap in vacuum systems.

A more successful set of experiments along these lines was then performed. "Saran" charcoal* or pyrolyzed polyvinyl chloride was made to adhere to the inside of the removable portion of a liquid nitrogen trap in the usual manner (by the use of water glass), and then outgassed at about 250° C over-night. Hydrogen was then introduced at various flow rates into a helium flowing system, and trapped out quantitatively

---

*Kindly supplied by Dr. S. S. Barton, Royal Military College of Canada, Kingston, Ontario.

FIGURE XVIII

Typical "desorptigram"

0
10
20
30
40
50
60
70
80
90
100
8/8/62
DYNATRONIC INSTRUMENTS CORP./ELECTRONICS DIV. OF LABLINE, INC.
CHICAGO, ILL.

FIGURE XIX

Diagram of "saran" charcoal trap and gas handling system

P : to pumps

L : to low vacuum

S : "saran" charcoal adsorbate

D : dewar

G : to gas chromatograph

T : Toepler pump

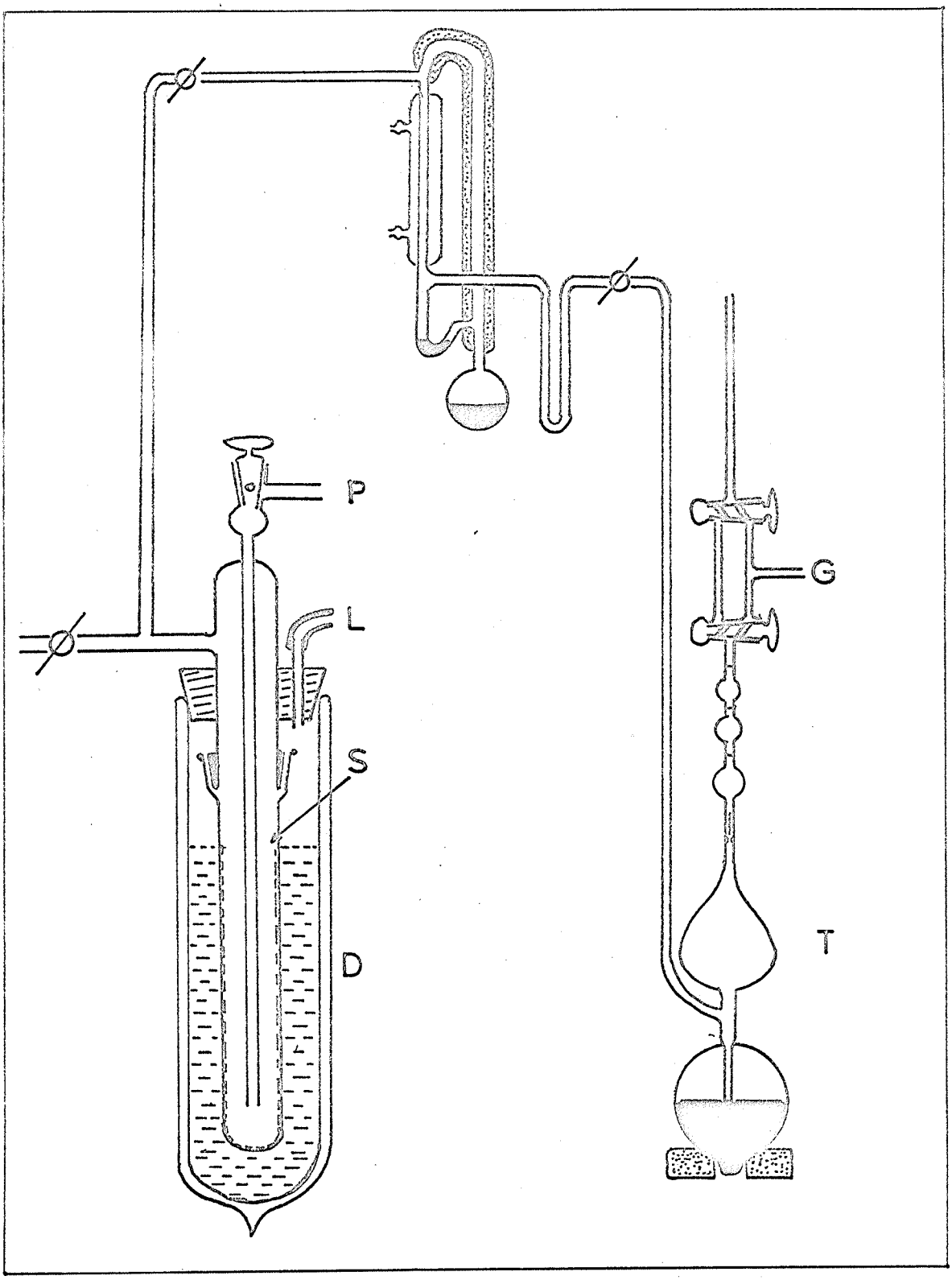
P
L
S
D
G
T

TABLE IX

Trapping of hydrogen from a helium flowing system

H_2 flow-rate (moles x 10^6/min)	H_2 in (moles x 10^6)	H_2 out (moles x 10^6)
8.8	89	90
14	96	98
15	75	76
25	128	128
40	119	120
61	183	196
74	149	142
206	205	207

Note: The above experiments were performed under the following conditions:

Total pressure: 1.04 mm Hg

Helium flow : 2700 moles x 10^6/min

A "blank" experiment showed that less than 1 micromole/min of helium was adsorbed.

downstream. It was found that a temperature slightly lower than -196° C was necessary for the quantitative adsorption, and this was achieved by pumping on the liquid nitrogen coolant. The hydrogen was then desorbed at 200° C and removed by means of a small diffusion and Toepler pump combination into a gas burette where its amount was determined by P.V.T. measurements. The following table shows that the adsorption is quantitative even at large hydrogen flows.

This study became even more interesting when it was found that D_2 is even more strongly adsorbed on a charcoal surface[48], and that under these conditions there is less than 0.25% exchange between H_2 and D_2 (i.e. to form HD) when a mixture of the above gases was trapped and collected in the above manner. This provided the way for the study of the $H + D_2$ reaction (see Section G). It is not necessary to mention that it could be of great value in any reaction where H_2, HD and D_2 are involved in a helium flowing system (eg. thermal and photochemical studies).

F. Estimation of Atoms

Introduction

By far the most difficult part of the research was to determine the atom concentration and to maintain its value constant over a series of experiments. During the work thus far chemical scavengers were employed for this purpose (CCl_4 and C_2H_5Cl), but especially at the low temperature experiments it was thought that an independent method for estimating the hydrogen atom concentration prior to each experiment would be of great value. It was first decided to use a hot wire according to the method described by Bak and Rastrup-Andersen[49].

Apparatus

a) First arrangement

The reaction vessel was so designed as to make it possible to remove the hot-wire probe from the reaction zone after the H-atom concentration has been determined. Also, a water-cooled discharge tube was constructed to prevent any possibility of excessive heat transfer from the discharge zone to the reaction vessel (see Fig. XX). An A.C. discharge was used for these experiments with a 200 V primary - 4500 V secondary transformer (Moloney #5948) connected directly across

FIGURE XX

Diagram of water-cooled dissociator, hot-wire probe, and reaction vessel.

H : Hydrogen inlet

D : Water-cooled dissociator

T : Taper for raising or lowering probe

P : To pumps

V : 250 ml. reaction vessel

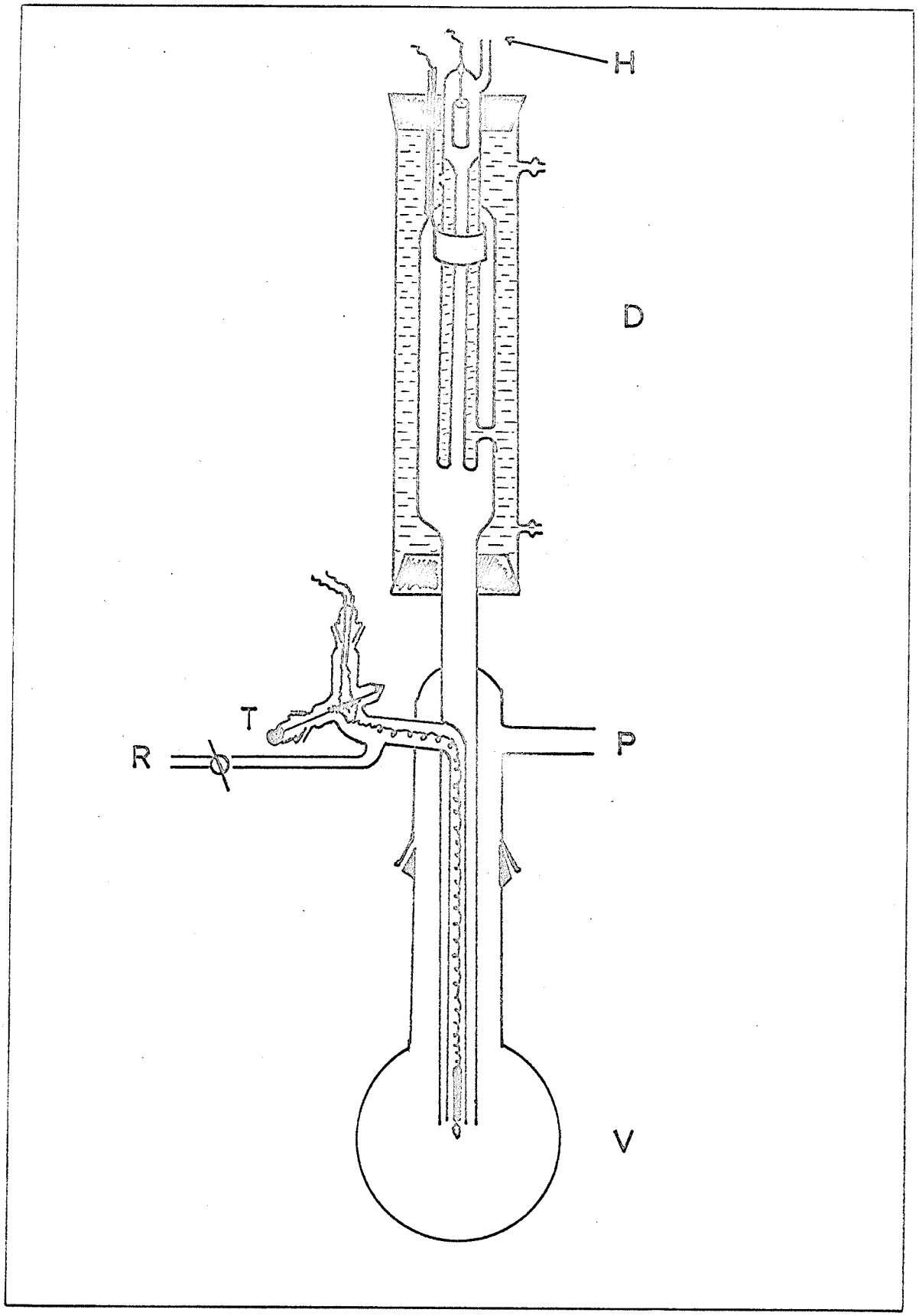
H
D
T
R
P
V

the electrodes.

The discharge zone and atom flow tube were poisoned with H_3PO_4 (2% by vol.) while $NaH_2PO_4.H_2O$ (5% by weight) was used for the reaction vessel. For a typical experiment the system was evacuated for one hour during which the probe was outgassed at red heat. Then hydrogen was introduced at a pressure of 1.03 mm Hg and a flow rate of 2700 micromoles/min. The probe current was adjusted by means of resistor, R_4, so that its temperature was just below that of red heat. The bridge was then balanced using resistor R_1 and the current through the filament and voltage across it were noted (I_o and V_o respectively). Next, the discharge was switched on and the temperature of the tube was kept at 21° C by circulating water through its outer jacket. Due to atom recombination, the temperature of the filament increased and this caused an imbalance in the bridge circuit. R_1 was re-adjusted until the bridge was again in balance and the new values for current and voltage were recorded (I and V respectively). From this information the atom concentration was calculated as shown in Appendix II.

The above values are then compared with those obtained by chemical scavengers in Table X. In each case the scavenger

FIGURE XXI

Diagram of probe detail

L : copper leads with teflon sheathing to bridge

A : chord for raising or lowering probe

C : brass

D : high-voltage teflon insulated wire

E : teflon holder for filament

F : portion of 150 watt light bulb filament

V : voltmeter

A : ammeter

R_1 : variable resistor

μA : micro-ammeter

R_3, R_2 : matched resistors

B : 12 volt battery

R_4 : variable resistor for current control

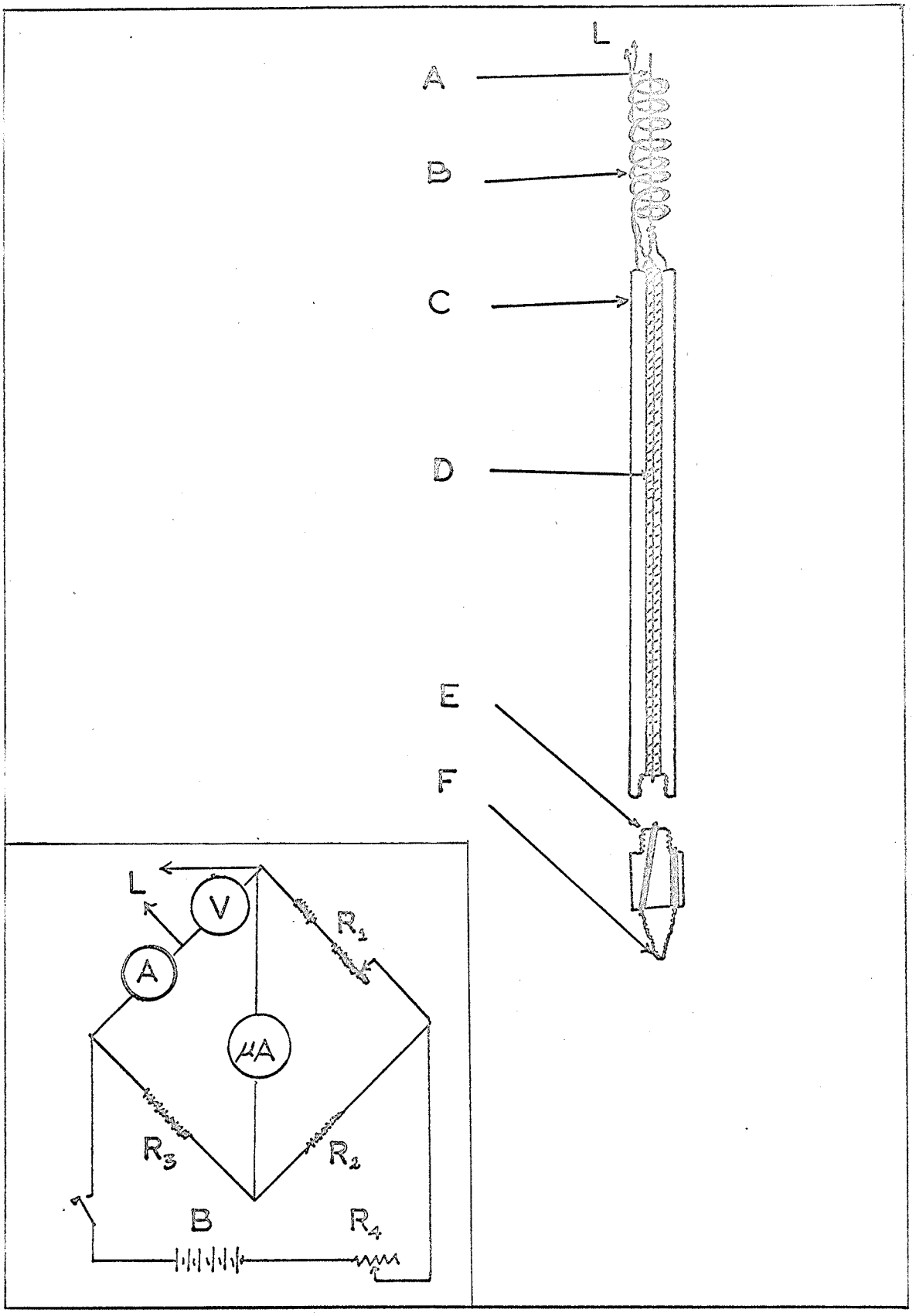
L
A
B
C
D
E
F
L
V
A
μA
R1
R2
R3
R4
B

TABLE X

Estimation of atoms at various temperatures using chemical and hot-wire scavengers

Temp. (°C)	Voltage across primary	ATOM CONCENTRATION Hot wire (moles x 10^6/min)	Chemical scavenger (moles x 10^6/min)
234	30	24	40 (HCl from CCl_4)
"	40	30	49 (" " ")
"	50	33	87 (" " ")
67	30	23	42 (HCl from C_2H_5Cl)
"	40	47	96 (" " ")
"	50	51	99 (" " ")
-96	30	194	433 (CH_2CO decomp.)
"	25	160	177 (" ")
"	25	150	223 (" ")

Note: See Appendix II and Appendix III

concentration was in large excess and for the C_2H_5Cl experiments the HCl formed was multiplied by a factor of three to arrive at the estimate of the atom flow rate[50].

Discussion

It can be seen that the atom concentration, as determined by the hot-wire method is generally lower than that estimated by the chemical scavengers in each case. This is probably due to one or more of the following reasons:

(a) The hot-wire arrangement of the probe is one-dimensional and Shaw[51] has shown that in his system this was at least 0.25 as effective for scavenging as a three-dimensional detector.

(b) The tungsten metal has a low accommodation coefficient for hydrogen atoms (see Ref. 57, p. 71).

(c) A reaction was seen to take place in the probe area to form a blue coating on the walls of the glass. This is probably due to WO_2 (or more commonly "tungsten blue") formed by the reaction, $H + WO_3$, which would remove atoms in a manner other than direct recombination.

b) Second arrangement

Some difficulty was encountered with the dissociator and in the movement of the probe. Thus the system was

FIGURE XXII

Diagram of improved "sandwich" probe

A : arm A of probe over which F folds

B : arm B of probe, coated with Sauereisen and H_3PO_4

L_1: thermocouple leads to galvanometer

L_2: copper leads to current supply

S : glass sheathing

T : iron-constantin thermocouples

R : five ohm Nichrome resistance wire

F : 1 cm^2 Al foil

V : Voltmeter

I : Ammeter

B : six volt battery

R_c,R_f: coarse and fine current adjust

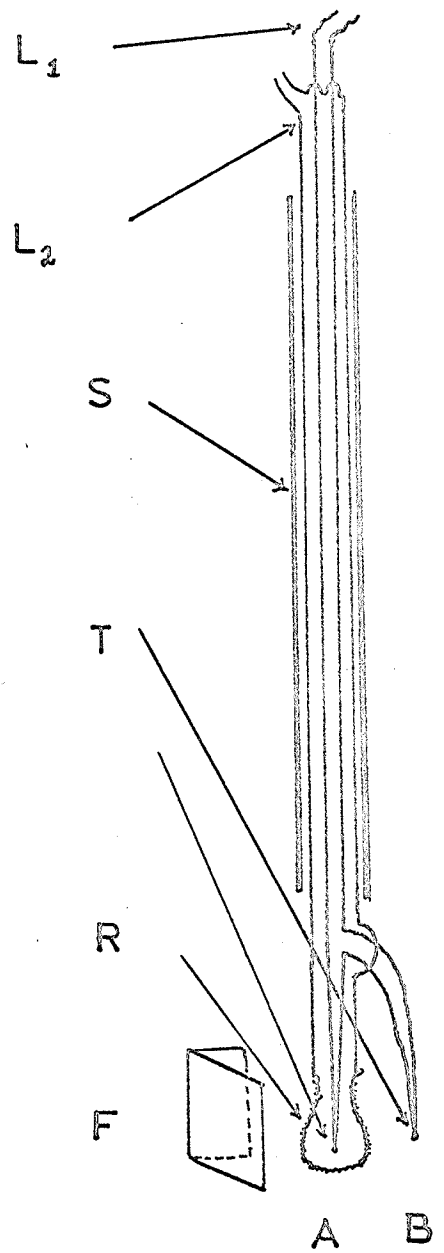
L1
L2
S
T
R
F
A
B

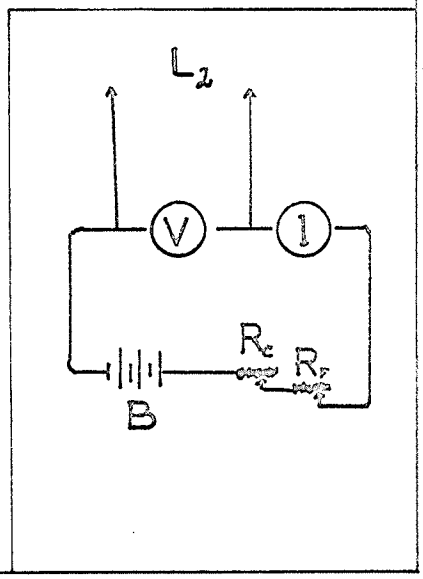
L2
V
I
Rc
Rv
B

temperature rise was produced by passing a known amount of current through the resistance wire. The absolute atom concentration could then be estimated by the wattage dissipated as in the case of the hot-wire detector described previously. This is really a combination of a hot-wire detector and a thermocouple probe. Using such an arrangement it was now convenient to determine the hydrogen atom concentration as a function of some of the variables which may influence it in a helium flowing system. Two types of arrangements were used as shown in Fig. XXIII. For these experiments an A.C. discharge was used with a 110 V primary - 31000 V secondary transformer (American Transformer Co. #18606).

Results

The results obtained are summarized in the following tables:

Discussion

When the helium pressure in the reaction vessel is increased two things happen:

1) There is an increase in the flow-rate of the helium. This effect tends to increase the atom concentration, as more atoms are swept out of the discharge zone.

FIGURE XXIII

Diagrams of two types of dissociators and reaction vessels for hydrogen atom studies.

H : hydrogen inlet

L_1: A.C. transformer leads

L_2: probe leads

D : dissociator

P : probe handling system with probe in "normal" position

R : reactant inlet

M : to McLeod pressure gauge

T : thermocouple well

V : 550 ml reaction vessel

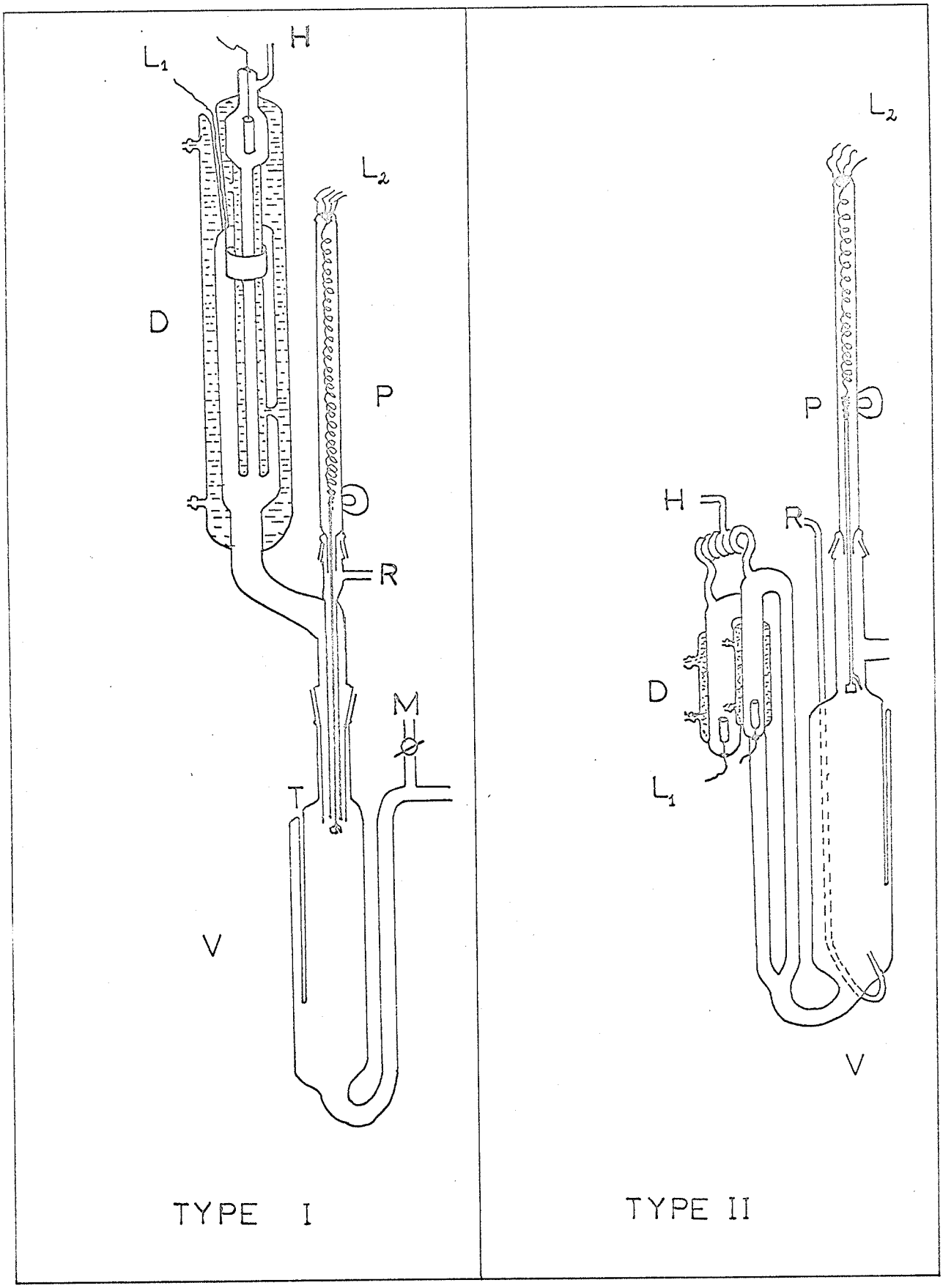
H
L1
L2
D
P
R
M
T
V
TYPE I
L2
P
H
R
D
L1
V
TYPE II

FIGURE XXIV

Photograph of the TYPE I system

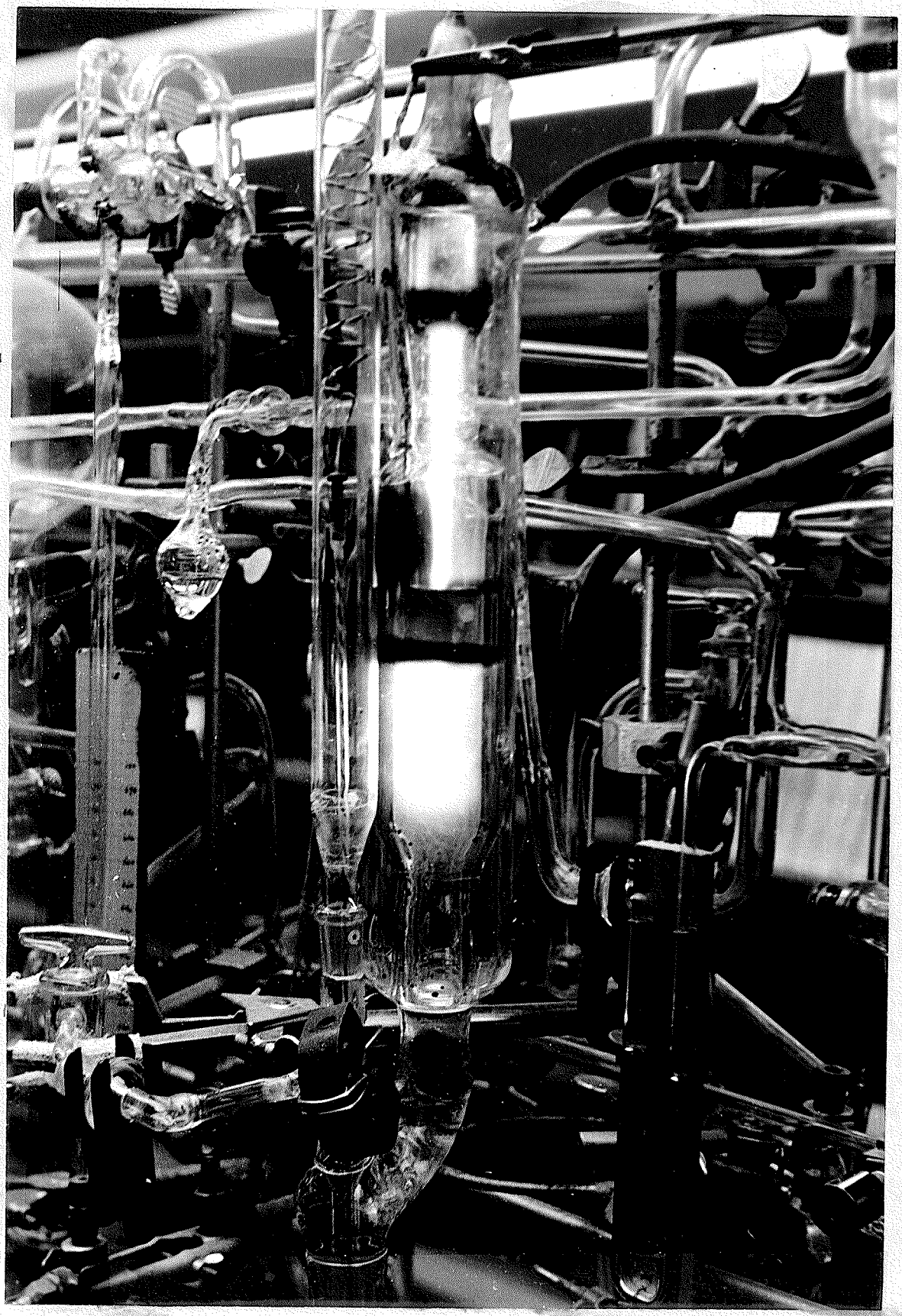

FIGURE XXV

Photograph of the TYPE II system

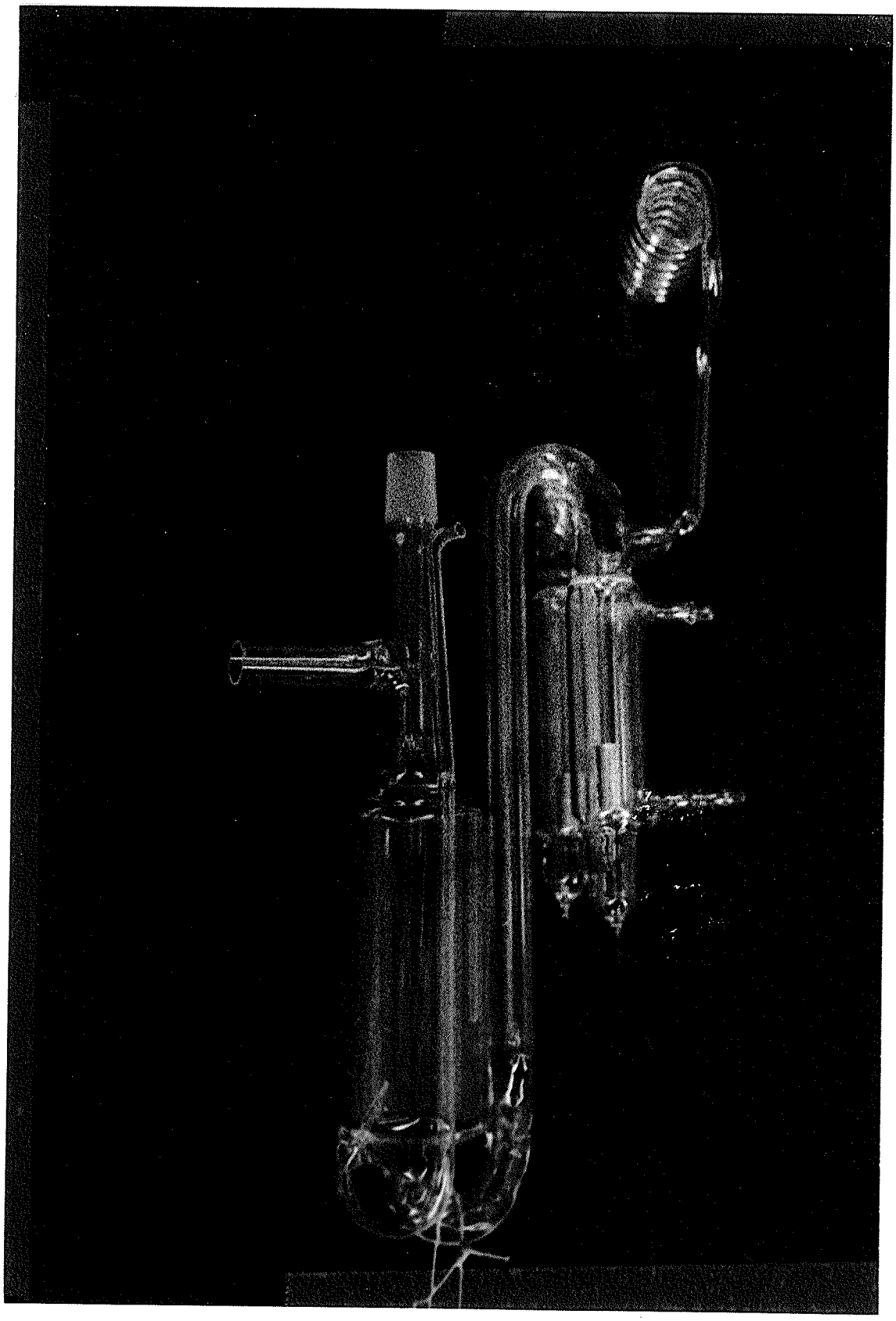

TABLE XI

a) Hydrogen atom concentration as a function of the helium pressure

Type I p_{H_2}: 98 microns			Type II p_{H_2}: 120 microns		
p_{He} (mm)	watts	atoms (moles x 10^6/min)	p_{He} (mm)	watts	atoms (moles x 10^6/min)
0.75	0.020	5.4	0.47	0.20	54
0.92	0.038	10	0.64	0.27	73
1.12	0.059	15	0.85	0.28	75
1.33	0.090	24	0.98	0.21	57
1.52	0.141	38	0.18	0.20	54
			0.41	0.19	51
			1.58	0.15	41

Note: Temperature: Ambient
Discharge conditions: 1 amp. and 25 volts (primary)
Position of probe: Normal

TABLE XII

b) Hydrogen atom concentration as a function of the molecular hydrogen pressure

Type I p_T: 1.52 mm			Type II p_T: 1.07 mm		
p_{H_2} (microns)	watts	atoms (moles x 10^6/min)	p_{H_2} (microns)	watts	atoms (moles x 10^6/min)
9.0	0.01	2.7	25	0.0315	8.5
26	0.04	11	55	0.106	29
42	0.07	19	112	0.263	71
63	0.13	35	150	0.303	82
85	0.14	38	340	0.416	112
98	0.17	46	1070 (pure H_2)	0.650	175
143	0.24	65			

Note: Temperature: Ambient
Discharge conditions: 1 amp. and 25 volts (primary)
Position of probe: Normal
One micron H_2 pressure gives approx. one μmole/min H_2 flow

TABLE XIII

c) Hydrogen atom concentration as a function of discharge current

Type I p_{He}: 1.52 mm, p_{H_2}: 50 microns				Type II p_{He}: 1.06 mm, p_{H_2}: 80 microns			
Amps. (Dis.)	Volts (Dis.) (primary)	Watts (probe)	Atoms (moles x 10^6/min)	Amps. (Dis.)	Volts (Dis.) (primary)	Watts (probe)	Atoms (moles x 10^6/min)
0.25	15	0.031	8.4	1.0	25.5	0.143	39
0.60	20	0.045	12	2.0	33	0.170	46
1.3	25	0.057	15	3.0	39	0.189	51
1.8	30	0.050	13.5	4.0	43	0.221	60
2.8	35	0.050	13.5	5.0	51	0.248	67
				6.0	57	0.248	67

Note: Temperature: Ambient
Position of probe: Normal

TABLE XIV

d) Hydrogen atom concentration as a function of the position of the probe

Type I		Type II	
Position	Atoms (moles x 10^6/min)	Position	Atoms (moles x 10^6/min)
normal (see Fig. XXIII)	11	normal (see Fig. XXIII)	41
2.5 cm down	11	2 cm down	45
1 cm up	5.2	4 cm down	43
3 cm up	2.3	10 cm down	26
7 cm up	0.58		

Note: Temperature: Ambient
Discharge current: 1 amp. and 25 volts (primary)
p_{He} and p_{H_2} as in (c)

TABLE XV

e) Hydrogen atom concentration as a function of the temperature of the reaction vessel

Type I p_{He}: 1.52 mm p_{H_2}: 15 microns			Type II p_{He}: 1.07 mm p_{H_2}: 12 microns		
Temp.(°C)	watts	atoms (moles x 10^6/min)	Temp.(°C)	watts	atoms (moles x 10^6/min)
-196	0	0	-196	0	0
-78	0.0078	2.1	-70	0.032	8.7
0	0.0060	1.6	31	0.043	11.6
50	0.0075	2.0	154	0.030	8.1
100	0.0086	2.3			
170	0.0127	3.4			
>220	very few or no atoms		>220	very few or no atoms	

Note: Discharge current: 1 amp. and 25 volts (primary)
Position of probe: Normal
Wall conditions: $NaHPO_4.H_2O$ (5% by wt.)

2) There is an increase in the number of third-body collisions of the type H + H + He = H_2 + He. This effect lowers the atom concentration as the helium pressure is increased.

From Table XI it can be seen that factor (1) is prominent in the Type I system and that both factors come into play in the Type II system due to the fact that the scavenger probe is farther away from the discharge area.

Table XII indicates that even at very low partial pressures of hydrogen only about 25% of it remains dissociated by the time it reaches the reaction vessel. This is true for both types of systems and is discouraging since a pure H + He binary system would be highly desirable for accurate H-atom studies. Harteck and Roeder[54] have also found this to occur for H, N, O-atoms using Ne as a carrier.

Table XIII illustrates that there is little hope for increasing the atom concentration simply by increasing the discharge current. An increase in the latter by a factor of six increases the atom concentration only by a factor of 1.5. Beyond this the number of atoms seems to level off in system II and actually decreases slightly in system I probably due to the over-heating of the electrodes.

Using H_3PO_4 and its salts ($Na_2HPO_4.H_2O$ in particular) produces a relatively constant atom concentration over a number of centimeters length of the reaction vessel. The large decrease of atoms shown in the Type II system as one moves the probe downward was probably due to the fact that many of the atoms were missed by the probe as one gets farther and farther away from the constricted area. System II shows that there is considerable "back diffusion" of atoms into the upper region of the inlet system and great care should be taken to insure that this whole region is at the same temperature as that of the reaction vessel or else a reaction may be occurring outside the desired temperature zone. However, this effect would be greatly reduced when an excess of reactant molecules flow through the inlet system and cause a pressure gradient in the inlet system opposite to that of diffusion of atoms.

Very little can be said about the temperature studies of the atom concentration as the set of experiments listed in Table XV was conducted over a period of days during which the walls may have varied significantly. The most outstanding feature of this study is that there are no atoms at -196° C and very few beyond 220° C under the above pressure and flow

conditions. This is in accordance with the results of other workers[55,56], and is believed to be due to two kinds of mechanisms operative in different regions of the temperature range[57]. At high temperatures atoms are destroyed by the Rideal mechanism

$$S\text{-}H + H = S + H_2 \qquad (54)$$

where S-H represents a chemisorbed atom on the surface. This reaction has an activation energy of about 6.5 kcal and begins to proceed at a considerable rate above 200° C.

At very low temperatures the activation energy for atom removal is close to zero[58]. According to the Hinshelwood scheme this is due to the fact that chemisorption decreases and surface diffusion of atoms becomes important:

$$S...H + S...H = 2\,S + H_2 \qquad (55)$$

Shuler and Laidler[58] indicate that water plays a role here as well since at low temperatures it is strongly adsorbed by van der Waals forces on glass, and forms a layer on the glass surface on which hydrogen atoms can rapidly move about and recombine, or be removed by the following reaction:

$$S...H_2O...H + H = S...H_2O + H_2 \qquad (56)$$

Another possibility postulated by the author for the low activation energy at low temperatures is "tunnelling" (see Appendix VII) since a plot of $\ln \gamma T$ vs. $1/T$ given by Shuler and Laidler is not unlike some theoretical plots generated by Bell's equation[59] in which quantum mechanical "tunnelling" is taken into account by virtue of the small mass of the hydrogen atom. This study is now being continued by E.S.R. in this laboratory[60] and preliminary results show that H-atoms formed on a porous glass surface recombine quite rapidly even at temperatures as low as -196° C.

Besides the above studies on atom recombination a few other points of interest may be mentioned:

a) It was found that the atom concentration could vary by a factor of at least two within a matter of hours and this cast a considerable amount of doubt on the validity of some of the "flow curve" experiments conducted previously with CH_2CO and C_3O_2. This is probably due to the dehydration of the acid (or its salt) under vacuum conditions giving rise to a different surface for atom recombination (see Smith[55]).

b) Trace amounts of water vapour in the molecular hydrogen stream tended to stabilize and increase the atom concentration by a factor of 2 to 10 contrary to the findings of Rony[53].

c) A teflon coating as described by Berg and Kleppner[61], gives little or no atoms under the above conditions.

d) The most suitable poisoning combination was H_3PO_4 (50% by volume) in the discharge tube and $Na_2HPO_4.H_2O$ (5% by weight) in the reaction vessel. The latter was used because it was found that H_3PO_4 tends to distill away and decompose under prolonged heating even at moderate temperatures ($\sim$ 150° C).

e) The aluminum surface of the probe must be out-gassed (by heating to $\sim$ 300° C) for maximum scavenging efficiency).

f) The Type II system would seem to be advantageous due to the fact that the atoms are pre-conditioned to the appropriate temperature before they enter the reaction zone. However, a great deal of difficulty was encountered in actual practice due to the fact that a large amount of heat liberated by the discharge zone caused the coolant to heat quickly and produced large temperature variations during a single experiment. Impurities present in the system tend to accumulate at the bottom bend of the reaction vessel between it and the dissociator giving rise to an extremely variable atom concentration. Consequently, the Type I system was chosen for the H + D_2 studies. Its disadvantage, however, is the possibility of diffusion of atoms and reactants above the desired temperature

zone in the reacion vessel. There is a certain possibility that the reaction could proceed beyond the reaction vessel region downstream towards the trapping system, although the author's experience with H-atoms leads him to believe that this is quite unlikely, as they tend to disappear rapidly around a "bend" or in a narrow, high pressure region of a fast-flow system. This cannot be said, however, for other longer-lived atoms and free radicals (eg. N, O, CH_2, or even CH_2CHO[4]).

G. The Reaction of Hydrogen Atoms with Deuterium

Introduction

The gas phase reaction of hydrogen atoms with p-hydrogen and its deuterium isotopes has been investigated both experimentally and theoretically by numerous workers (see Ref. 62 for a recent survey), and has served as a starting point for the modern theories of chemical kinetics[63]. However, one of the more thorough studies[64] of this topic reviews the experimental data and shows that it is far from being complete and conclusive. The above author suggests that future studies should take the following points into consideration:

1) The reactions should be studied over a wider temperature

range.

2) A technique should be employed which produces atoms by an external means similar to that of Geib and Harteck[15].

3) Careful attention should be paid to heterogeneous effects.

4) A better method should be developed for analyzing the gas mixtures.

5) Low temperature studies should be particularly stressed.

In an attempt to remedy some of the above weaknesses of previous workers, Schulz and LeRoy[19] investigated the H + D_2 reaction in 1964. An ordinary Arrhenius Law treatment of the data gave a straight line for the log k vs. 1/T plot in the 368-468° temperature range and gave an A factor of 4.37×10^{12} along with a classical activation energy, E_c, of 7.30 kcal/mole.

These early studies by the above authors could also be criticized as follows:

1) The temperature range is still quite narrow. The authors claim that not enough product was formed for analysis by their technique to extend the study to lower temperatures.

2) Quantum mechanical "tunnelling" was not taken into account.

3) The gases were analyzed after only a portion of their

total volume was collected in the exhaust of the main flow system pump.

4) The probe was kept inside the reaction zone and this could have served as a surface for a heterogeneous reaction of the type

$$H + D_2 + Pt\ (hot) \quad = \quad HD + D + Pt\ (hot) \qquad (57)$$

In subsequent publications on $H + p\text{-}H_2$ [20] and $D + H_2$ [21] the authors have corrected some of the above defects but nothing has been said about the original $H + D_2$ study.

Since a low temperature reaction vessel, a probe for determining atom concentration, and a method for the collection of H_2, HD, and D_2 in a fast-flow system has been developed previously in this research it was thought that the study of the $H + D_2$ reaction may prove to be a good test and application of some of the above techniques. It also seemed logical to the author that a study of this nature should be undertaken before any experiments with $H + CD_4$, and $H + CD_2CO$ (where HD and D_2 are likely products) be attempted.

Apparatus and materials

A diagram of the apparatus is shown in Fig. XXVI. It is a normal fast-flow low-pressure system and features a

FIGURE XXVI

Diagram of apparatus used for H + D_2 studies

B_1 : 1 liter bulb

B_2 : 150 ml storage bulb

B_3 : 2 liter storage bulb for H_2-He mixture

B_4 : 150 ml ballast

M_n : mercury manometers

S_n : stopcocks

Mc : McLeod gauge

T_n : Traps or Toepler pumps

t_n : tapers

i : to inlet system for reactant

j : ball joints

b_n : gas burettes

L : to low vacuum

V_1 : Edwards High Vacuum metal valve (Type OSIC)

V_2 : Ideal Aerosmith metal valve #54-2-11

V_3 : Matheson Capillary valve #150

P_n : pumps

G : to sampling system for gas chromatography

C : quartz CuO furnace

H : He or H_2 inlet

D : dissociator

R : reaction vessel

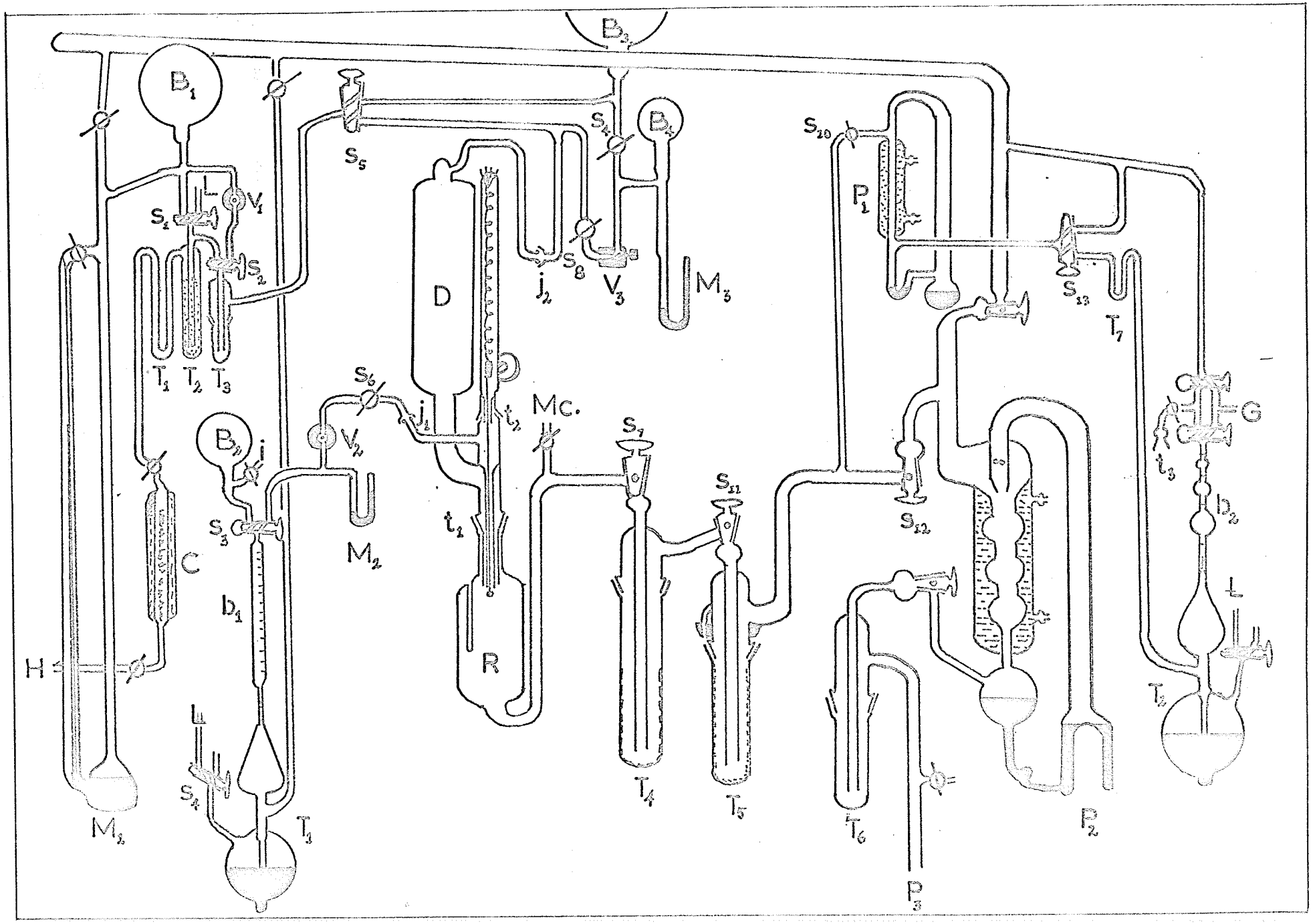
B1
B2
B3
S1
S2
S3
S4
S5
S6
S7
S8
S9
S10
S11
S12
S13
V1
V2
V3
T1
T2
T3
T4
T5
T6
T7
D
R
Mc.
C
M1
M2
M3
P1
P2
P3
H
G
b1
b2
j1
j2
t1
t2
t3

capillary manometer, M_1, for regulating the helium flow, a Toepler pump-gas burette inlet system, T_1, the Type I dissociator-reactor assembly, D - which could be disassembled easily for poisoning, an inlet system for introducing trace amounts of H_2 into the helium stream, and SiO_2 gel and "saran" charcoal traps. A large Hg diffusion pump has been included and served for rapid out-gassing of the reaction vessel and traps prior to a reaction but had very little effect on the helium flow. The small Hg diffusion pump served to carry the products over to the Toepler pump where they were collected in the gas burette, b_2.

After determining the total volume of H_2, HD, and D_2, the isotopic composition was quantitatively analyzed by gas chromatography. A diagram of this arrangement is given in Fig. XXVIII. It features a gas sampling system*, a Gow-Mac micro-cell detector (Model 470) with thermistors, a 1/8 in. activated alumina column prepared according to the method of Yasumori and Ohno[65]. An attempt to duplicate the results of the above authors gave broad unsymmetrical peaks at -196° C (seven foot column with an He flow of approximately 17 cc/min). This undesirable situation was improved slightly by adding liquid

---

*I am indebted to Dr. A. Cohen (Postdoctoral Fellow, U. of M. 1965-66) for the idea of using a brass sampling valve in the above arrangement, and to Professor H. D. Gesser who made the original suggestion.

O_2 to the coolant giving a column temperature of about -190° C. Sharper peaks were obtained but the separation was now reduced (see Fig. XXIX). Consequently, hydrogen was used as a carrier gas. This not only eliminated the large undesirable H_2 peak and gave more symmetrical HD and D_2 peaks for area determination but also gave a better separation and enabled one to operate at the more constant temperature of -196° C (see Fig. XXX). A three foot length of 1/8 in copper tubing used as a pre-column eliminated some of the prolonged baseline drift due to the unequal cooling of the thermistors when the temperature of the column was suddenly lowered to -196° C. Under the above conditions and with a hydrogen flow of approximately 15 cc/min and a column length of 10 ft the HD and D_2 retention times were approximately 5.5 and 6.5 mins. Using such an arrangement it is estimated that 0.1% HD in D_2 could easily be detected although an error of about 5% was observed in the quantitative determination as a result of an unsteady baseline at maximum sensitivity (probably caused by a faulty bridge circuit) and also due to the fact that peak areas were found to vary from day to day for the same amount of sample injected (probably due to changes in the characteristics of the column caused by adsorption of water vapor). Nevertheless,

it is estimated that the accuracy was sufficient for the present work since it is difficult to claim better than 5% overall reproducibility in the determination of a rate constant employing a fast-flow Wood-Bonhoeffer apparatus.

The peak areas were determined by weighing or by means of a planimeter, and the analysis was conducted in the following manner. Known amounts of D_2* were injected and the area response per sample size was noted. Then a known mixture of H_2 and D_2 was placed into the gas burette and a sample of it was injected. This gave a D_2 peak corresponding to the amount of D_2 in the sample. Next, the mixture in the gas burette was sparked by means of a Tesla coil and known amounts of it were again injected into the chromatograph. The HD and D_2 areas were now measured and the absolute amount of HD produced (by the reaction $H_2 + D_2 = 2\ HD$) was estimated by taking twice the absolute amount of D_2 decrease from that of the pure H_2 - D_2 system. See Table below for a typical series of such experiments and Fig. XXVII for a plot of the response curves.

---

*The deuterium for the above experiments was kindly supplied by Dr. D. Safrany, A.E.C.L., Pinawa, Manitoba and found to contain 0.51 ± 0.03% HD as estimated by gas chromatography, along with 0.25% of M/e = 32 (oxygen) contaminant, and 0.20% M/e = 28 (nitrogen) contaminant as analyzed by mass spectrometry.

TABLE XVI

Data for a typical set of response curves for deuterium and hydrogen deuteride

a) Deuterium

Volume of D_2 injected (cc-cm) (temp: 33° C)	Weight of D_2 peak (grams)
2.81	0.0188 x 5 = 0.094
6.40	0.0100 x 25 = 0.250
17.5	0.0275 x 25 = 0.688

b) Hydrogen deuteride (produced by sparking a D_2-H_2 mixture, which had 37% D_2 by volume)

Orig. D_2 (cc-cm) if no reaction occurred	Weight of D_2 peak (g)	Vol. of D_2 (from (a) plot) (cc-cm)	Diff. in D_2 (cc-cm) (Col. 1 - Col. 3)	Vol. HD (cc-cm)	Weight of HD peak
2.11	0.0198	0.55	1.56	3.12	0.0640
2.18	0.0310	0.85	1.33	2.66	0.0540
4.01	0.0854	2.23	1.78	3.56	0.0755
7.80	0.1675	4.30	3.50	7.00	0.1648

FIGURE XXVII

Diagram of deuterium and hydrogen deuteride response curves for gas chromatography.

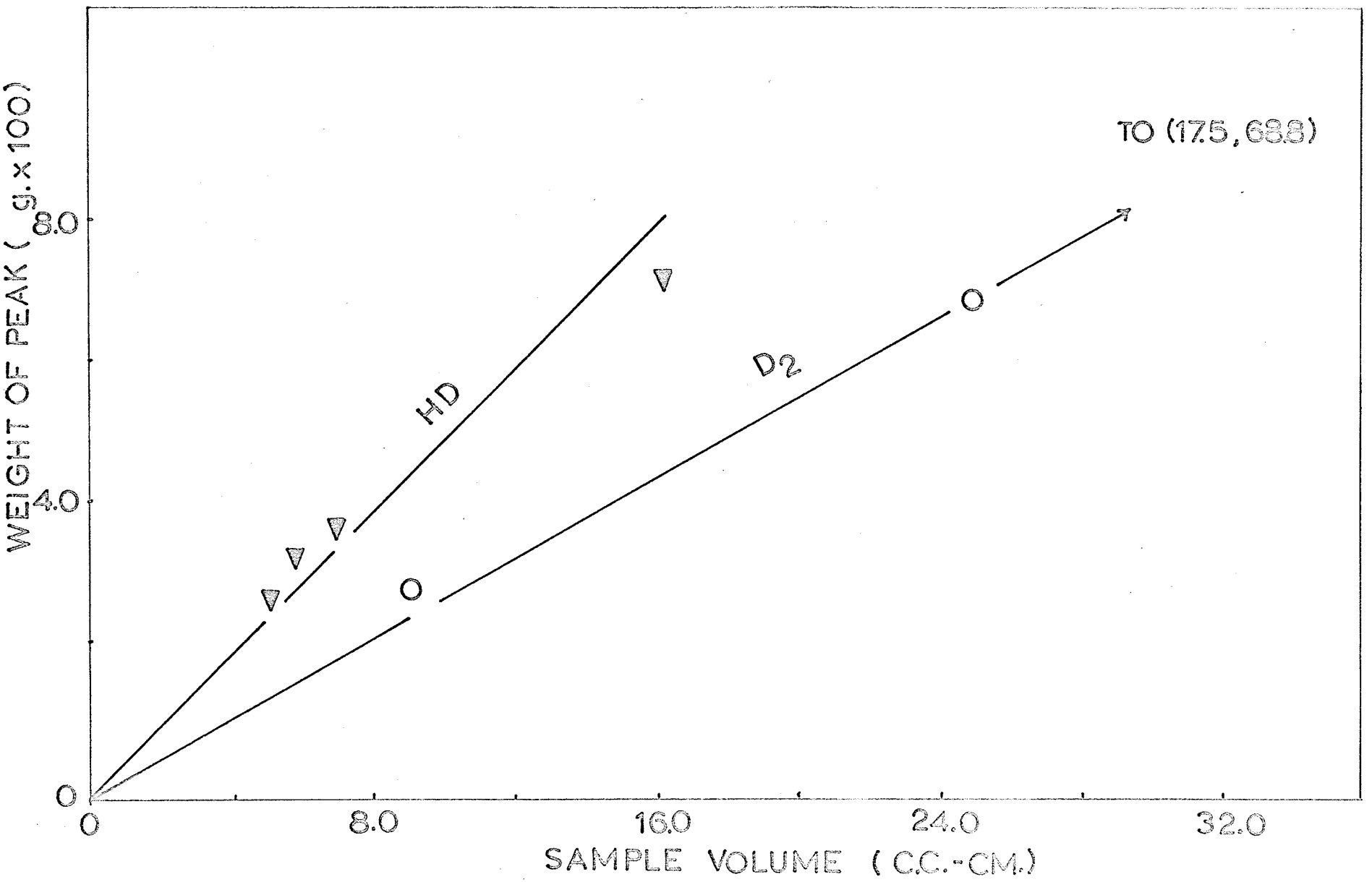
WEIGHT OF PEAK (g. x 100)
8.0
4.0
0
0
8.0
16.0
24.0
32.0
SAMPLE VOLUME (C.C.-CM.)
HD
D2
TO (17.5, 68.8)

FIGURE XXVIII

Diagram of the gas chromatographic system for the analysis of H_2, HD, and D_2.

P : Toepler pump

S_1,S_2: Two way stopcocks

S_3: Springham 2 mm Capillary Stopcock

V_1: 4-way valve (#BR 4T, Brass body, teflon plug)
Obtained from: Conant Bros. Co.
427 Riverside Ave.,
Medford, Mass.

Pr: Pre-column (3 ft. 1/8 in. copper tubing)

C : Activated alumina (60-100 mesh) column treated with $MnCl_2$

G : Gow-Mac Micro-cell (type 9689 - TH; Model 470)

B : to soap bubble meter or exhaust system

V_2: Ideal-Aerosmith metal valve #54-2-12

T : Molecular sieve trap (Linde 5X)

V_3: Reducing valve

H_2 or He: Storage cylinder

a : 0-20 milliamps

b : 12 volt battery

t_1 and t_2: 8K matched resistors

0 : Bristol's Dynamaster recorder (1 mv)

r_1: 2000 ohm variable resistor

FIGURE XXVIII (CONT'D)

r_2: 100 ohm pot.

r_3, r_4: 500 ohm matched resistors

r_5, r_6: 50 ohm matched resistors

r_7: 5000 ohm pot.

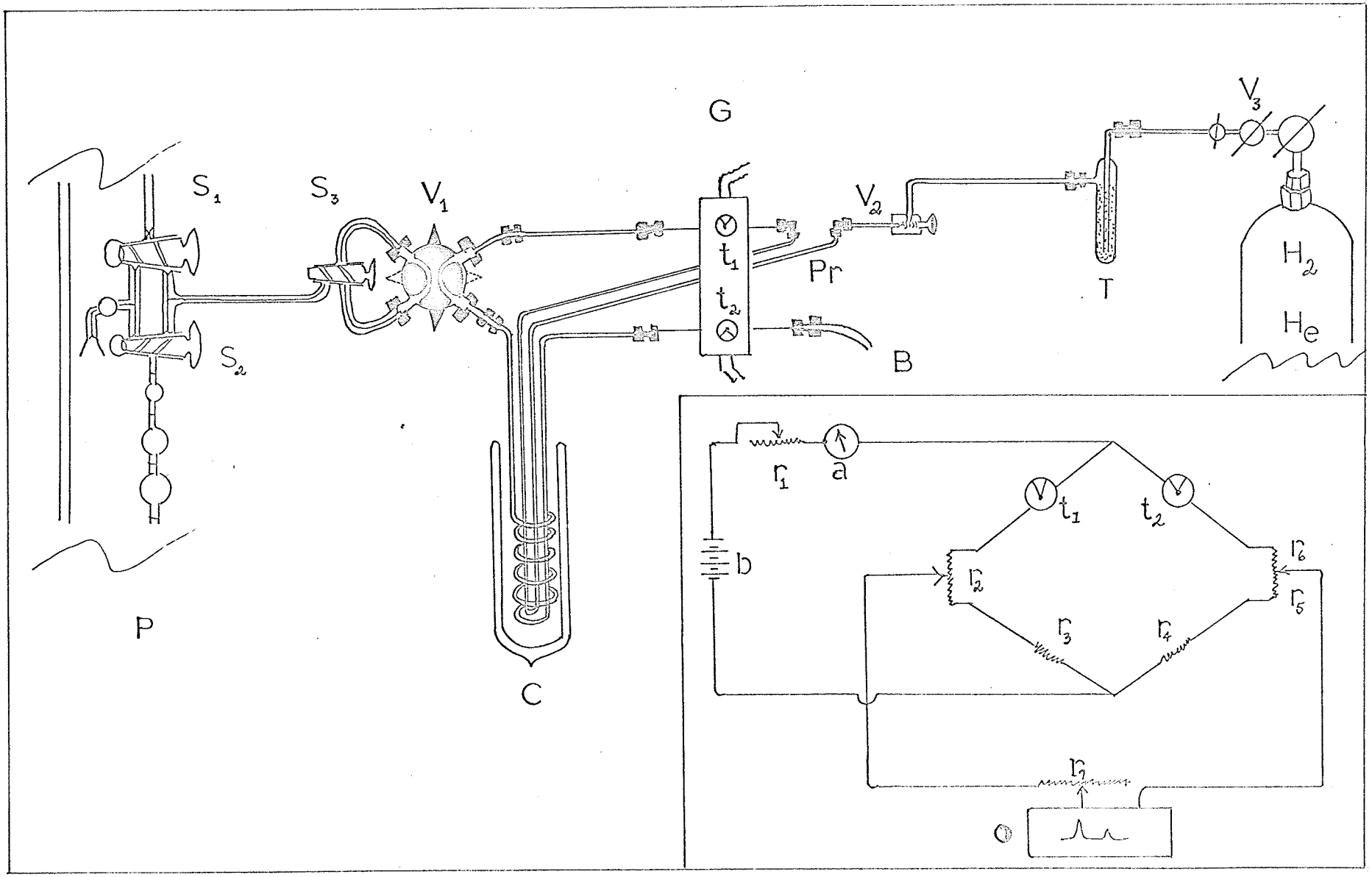
G
S1
S3
V1
V2
V3
S2
t1
t2
Pr
B
T
H2
He
P
C
a
r1
b
r2
r3
r4
r5
r6
r7
O

FIGURE XXIX

Chromatogram of H_2, HD, and D_2 using helium carrier gas under the following conditions:

Gow-Mac thermistor detector

Seven ft., 1/8 in., activated alumina column treated with $MnCl_2$

Helium flow: 17 cc/min

Column temp: -190° C

Sample size: $\frac{25}{76}$ x 1.90 = 0.63 cc

Recorder: 10 mv "Graphicorder" (Dynatronic Instruments Corp., Labline, Chicago)

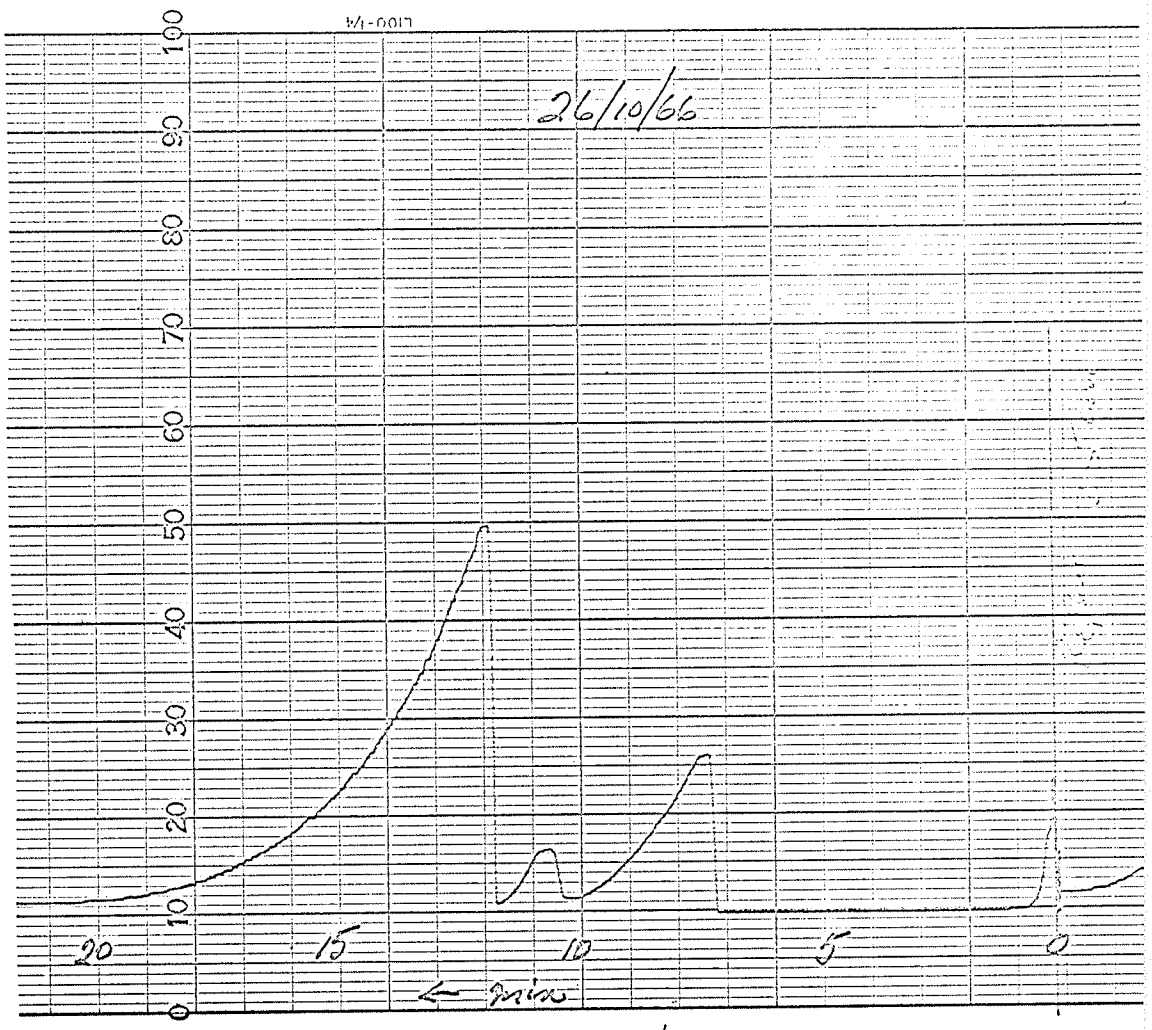

DYNATRONIC INSTRUMENTS CORP. / ELECTRONICS DIV. OF LABLINE, INC.

FIGURE XXX

Chromatogram of HD and D_2 using hydrogen gas under the following conditions:

Gow-Mac micro-cell with thermistor detector

Ten ft., 1/8 in., activated alumina column treated with $MnCl_2$

Hydrogen flow: 15 cc/min

Column temp: -196° C

Sample size: 0.71 cc

Recorder: 1 mv (Bristol's Dynamaster)

26/1/67

Exp C1 : $\frac{28.5}{76} \times 1.90 = 0.71$ cc.

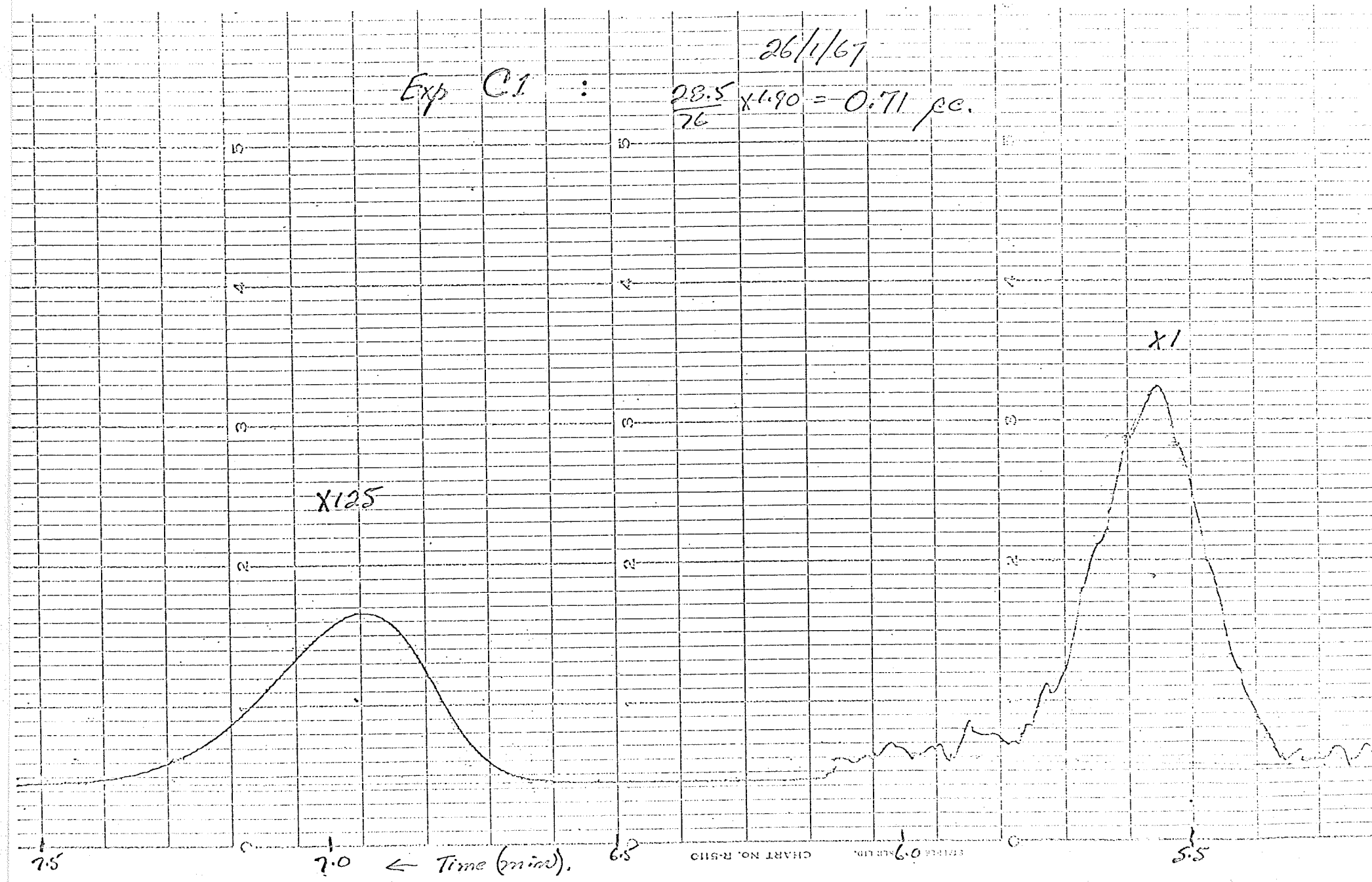

The above series of experiments was conducted at least three times on separate occasions and the ratio of response for D_2 vs. HD per equivalent sample size was found to be 1.75, 1.92, and 2.17. This gives an average of 1.95 ± 0.13 or 2.0 ± 0.1 to two significant figures.

Consequently, the percentage of HD in a HD-D_2 mixture could now be easily determined simply by using the following formula:

$$\frac{2\,(HD)_{\text{peak area}}}{2\,(HD)_{\text{peak area}} + (D_2)_{\text{peak area}}} \times 100 \qquad (58)$$

after injecting an arbitrary amount of the mixture into the G.C. The absolute amount of HD produced in a typical reaction could then be calculated by taking the above percentage, subtracting from it the total "blank" (due to original impurity and exchange on the charcoal surface during collection), and multiplying the result by the total amount of D_2 put into the reaction vessel (since the amount of D_2 reacted in the forthcoming experiments was always less than 5% of the total amount of it put into the reaction vessel). The above method was used since it utilizes relative areas of HD and D_2 and consequently would be expected to be less dependent upon variations of the

absolute areas caused by changes of the condition of the column from day to day.

Procedure for a typical experiment

The apparatus was evacuated to less than one micron Hg for at least a day. Tank hydrogen (Linde 99.5% pure) was then introduced through the CuO furnace (quartz, maintained at approximately 500° C), the three traps T_1, T_2, and T_3 (all at -196° C) and stored in bulb B_3 at a pressure of 10.0 cm Hg (manometer M_3). Next, helium (Linde 99.995% pure) was purified in the same manner and introduced into the same bulb until the total pressure was 80.0 cm as read on manometer M_1. During an experiment this H_2-He mixture was bled into the reaction vessel through valve V_3 (Matheson metal capillary valve #150) at a pressure of 120 microns, (i.e. p_{H_2} = 15 μ), and a flow rate of approximately 20 micromoles/min. Stopcock S_5 was opened to the dissociator side during a run and He was introduced into the flow system at a pressure of about 1.90 mm Hg and a flow rate of 5430 micromoles/min by the use of metal valve V_1 (Edwards high-vacuum type OSIC). The pumping for this fast-flow system was accomplished by a Welch Duo-Seal vacuum pump (serial no. H-1402B) which gave an ultimate vacuum of 10^{-5} cm of Hg and a pumping speed of 140 liters per minute.

The reaction vessel was then brought to the desired temperature (by a furnace or coolant) and traps T_4 and T_5 were outgassed at about 200° C. Deuterium (unpurified) was fed from bulb B_2 into the gas burette b_1 through stopcock S_3 and its volume determined by P.V.T. measurements before and after an experiment.

The probe was lowered to the "normal" position into the reaction vessel and was outgassed for about one-half hour at approximately 300° C by passing about 0.5 amp of current through its internal resistance wire. After this treatment it was brought back to the temperature of the reaction vessel and stopcocks S_5 and S_8 were opened to begin the helium and hydrogen flows. The dissociator was switched on and the current through the primary circuit of the transformer was maintained constant at 2 amps. by a variac. This gave a deflection on the probe galvanometer due to recombination of atoms on the aluminum surface. The extent of the deflection was noted and the dissociator switched off. An exactly equivalent deflection was then produced by adjusting the current through the heating wire within the probe. The wattage dissipated was recorded, and assuming complete scavenging of the atoms, the atom concentration was now estimated according

to the procedure shown in Appendix III.

The He and H_2-He flows were stopped and the probe was raised out of the reaction vessel (about 10 cm up). Trap T_4 was cooled to -196° C while trap T_5 was taken below -196° C by pumping on the liquid N_2 coolant. The He flow was begun again and the discharge was switched on. Stopcocks S_8 and S_6 were opened as simultaneously as possible and the reaction was allowed to proceed for periods of 2.0 to 7.0 mins (depending on the rate of the D_2 flow). During this period the H_2-He mixture flow was maintained constant using scratched stopcock S_9 and ballast bulb B_4. The D_2 was also maintained at a constant inlet pressure by slowly raising the Hg level in the gas burette (using scratched stopcock S_4). The pressure during the reaction period was checked by means of a McLeod gauge.

After the reaction period was over, the dissociator was switched off, the D_2, He, and H_2-He mixture flows were terminated, and the system evacuated to less than one micron Hg. Stopcocks S_{11} and S_{12} were closed and S_{10} along with S_{13} were opened to the Toepler pump T_2. The liquid N_2 coolant from T_5 was removed and a hot ($\sim$ 200° C) furnace was slipped over the trap. The product along with the excess H_2 and D_2 were pumped continuously over into the gas burette, where the total volume was noted by

P.V.T. measurements. After this the mixture was "stirred" in the burette by raising and lowering the level of the Hg in the Toepler pump a few times, and a top and bottom portion of it was injected into the gas chromatograph by means of the sampling system.

For analysis, the H_2 carrier gas was purified by means of a molecular seive trap, T, and its pressure adjusted at 10 p.s.i. by means of valve V_3. The column was immersed into a -196° C bath and the current through the thermistors controlled at 5 milliamps. A Bristol's recorder (Model #M 1P 560-51-T24-T38-T71-T13-T82-T74, converted to 1 mv) served as the output device at a chart speed of 4 1/2 in/min. To save chart paper it was turned on about 4.5 min after the injection of the sample. A representative chromatogram from experiment C1 is shown in Fig. XXX.

A series of 5 to 6 experiments as described above was conducted at five different temperatures, varying only the D_2 flow rate. During such a series the G.C. was left on to obtain maximum reproducibility of conditions. Also, the atom concentration was determined only at the beginning and at the end of each series. As a rule this was found to be constant over such a short period.

Results

The results for each series are given in Tables XVII to XXI. Listed in each table are the rate constants as determined by the use of a Olivetti Underwood Programma 101 calculator (see Appendix VI). Two different methods were used to calculate the rate constants, namely streamlined and turbulent flow of the gases through the reaction vessel (after Jamieson[66]), and relatively good agreement was obtained between the two methods. The "contact time" or the time the reactants spent in the reaction vessel was estimated as follows:

$$t = \frac{n}{r} \text{ sec.} \qquad (59)$$

where n is the total number of moles of gas in the vessel during a reaction. This was estimated from the Ideal Gas Law:

$$n = \frac{PV}{RT} \qquad (60)$$

where each term has the usual connotation (e.g. T = absolute temp), and V is the volume of the vessel assuming that the "reaction volume" is equivalent to the size of the reaction vessel.

The denominator r in formula (59) is the total flow rate of the gases in moles per sec. and was taken to be equivalent

to the helium flow rate since in the experiments the combined H_2 and D_2 flows were never greater than 2% of the helium flow-rate.

A typical calculation of the contact time for the A series of experiments is given in Appendix IV.

The deuterium consumption during a reaction was determined as follows. The main reactions occurring are expected to be:

$$H + H_2 = H_2 + H \quad (61)$$

$$H + D_2 = HD + D \quad (62)$$

$$H + HD = H_2 + D \quad (63)$$

$$H + DH = HD + H \quad (64)$$

$$D + H_2 = DH + H \quad (65)$$

$$D + HD = DH + D \quad (66)$$

$$D + DH = D_2 + H \quad (67)$$

$$D + D_2 = D_2 + D \quad (68)$$

along with wall reactions such as:

$$H + H + W = H_2 + W \quad (69)$$

$$H + D + W = HD + W \quad (70)$$

$$D + D + W = D_2 + W \quad (71)$$

Reactions (66) and (68) would not be noticeable in our case. The primary source of HD would be (62). This would be immediately followed by (65) in which another HD molecule is formed and an H-atom is regenerated. Consequently the D-atom concentration would never "build up" to a large value. Hydrogen deuteride formation, however, would proceed continuously along the reaction vessel, and the H-atom concentration would tend to level off at some value slightly below the original concentration at the entrance of the reaction vessel. Due to the low steady-state D-atom concentration, and also due to the fact that the HD concentration is never more than 10% of the amount of D_2 put into the reaction vessel, reactions (66) and (67) would be of minor importance. Since reaction (64) is not noticeable, the only other significant reaction may be (63). Let us take Exp. C5 as an example. Here the D_2 flow rate is 47.0 micromoles /min., the HD produced is 0.424 (0.212 x 2) micromoles/min., and

TABLE XVIIa

Hydrogen deuteride formation from H + D_2 at -78° C (Room temperature: 32° C)

Exp.	D_2 in (cc-cm)	HD area (arb. uni.)	D_2 area (arb. uni.)	% HD from formu. (58)		HD abs. (cc-cm)		Reaction time (min)	HD μmoles/min / 2
N.R.		371	136000	0.55					
Blank	180	403 338	99500 98200	0.80 0.68	0.74	Note: Exchange = 0.19%			
A1	36	221 350	13200 20100	3.24 3.37		0.90 0.95	0.93	7.0	0.035
A2	64	294 449	28200 47100	2.04 1.87		0.83 0.72	0.78	5.0	0.041
A3	98	453 611	43900 56100	2.02 2.13		1.25 1.36	1.30	5.0	0.063
A4	150	785 885	75700 89400	2.03 1.94		1.94 1.80	1.87	4.25	0.11-
A5	183	1350 1300	132000 118000	2.00 2.16		2.31 2.59	2.45	2.0	0.31

TABLE XVIIb

Rate constant for H + D_2 at -78° C (contact time = 0.96 sec.)

Exp.	D_2 in (moles x 10^6/min)	D_2 consumed (moles x 10^6/min)	Atoms (moles x 10^6/min)	k_t x 10^{-8} (cc-mole^{-1}-sec^{-1})	k_s x 10^{-8} (cc-mole^{-1}-sec^{-1})
A1	2.73	0.035	2.10	2.25	2.22
A2	6.68	0.041	2.10	1.07	1.06
A3	10.40	0.068	2.10	1.15	1.14
A4	18.7	0.114	2.10	1.10	1.07
A5	48.5	0.319	2.10	1.32	1.22
			Ave.	1.38 ± 0.35	1.37 ± 0.35

TABLE XVIIIa

Hydrogen deuteride formation from H + D_2 at 0° C (Room temperature: 31° C)

Exp.	D_2 in (cc-cm)	HD area (arb. uni.)	D_2 area (arb. uni.)	% HD from formu. (58)	HD abs. (cc-cm)	Reaction time (min.)	HD μmoles/min 2
N.R.		603	248000	0.48			
Blank	209	440 587	121600 190500	0.72 0.61	0.66	Note: Exchange = 0.18%	
B1	61	322 248	59700 56300	1.07 0.87	0.25 0.13	0.19	4.0	0.0124
B2	47	257 465	25400 45500	1.98 2.00	0.62 0.63	0.62	5.0	0.032
B3	151	584 647	89250 104600	1.29 1.22	0.95 0.85	0.90	5.0	0.047
B4	126	478 596	72000 84000	1.31 1.40	0.82 0.93	0.87	5.0	0.045
B5	192	813	63200	2.51	3.55		3.0	0.31
B6	249	662 673	120000 158000	1.09 0.85	1.07 0.47	0.77	2.0	0.1[illegible]

TABLE XVIIIb

Rate constant for H + D_2 at 0.00° C (contact time = 0.67 sec.)

Exp.	D_2 in (moles x 10^6/min)	D_2 consumed (moles x 10^6/min)	Atoms (moles x 10^6/min)	k_t x 10^{-8} (cc-mole^{-1}-sec^{-1})	k_s x 10^{-8} (cc-mole^{-1}-sec^{-1})
B1	8.10	0.0124	1.62	0.70	0.70
B2	5.00	0.032	1.62	2.99	2.94
B3	16.0	0.047	1.62	1.38	1.35
B4	13.4	0.045	1.62	1.57	1.54
B5	34.0	0.31	1.62	5.16	4.61
B6	66.0	0.10	1.62	0.72	0.70
				Ave. 2.50 ± 1.46	1.97 ± 1.30

TABLE XIXa

Hydrogen deuteride formation from H + D_2 at 50° C (Room temperature: 26° C)

Exp.	D_2 in (cc-cm)	HD area (arb. uni.)	D_2 area (arb. uni.)	% HD from formu. (58)	HD abs. (cc-cm)		Reaction time (min.)	HD μmoles/min. / 2
Blank:	same as for B series							
C1	30	300	25150	2.33	0.50		5.0	0.026
C2	57	280	27500	2.00	0.76	0.75	5.0	0.040
		498	50500	1.95	0.74			
C3	123	667	74750	1.75	1.34	1.27	5.0	0.066
		768	92300	1.64	1.21			
C4	187	742	108000	1.36	1.30	1.38	3.0	0.120
		925	126000	1.44	1.47			
C5	222	860	115600	1.47	1.79	2.02	2.5	0.212
		935	109000	1.68	2.26			

TABLE XIXb

Rate constant for H + D_2 at 50° C (contact time = 0.565 sec.)

Exp.	D_2 in (moles x 10^6/min.)	D_2 consumed (moles x 10^6/min.)	Atoms (moles x 10^6/min.)	k_t x 10^{-8} (cc-mole^{-1}-sec^{-1})	k_s x 10^{-8}
C1	3.18	0.026	2.03	4.25	4.19
C2	6.03	0.040	2.03	3.46	3.42
C3	13.1	0.066	2.03	2.66	2.61
C4	33.0	0.120	2.03	1.98	1.91
C5	47.0	0.212	2.03	2.57	2.43
			Ave.	2.98 ± 0.70	2.91 ± 0.71

TABLE XXa

Hydrogen deuteride formation from H + D_2 at 100° C (Room temperature: 30° C)

Exp.	D_2 in (cc-cm)	HD area (arb. uni.)	D_2 area (arb. uni.)	% HD from formu. (58)	HD abs. (cc-cm.)		Reaction time (min.)	HD μmoles/min. / 2
Blank	129	540	165400	0.65				
D1	26	412	11900	6.48	1.52	1.33	5.0	0.069
		548	20700	5.03	1.14			
D2	41	434	17200	4.80	1.70	1.75	5.0	0.091
		548	20700	5.03	1.80			
D3	73	804	26700	5.68	3.67	3.77	5.0	0.196
		995	31500	5.94	3.86			
D4	109	1335	56800	4.49	4.19	4.14	3.0	0.357
		1830	79600	4.40	4.09			
D5	148	1480	76900	3.70	4.51	4.74	3.0	0.410
		1885	90100	4.01	4.97			
D6	181	2230	96600	4.41	6.80		3.0	0.590

TABLE XXb

Rate constant for H + D_2 at 100° C (contact time = 0.494 sec.)

Exp.	D_2 in (moles x 10^6/min.)	D_2 consumed (moles x 10^6/min.)	Atoms (moles x 10^6/min.)	$k_t \times 10^{-8}$ ($cc\text{-}mole^{-1}\text{-}sec^{-1}$)	$k_s \times 10^{-8}$ ($cc\text{-}mole^{-1}\text{-}sec^{-1}$)
D1	2.76	0.069	2.33	15.3	14.8
D2	4.35	0.091	2.33	12.9	12.5
D3	7.73	0.196	2.33	16.5	15.7
D4	19.3	0.357	2.33	12.9	11.8
D5	26.1	0.410	2.33	11.2	10.1
D6	32.0	0.590	2.33	14.6	12.5
				Ave. 13.9 ± 1.6	12.9 ± 1.6

TABLE XXIa

Hydrogen deuteride formation from H + D_2 at 170° C (Room temperature: 30° C)

Exp.	D_2 in (cc-cm)	HD area (arb. uni.)	D_2 area (arb. uni.)	% HD from formu. (58)	HD abs. (cc-cm)		Reaction time (min)	HD μmoles/min / 2
Blank:	same as for D series							
E1	35	628	12600	9.06	2.94	3.09	5.0	0.160
		802	14600	9.90	3.23			
E2	65	1335	29000	8.42	5.05	5.10	5.0	0.266
		1675	35600	8.59	5.16			
E3	104	1840	32500	10.20	9.93	9.80	5.0	0.510
		2205	39900	9.95	9.67			
E4	131	2640	53500	8.98	10.9	10.7	4.0	0.695
		3070	64500	8.69	10.5			
E5	175	2930	66400	8.11	13.0	13.2	3.0	1.14
		3565	79400	8.24	13.3			
E6	178	2940	60700	8.84	14.6		2.5	1.52

TABLE XXIb

Rate constant for H + D_2 at 170° C (contact time = 0.41 sec.)

Exp.	D_2 in (moles x 10^6/min.)	D_2 consumed (moles x 10^6/min.)	Atoms (moles x 10^6/min.)	k_t x 10^{-8} (cc-mole^{-1}-sec^{-1})	k_s x 10^{-8} (cc-mole^{-1}-sec^{-1})
E1	3.71	0.160	3.43	27.5	26.2
E2	6.90	0.266	3.43	25.2	23.8
E3	11.0	0.510	3.43	33.2	29.9
E4	17.4	0.695	3.43	30.3	26.5
E5	30.9	1.14	3.43	33.3	26.6
E6	37.7	1.52	3.43	43.8	31.6
				Ave. 32.2 ± 4.6	27.4 ± 2.2

the H-atom concentration is 2.03 micromoles/min. From theoretical estimates[68] it is noted that the rate constants for reactions (62) and (63) are approximately equal. Consequently, the ratio of the rates of these two reactions would be $[H][D_2] : [H][HD]$ or $[D_2] : [HD]$ or 47:0.424 or about 100:1. In other words reaction (63) contributes only about 1% to the overall scheme and could thus be neglected. Beyond the poisoned zone of the reaction vessel, reactions (69), (70) and (71) would become significant, of which (70) is the only other major HD forming step. However, it must always be preceded by (62). Consequently, to a good approximation the D_2 consumed by reaction (62) is always the total HD formed divided by two. It is this value that is used in the calculation of the second order rate constant for reaction (62).

Discussion

Table XXII gives a summary of the results. These are plotted in Fig. XXXI and the deviation from the average value indicated at each temperature. As could be seen from this figure, with the exception of the B series of experiments (where it is quite probable that a great deal of "human" error was involved in at least two of the trials), the deviation is within 0.3 of a log k unit or within a factor of two in the rate

TABLE XXII

Summary of the rate constants obtained for $H + D_2$

t(°C)	T(°K)	1/T x 10^3	k_t ($cc\text{-}mole^{-1}\ sec^{-1}$)	k_s	log k_t	log k_s	log $k_{ave.}$
-78	195	5.13	$1.38 \pm 0.35 \times 10^8$	$1.37 \pm 0.35 \times 10^8$	8.14	8.14	8.14
0.00	273	3.67	$2.50 \pm 1.46 \times 10^8$	$1.97 \pm 1.30 \times 10^8$	8.40	8.30	8.35
50	323	3.10	$2.98 \pm 0.70 \times 10^8$	$2.91 \pm 0.71 \times 10^8$	8.47	8.46	8.47
100	373	2.69	$1.39 \pm 0.16 \times 10^9$	$1.29 \pm 0.16 \times 10^9$	9.14	9.11	9.13
170	443	2.26	$3.22 \pm 0.46 \times 10^9$	$2.74 \pm 0.22 \times 10^9$	9.51	9.44	9.48

FIGURE XXXI

Arrhenius plot for the H + D_2 reaction indicating the spread in the values at each temperature.

2.0
3.0
4.0
5.0
1/T x 10^3
8.0
8.4
8.8
9.2
9.6
LOG k

FIGURE XXXII

Arrhenius law plot for H + D_2; present results compared with those of Schulz and LeRoy.

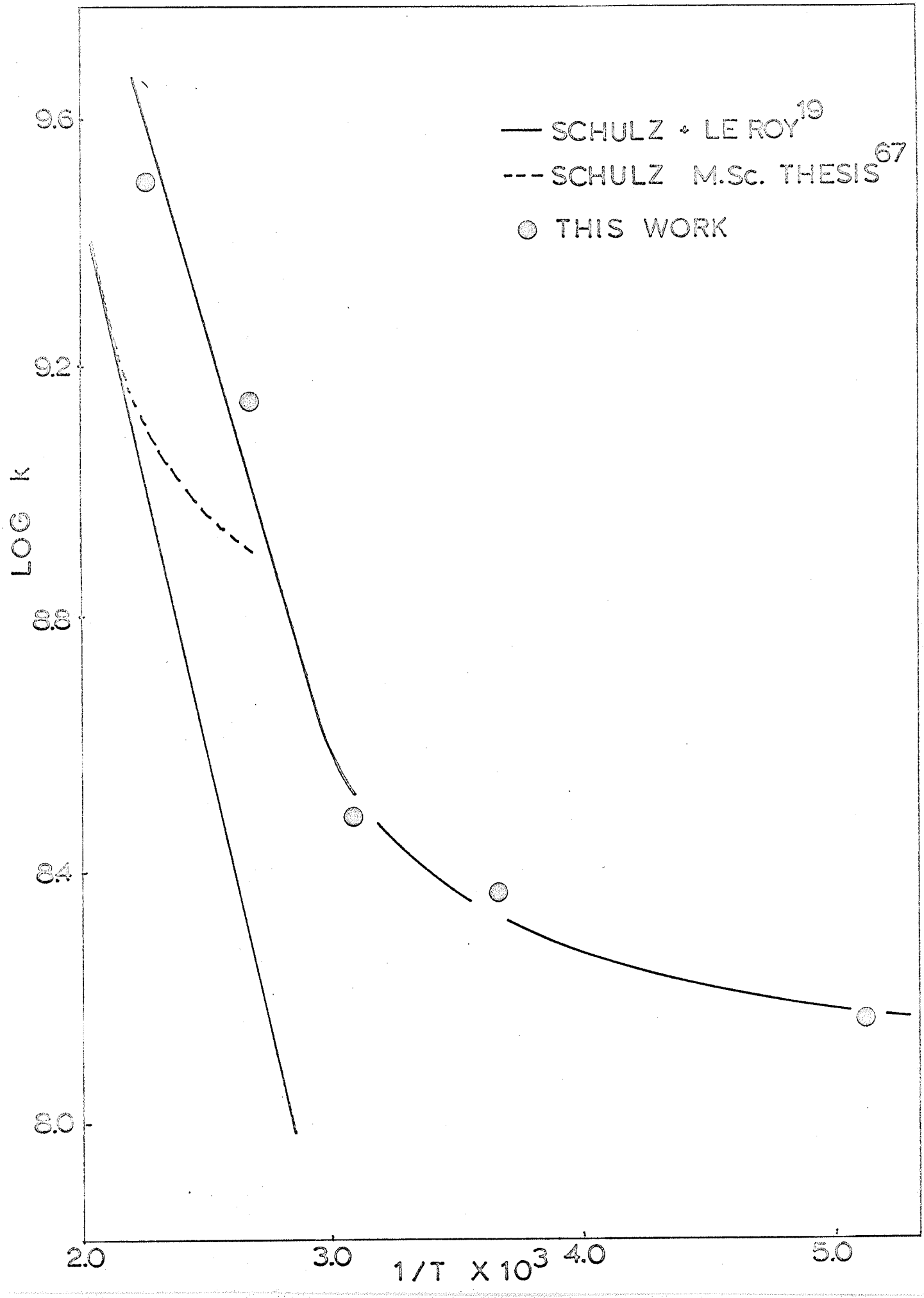
SCHULZ + LE ROY[19]
SCHULZ M.Sc. THESIS[67]
THIS WORK
LOG k
9.6
9.2
8.8
8.4
8.0
2.0
3.0
4.0
5.0
1/T X 10^3

constant k. This is not a very large improvement over the data of Schulz[67]. It is interesting to note, however, that his data also indicate a "levelling off" in the rate constant below 150° C but he did not interpret his results in terms of quantum mechanical tunnelling during this early work.

Figure XXXII is a comparison of the present results with those of Schulz and LeRoy[19]. The main feature is the upward displacement of our values with respect to their data, and indicates that the rate constant for the present work is about a factor of 10 higher than that reported by the above authors. From the present results the rate constant at 400° K would be about 1.6×10^9 cc-mole^{-1}-sec^{-1} and is in good agreement with a recent theoretical estimate by J. C. Polanyi[68] who reports a value of 1.68×10^9 cc-mole^{-1}-sec^{-1} at 400° K using a symmetrical energy surface calculated according to Gorin, Kauzmann, Walter and Eyring[69] with a classical barrier height of 7.5 kcal/mole.

These results may now be interpreted in two ways:

a) Classical interpretation in terms of the ordinary Arrhenius law.

Figure XXXIII is an Arrhenius plot using only the three values for the rate constant obtained above room temperature.

FIGURE XXXIII

Arrhenius law plot for H + D_2, using the three high temperature values only.

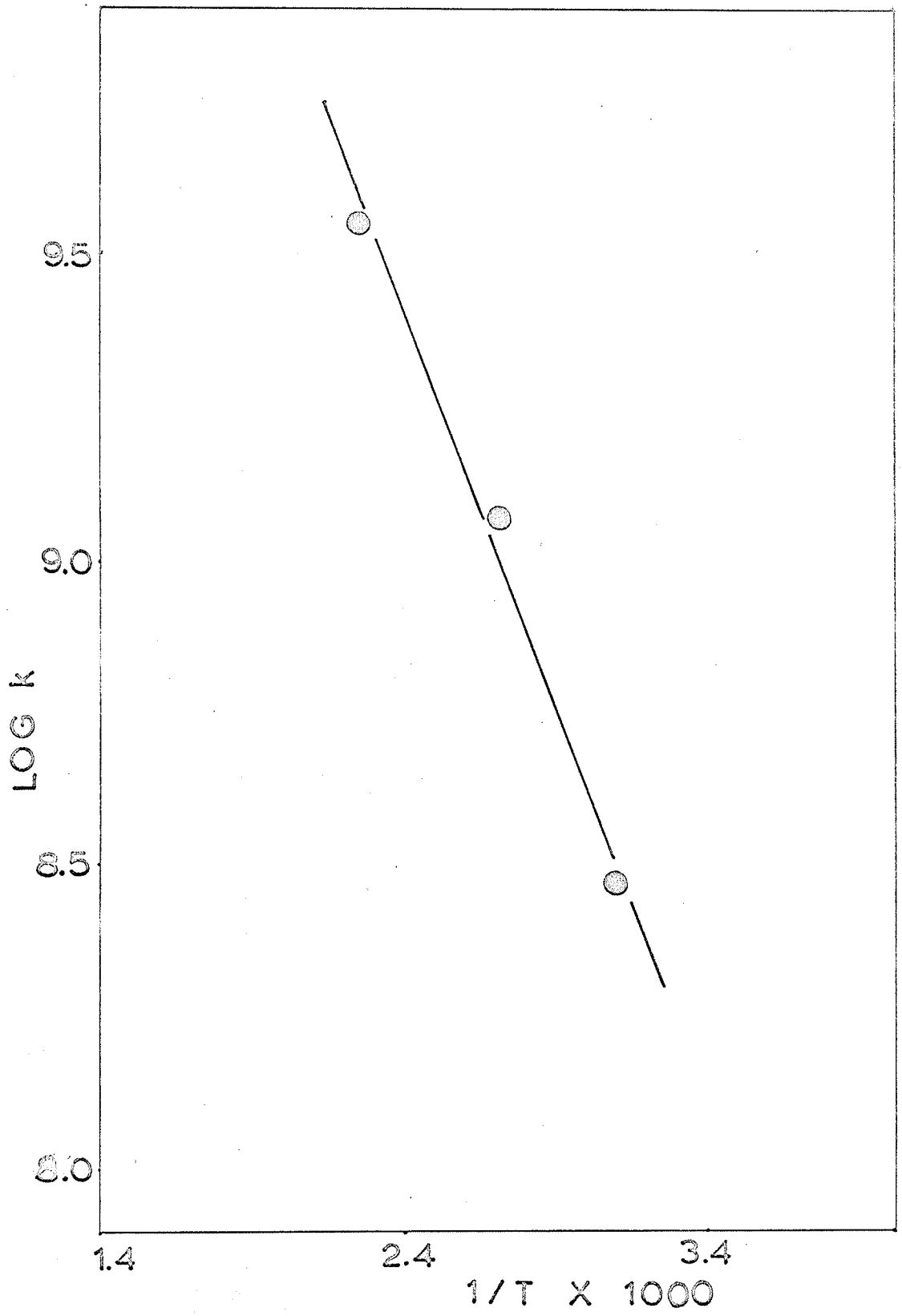
9.5
9.0
8.5
8.0
LOG k
1.4
2.4
3.4
1/T X 1000

A fairly good straight line is obtained; taking its slope gives a value of 5.95 kcal/mole as the average activation energy over the 50° C - 170° C temperature range. Figure XXXIV shows the same values plotted along with those of Farkas and Farkas, and van Meersche. Drawing the best straight line now gives a value of 8.01 kcal/mole for ΔE_o over the 50° C - 727° C temperature range.

b) Interpretation of results in terms of quantum mechanical tunnelling.

The other striking result is the large curvature in the plot of Figure XXXI at low temperatures. This could be caused by one or more of the following factors:

1) There is a change in the mechanism for the reaction at low temperatures.
2) A heterogeneous reaction comes in to effect at 0° C and lower.
3) The reaction is occurring partially at a higher temperature beyond the low-temperature zone of the reaction vessel.
4) Quantum mechanical tunnelling.

Factor (1) has been postulated to explain the deviations from the Arrhenius law in the homogeneous gas-phase pyrolysis of di-isopropyl mercury[77]. Between 240° C and 300° C the activation energy, ΔE_o, is 40.4 kcal/mole but in the range

FIGURE XXXIV

Arrhenius law plot for H + D_2; present high temperature results along with those of Farkas and Farkas, and van Meersche.

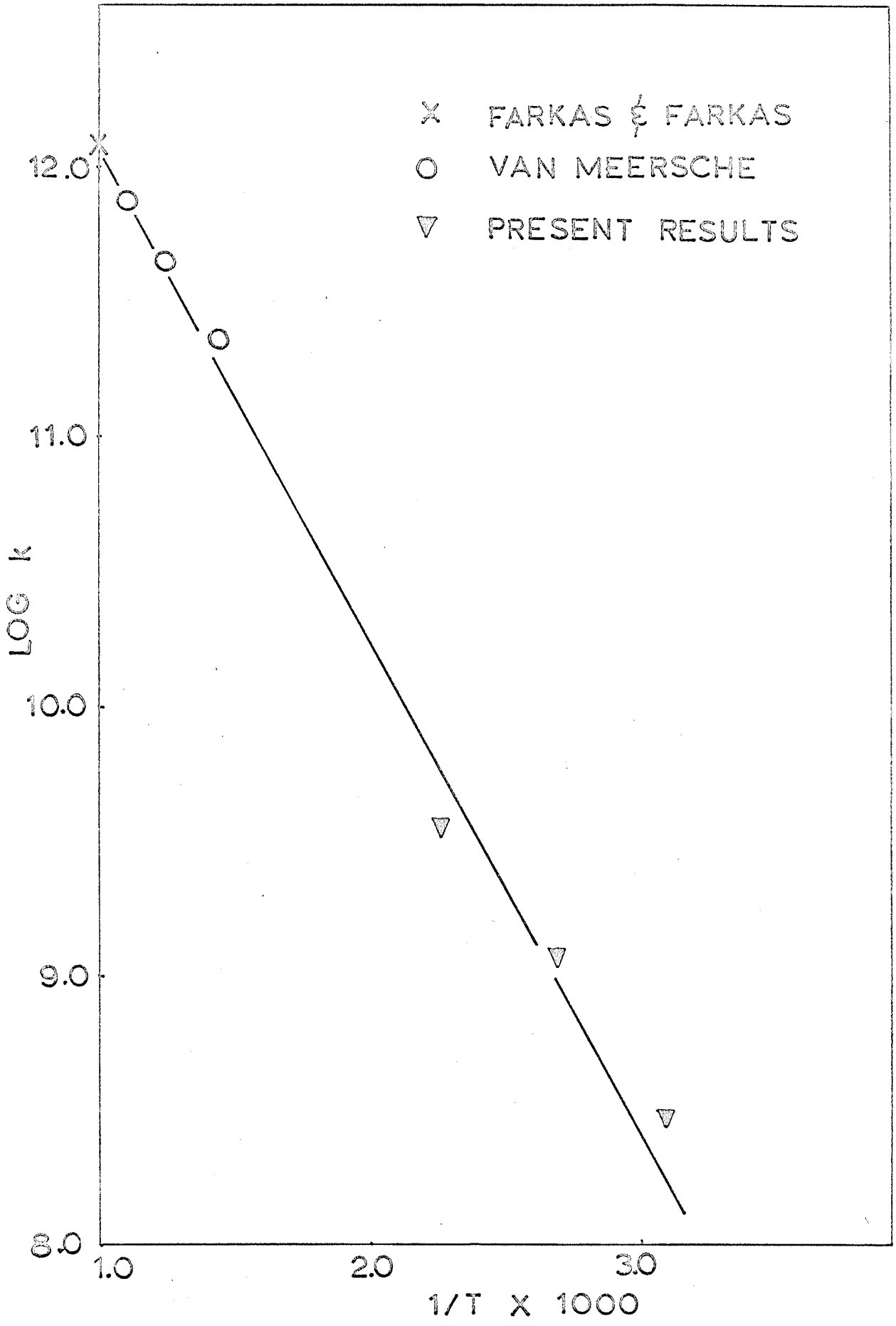
X FARKAS & FARKAS
O VAN MEERSCHE
▽ PRESENT RESULTS
12.0
11.0
10.0
9.0
8.0
LOG k
1.0
2.0
3.0
1/T X 1000

170° C to 240° C it falls to 07 kcal/mole. It is thought that the high temperature process is

$$HgR_2 = 2\,R\cdot + Hg \qquad (72)$$

whereas at low temperatures the process becomes

$$HgR_2 = R\cdot + HgR\cdot \qquad (73)$$

However, it seems unlikely that such an effect is operative in the present results.

Factor (2) is a more likely possibility and has been postulated previously[78] for the H + NH_3 reaction at low temperatures as well as for the rapid recombination of H-atoms at -196° C [58]. It could readily be checked by altering the surface-to-volume ratio of the reaction vessel.

Factor (3) is a very attractive explanation but if this were the case, the rate constant should increase consistently with an increase in the D_2 flow rate. No such effect, however, is observed in Tables XVIIb, XVIIIb, and XIXb.

Assuming factor (4) to be the only significant one, simple collision theory along with Bell's tunnelling equations were used to generate curves similar to the experimental one using an Olivetti Underwood Programma 101 calculator (see

Appendix VII), varying constants E_c and 2a.

By trial and error it was found that a close fit could be obtained for E_c = 7.8 kcal/mole and 2a = 0.50 Å, but the entire curve is shifted upward by a factor of 2 log units or 100 in the rate constant. This indicates a p factor of about 0.01. Fig. XXXV shows the close correspondence between the experimental data and the calculated values when this factor is inserted into the theoretical formulae.

Later, however, it was found that the above values (i.e. E_c = 7.8, 2a = 0.50, and p = 0.01) did not give a good fit when the high temperature value of Farkas and Farkas[14] was included. Figure XXXVI shows that good harmony is obtained, however, when E_c = 11.7 kcal/mole, and 2a = 0.582 Å. Under these conditions the two curves practically coincide. This now not only gives experimental data over the 727° C to -78° C temperature range but indicates that the p factor is approximately unity.

The above value for E_c is approximately equal to the average of the two values reported by Schulz[52] using sophisticated transition theory with parabolic and Eckart barriers (9.8 kcal and 14.0 kcal respectively). However, the present value of 2a is rather small when compared with

FIGURE XXXV

Arrhenius law plot for H + D_2; present results compared with theoretical values generated by Bell's equation for E_c = 7.8 kcal/mole, 2 a = 5.0 Å, and a steric factor, p, of 0.01.

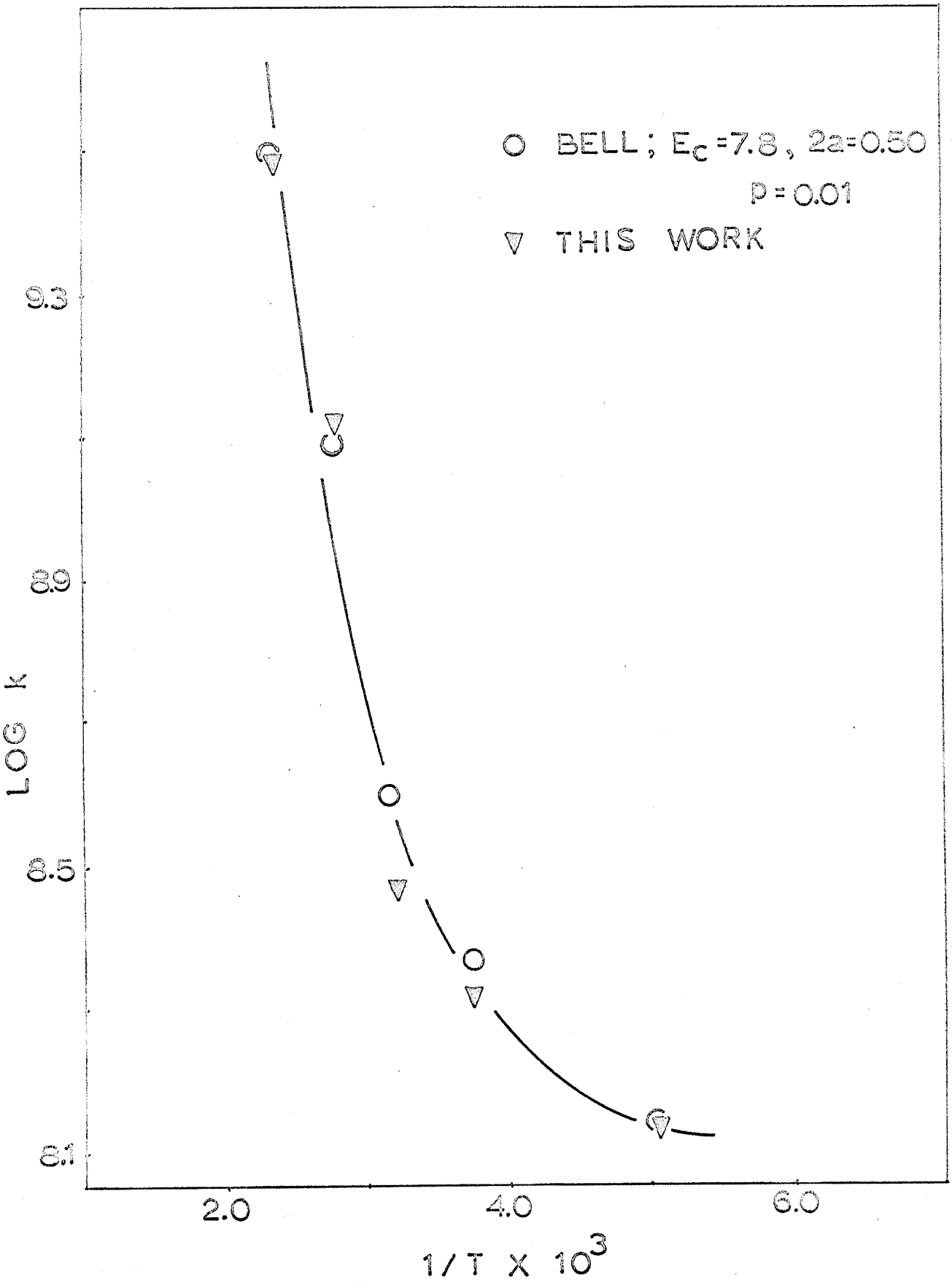
O BELL; E_c=7.8, 2a=0.50
p=0.01
▽ THIS WORK
9.3
8.9
8.5
8.1
LOG K
2.0
4.0
6.0
1/T X 10^3

FIGURE XXXVI

Arrhenius law plot for H + D_2; a comparison of the experimental data of the present work (including the high temperature value of Farkas and Farkas) with values generated by Bell's equation using E_c = 11.7 kcal/mole, 2 a = 0.582 Å, and a steric factor of unity.

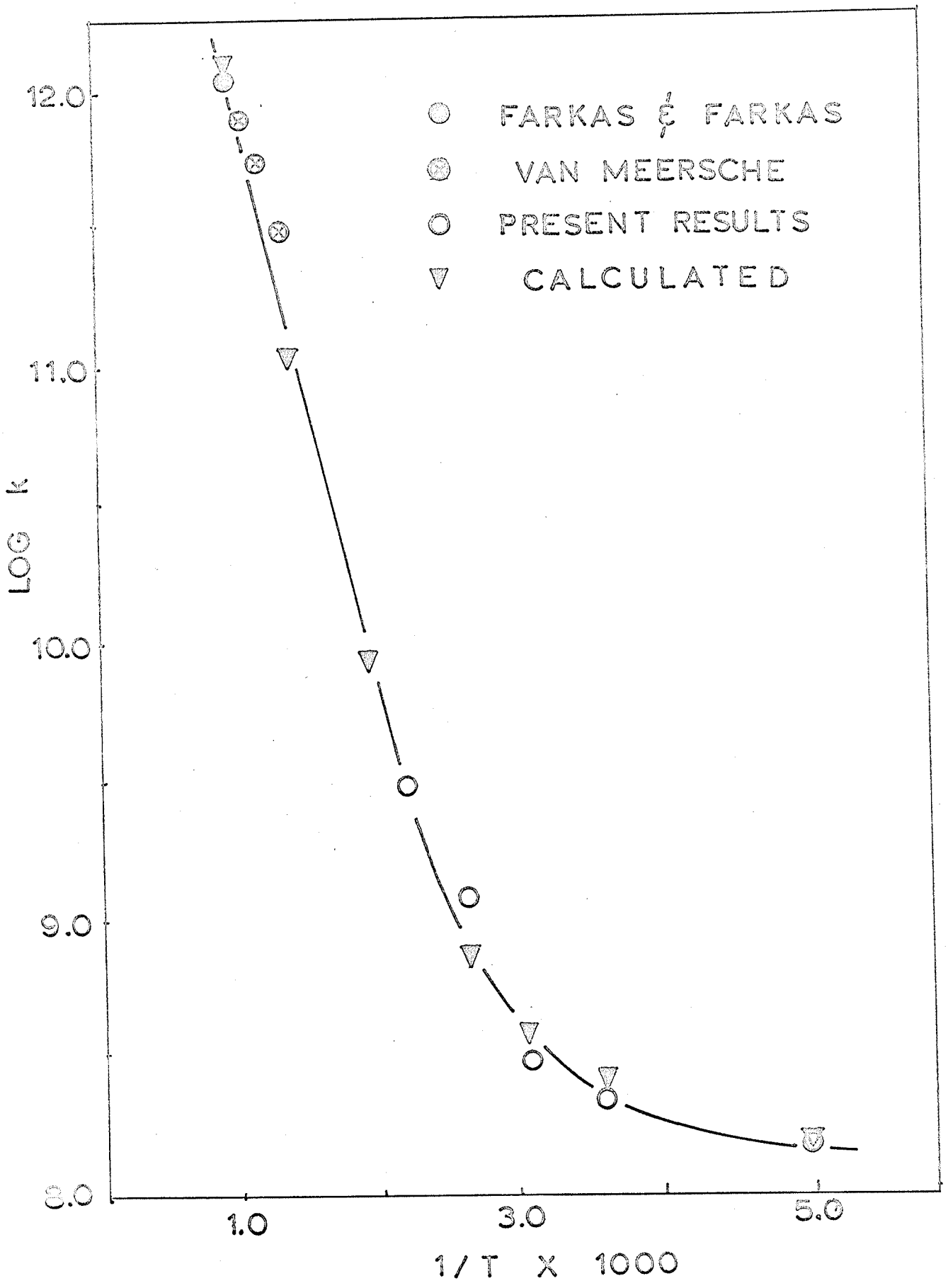
FARKAS & FARKAS
VAN MEERSCHE
PRESENT RESULTS
CALCULATED
LOG K
12.0
11.0
10.0
9.0
8.0
1.0
3.0
5.0
1/T X 1000

Shavitt's[64] theoretical estimates of 1.75 and 1.77 Å, and Hulett's[70] results for proton transfer studies in solution of approximately 1.2 Å. On the other hand, it is difficult for the author to see why this value should be so large for a gas phase reaction when the reaction shell thickness for an H-atom colliding with a hydrogen molecule is only about 0.6 Å (see Glasstone, Laidler, and Eyring; p. 94)[71].

It is tempting to speculate on the implications of such a set of results (i.e. thin energy barrier and a p factor equal to unity), but it is believed this would be premature at this time since it has not been firmly established that the large curvature in the data is entirely due to tunnelling. However, it may be said that the data seem to imply that beyond a certain threshold energy (11.7 kcal/mole for $H + D_2$) there is no preferred orientation for reaction upon collision and each atom-molecule encounter is effective. This may perhaps be due to the formation of a long-lived association complex of the form HDD but this is only a guess and a great deal more work is required before anything of this nature may be postulated. It is interesting to note, however, that such an association complex (CH_5) has been previously postulated in the $H + CH_4$ reaction[69], to account for the rapid recombination

of H-atoms in the presence of CH_4. A summary of the estimates for the activation energy and barrier height is given in Table XXIII.

Conclusion

The data certainly do illustrate the applicability of some of the newly developed techniques to studies of atom reactions in the gaseous phase. With a few minor improvements in the reaction vessel, the inlet systems, and the gas chromatographic column and bridge, it ought to be possible to determine rate constants with an accuracy of 1% over a 200° C to -135° C temperature range. Using a quartz reaction vessel the temperature range may even be extended higher. Also, with the independent method for determining absolute H-atom concentrations, studies of the mechanism of these reactions should now be approached with a little more confidence.

In conclusion it seems appropriate to mention three other points of interest:

1) There is an added note in Bell's paper[59] that the equation (95) for q should really include a factor of $\sqrt{\overline{W}/RT}$ in the expressions, where $\overline{W}$ is the average energy of the molecules

TABLE XXIII

Summary of the values for the activation energy (ΔE_o) and energy barrier height (E_c) for the H + D_2 reaction

	ΔE_o	ΔE_o + zero point energy correction	ΔE_o + tunnelling correction	E_c
From present values only	5.95	5.95 + 0.76 = 6.71	7.8	7.8 + 0.76 = 8.56
From present values along with those of other workers	8.01	8.01 + 0.76 = 8.77	11.7	11.7 + 0.76 = 12.46

Note: (1) Units for the above values are kcal/mole.

(2) See Figure XXXVII for an explanation of terms involved in the above Table.

(3) The zero point energy correction is based on Farkas and Farkas'[14] values of 4.39 kcal/mole and 3.63 kcal/mole for the zero point energies of D_2 and HDD respectively.

(4) The 8.01 and 12.46 kcal/mole values are taken as the more accurate ones since in this case the reaction is considered over a wider temperature range.

FIGURE XXXVII

One dimensional energy barrier diagram showing the potential energy as a function of the reaction co-ordinate for a typical hydrogen-atom - plus - hydrogen reaction.

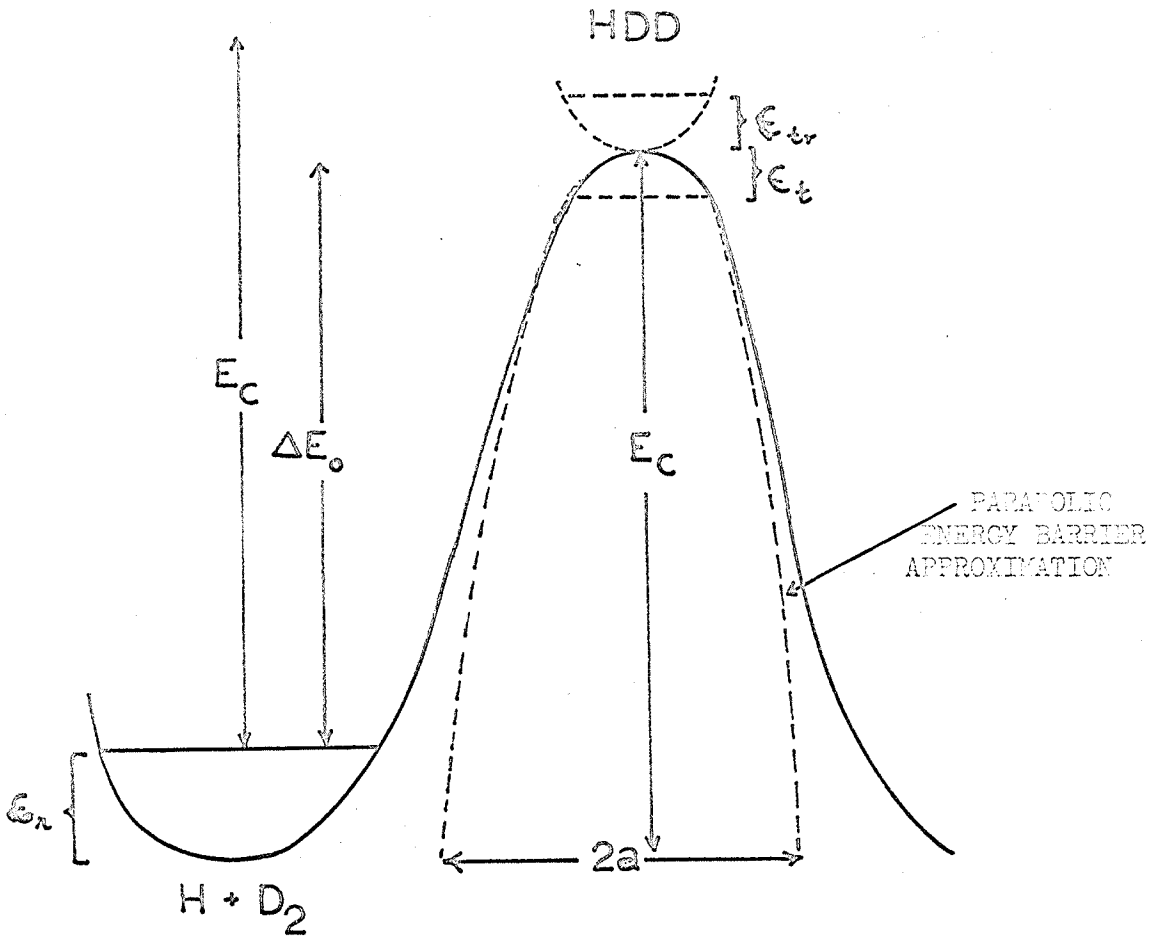

$$\Delta E_o = E_c - \text{ZERO POINT ENERGY CORRECTION} - \text{TUNNELLING CORRECTION}$$

$$\Delta E_o = E_c - (\epsilon_R - \epsilon_{t_R}) - \epsilon_t$$

$$E_c = \Delta E_o + (\epsilon_R - \epsilon_{t_R}) + \epsilon_t$$

where E_c = classical energy barrier height

ΔE_o = apparent activation energy

ϵ_R = zero point energy due to vibrational energy of reactants

ϵ_{t_R} = zero point energy of complex due to bending and symmetric modes

ϵ_t = tunnelling correction due to assymetric mode

crossing the barrier. Estimating this to be approximately 6.3 kcal/mole $(\frac{12.5 + 0}{2})$ one could see that the results would be higher by $\sqrt{\frac{6300}{2.0 \times 1000}}$ or 1.8 at 1000° K and $\sqrt{\frac{6300}{2.0 \times 195}}$ or 4.0 at 195° K. This would necessitate the introduction of p factors of $\frac{1}{1.8}$ or 0.6 and $\frac{1}{4.0}$ or 0.3 at 1000° K and 195° K respectively and gives an average factor of about 0.5 over the whole temperature range. One may interpret this to mean that only one-half the collisions are effective and a plausible mechanism may be

$$H + D_2 = HDD^* \quad (74)$$

$$H + HDD^* = H_2 + D_2 \quad (75)$$

$$H + DDH^* = HD + HD \quad (76)$$

similar to one of the possibilities (IHH) recently postulated for the $I_2 + H_2$ reaction[72].

2) Since there is curvature in the true Arrhenius Law plot, the E_c estimated previously for H-atom reactions by a straight line over a short temperature range would vary depending on the temperature range over which the reaction was examined. This could be a cause of some of the discrepencies

observed when comparing the results of different workers.

3) The p factor and E_c are somehow interelated and seem to adjust themselves depending on the apparatus, the researcher, and the interpretation of the results. This is especially true for the H + CH_4 reaction where E_c varies from 12 to 4 kcal/mole and corresponding p factors of 10^{-1} and 10^{-5}. Jamieson[73] has shown that there is a linear relationship between log p and E_c for this reaction and it seems that depending on conditions, the system "adjusts" itself either to a large activation energy and a large p factor, or a small p factor and a small activation energy, the rate constant remaining approximately the same.

By accurate H-atom studies and extension of the experiments to the low temperature "tunnelling" region, the above situation could be rectified since such a study not only enables one to determine a barrier height E_c, but also the barrier width. It is a possibility that eventually H-atom reactions may not only be classified in terms of an activation energy but also in terms of a barrier width. This would be similar to the attempts already made to interpret experimental results in terms of a "collision cross-section".[74]

OVERALL DISCUSSION AND SUGGESTIONS FOR FURTHER STUDY

The section A experiments show that "clean up" of hydrogen atoms by ketene does occur at -96° C, and that molecular hydrogen is not only necessary for chain propagation at 232° C but also is necessary for CH_4 formation. This excludes reactions such as

$$H + CH_2{=}CO = CH_3{-}CO \quad (36)$$

$$H + CH_3{-}CO = CH_4 + CO \quad (77)$$

and $$H + CH_2{=}CO = CH_2{-}\overset{H}{C}O \quad (3a)$$

$$H + CH_2{-}\overset{H}{C}O = CH_3{-}\overset{H}{C}O \quad (78)$$

$$H + CH_3{-}\overset{H}{C}O = CH_4 + HCO \quad (79)$$

where methane is produced by a series of hydrogen atom additions to the original ketene molecule.

The approximate thermochemical data for each step of the proposed mechanism are as follows:

				ΔH (kcal/mole)
$H + CH_2{=}CO$	=	$CH_2{-}\overset{H}{C}O$	(3a)	-41

			ΔH (kcal/mole)
$H + CH_2{=}CO$	= $CH_3{-}CO^*$	(3b)	-41
$H + CH_2{-}\overset{H}{C}O^*$	= $CH_3 + HCO$	(80)	-14
$H + CH_3{-}CO^*$	= $CH_4 + CO$	(77)	-92
$CH_2{-}\overset{H}{C}O^* + H_2$	= $CH_4 + HCO$	(4)	-12
$CH_3{-}CO^* + H_2$	= $CH_4 + HCO$	(81)	-12
$2\ HCO$	= $(HCO)_2$	(5)	-80
$2\ HCO$	= $H_2 + 2\ CO$	(6)	-56
$HCO + CH_2CO$	= $CH_2{-}\overset{H}{C}O^* + CO$	(7)	-18
$HCO + CH_2CO$	= $CH_3{-}CO^* + CO$	(82)	-18
$2\ CH_3CO^*$	= $C_2H_6 + 2\ CO$	(8)	-68
$2\ CH_2{-}\overset{H}{C}O^*$	= $C_2H_4 + (HCO)_2$	(83)	-40
$CH_3{-}CO^*$	= $CH_3 + CO$	(84)	10
$CH_2{-}\overset{H}{C}O^*$	= $CH_2 + HCO$	(85)	72
HCO	= $H + CO$	(86)	24
$CH_2 + H_2$	= $CH_3 + H$	(2)	-1

		ΔH (kcal/mole)
$CH_3 + H + W = CH_4 + W$	(11)	-102
$CH_3 + HCO + W = CH_4 + CO + W$	(12)	-78
$CH_3 + H_2 = CH_4 + H$	(87)	-2
$CH_3 + CH_3 = C_2H_6$	(13)	-84

It is difficult to estimate ΔH for reaction (3a) because the heat of formation of the $CH_2\text{-}\dot{C}HO$ radical has not been reported in the literature. However, since the same bond is broken and a similar bond is formed (i.e. C-H) one would estimate the ΔH for reaction (3a) to be similar to that of (3b). Consequently, apart from resonance stabilization one must assume that ΔH_f^o for $CH_2\text{-}\dot{C}HO$ is similar to that of CH_3-CO. Using these data, and calculating the approximate ΔH values for the other reactions, it can be seen that all the reactions are thermochemically feasible except reactions (84), (85) and (86) which are endothermic by a large extent. It must be concluded, therefore, that the chain is propagated by HCO radicals even at high temperatures and that the C_2H_6 is probably formed as a result of a second

atom reacting with the long-lived free radical via the following scheme:

		Δ_H (kcal/mole)
$CH_2\text{-}\overset{H}{\underset{|}{C}}O^* + H = H_2 + CH_2 + CO$	(88)	11
$CH_2 + H_2 = CH_3 + H$	(2)	-1
$CH_3 + CH_3 = C_2H_6$	(13)	-84

Reaction (88) is about 11 kcal endothermic and thus would be almost thermoneutral if the original $CH_2\text{-}\overset{H}{\underset{|}{C}}O^*$ had at least 10 kcal of energy in excess. This would explain why C_2H_6 is only formed at higher temperatures and would necessitate the reaction of a second hydrogen atom with the ketene molecule.

The mass spectrometric identification of the $CH_2\text{-}\overset{H}{\underset{|}{C}}O$ radical in the H + CH_3CHO reaction tends to support the conclusions of this study that the primary addition of the H-atom is on the carbonyl carbon. This would seem to indicate that in this case the atom acts as a nucleophilic reagent similar to Cl^-, OR^-, and RNH_2 which in general attack ketenes as follows:

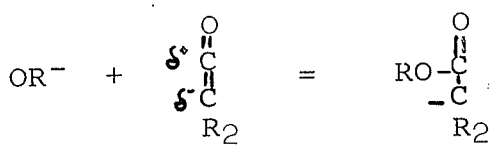

(89)

Such a conclusion is also supported by the H + C_3O_2 experiments of section B where the evidence points to a long-lived O=C=C-C=O, perhaps once again resonance stabilized by the two structures

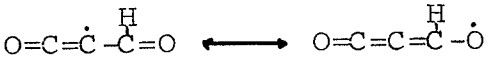

It is a possibility that the radical postulated by Back[46] is also of this nature, i.e.

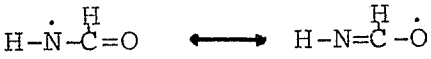

although more experiments with H + HNCO would have to be conducted to see whether this is actually the case.

As has been mentioned previously, the validity of the "second atom" theory in which another H-atom now reacts with the long-lived free radical could be tested by an accurate estimate of the H-atom concentration prior to each experiment. It is for this reason that the Type I and Type II reaction vessels with moveable calorimetric probes were designed. It would not be too surprising if this were the case since hydrogen atoms have previously[79] been observed to react with

Na, Tl, Pb, and S_2 in the gas phase according to reactions such as

$$H + H + Na = H_2 + Na^* \quad (90)$$

where the Na D-line emission has been directly observed. Also, halogen atoms have long been postulated to recombine in the presence of a third body according to the following mechanism[80]:

$$X + M = XM \quad (91)$$

$$X + XM = X_2 + M^* \quad (92)$$

Moreover, Evans, Freeman, and Winkler[81] have postulated that recombination of nitrogen atoms catalyzed by a reactant could explain most of the products observed in the reaction of methyl chloride, methyl cyanide, and methylamine with nitrogen atoms.

The H + D_2 experiments of Section G have demonstrated the usefulness of the moveable calorimetric probe, and the idea of using trace amounts of H_2 in a helium flowing system to produce H-atoms, and then studying the extent of their reaction by collecting the isotopic hydrogens in a "saran" charcoal trap. This method could now readily be applied to a D_2 system and the next study in this series should be the examination of

reactions such as D + H_2 and D + CH_4.

Once the rates and the mechanisms of these reactions have been established over a large temperature range one could readily proceed to a D + CH_2CO study. The best way to go about this would be to produce D atoms in a helium flowing system at a fairly large concentration (perhaps by the use of internal water-cooled electrodes similar to those recently devised by Safrany[82]), and then reacting them with a mixture of H_2 and CH_2CO. If the primary addition is as has been postulated, and the long-lived free radical does react with hydrogen one ought to obtain undeuterated CH_4 as one of the major products from the reaction:

$$CH_2\overset{D}{C}O^* + H_2 = CH_4 + DCO \qquad (93)$$

rather than CH_3D if the other possibility took place, i.e.

$$CH_2D\text{-}CO^* + H_2 = CH_3D + HCO \qquad (94)$$

Such isotopic experiments would be of great importance in establishing the mechanism and the role that hydrogen atoms play in the photolysis of simple molecules in the gaseous phase.

SUMMARY AND CONTRIBUTIONS TO KNOWLEDGE

1) Methane, carbon monoxide, and polymer are the major products in the reaction of hydrogen atoms with carbon suboxide at -96° C. At higher temperatures some CH_2CO and C_2H_6 are also formed. The major reaction at 235° C is the formation of a polymer. From stoichiometric considerations the composition of the polymer indicates a C:O ratio of 3:1. The mechanism most consistent with the results is as follows:

$$H + OCCCO = OCC-\overset{H}{C}O^* \quad (26a)$$

$$H + OCC-\overset{H}{C}O^* = OCC + CO + H_2 \quad (26b)$$

$$OCC + H_2 = H_2CCO^* \xrightarrow{W} CH_2CO \quad (27a)$$

$$H_2CCO^* \rightarrow CH_2 + CO \quad (27b)$$

$$CH_2 + H_2 \xrightarrow{W} CH_4 \quad (2a)$$

$$CH_2 + H_2 \rightarrow CH_3 + H \quad (2b)$$

$$CH_3 + CH_3 = C_2H_6 \quad (13)$$

$$\begin{matrix} OCC-\overset{H}{C}O \\ + \\ OCC-CO \\ \quad H \end{matrix} = \begin{matrix} OCC \\ | \\ OCC \end{matrix} + H_2 + 2\,CO \quad (28)$$

$$\begin{matrix} OCC \\ | \\ OCC \end{matrix} = OCCCO + C \quad (29)$$

$$C \overset{W}{=} \text{residue} \qquad (30)$$

$$C + H_2 = CH_2 \qquad (31)$$

$$OCC\overset{H}{C}O + H_2 = CH_2CO + HCO^* \qquad (32)$$

$$HCO^* + OCCCO = OCC\overset{H}{C}O^* + CO \qquad (33)$$

$$HCO^* + HCO^* \rightleftharpoons \begin{cases} \xrightarrow{} H_2 + 2\,CO & (6) \\ \xrightarrow{W} (HCO)_2 & (5) \end{cases}$$

$$CCO + C_3O_2 = \text{polymer} + 2\,CO \qquad (20)$$

2) Ammonia and large amounts of non-condensable products (probably N_2 and CO) are formed from the reaction of H-atoms with HNCO in the -76° C to 252° C range. The reaction may proceed via a $HN\text{-}\overset{H}{C}O$ intermediate.

3) From the H + CH_2CO, H + OCCCO, and H + $HN\text{-}\overset{H}{C}O$ studies there is considerable evidence that the primary attack of the hydrogen atom is on the carbonyl carbon of the molecule in each case.

4) A method for the quantitative collection and estimation of H_2, HD, and D_2 from a fast-flow low-pressure helium system has been developed by the use of "saran" charcoal.

5) A water-cooled discharge tube has been designed for the stable production of atoms and which could also be used as a Lyman-α lamp in photochemical studies. This along with the technique described in (4), an improved calorimetric probe, and a low-temperature reaction vessel have been used to study the $H + D_2$ reaction in a helium flowing system over the 443°K to 195°K temperature range. The experiments above 273°K indicate an activation energy of 8.01 kcal/mole. Considerable curvature has been obtained below 273°K and these results could be interpreted in terms of quantum mechanical tunnelling with E_c = 12.46 kcal/mole and a parabolic energy barrier width (2a) of 0.582 Å.

BIBLIOGRAPHY

1) Demchuk, N. M.Sc. Thesis, Univ. of Manitoba (1963).

2) Knox, K., Norrish, R.G.W. and Porter, G. J. Chem. Soc. 1477 (1952).

3) Gesser, H. and Steacie, E.W.R. Can. J. Chem. 34, 113 (1956).

4) Lambert, R. M., Christie, M. I., and Linnett, J. W. Chem. Commun. #8, 388 (1967).

5) Heicklen, J. American Institute of Aeronautics and Astronautics 5, 4 (1967).

6) Donahue, T. M. Planet. Space Sci. 12, 149 (1964).

7) Mitchell, A.C.G. and Zemansky, M. W. "Resonance Radiation and Excited Atoms", (Cambridge University Press, London, 1934).

8) Tanaka, I. and McNesby, J. R. J. Chem. Phys. 36, 3170 (1962).

9) Demchuk, N. and Gesser, H. Can. J. Chem. 41, 1645 (1963).

10) Jamieson, J.W.S. Private Communication.

11) Jamieson, J.W.S., Brown, G. R. and Hancock, W. K. Can. J. Chem. 43, 1973 (1965).

12) Rony, P. R., Lawrence Radiation Laboratory, Univ. of Calif., Berkeley, Calif. Report #16050, April, 1965.

13) Farkas, A. Z. Physik. Chem. 10B. 419 (1931).

14) Farkas, A. and Farkas, L. Proc. Roy. Soc. (London) A152, 124 (1935).

15) Geib, K. and Harteck, P. Z. Physik. Chem., Bodenstein Festband, 849 (1931).

16) Melville, H. W. and Robb, J. C. Proc. Roy. Soc. A196, 445 (1949).

17) van Meersche, M. Bull. Soc. Chim. Belges 60, 99 (1951).

18) Boato, G., Careri, G., Cimino, A., Molinari, E. and Volpi, G. J. Chem. Phys. 24, 783, (1956).

19) Schulz, W. R. and LeRoy, D. J. Can. J. Chem. 42, 2480 (1964).

20) Schulz, W. R. and LeRoy, D. J. J. Chem. Phys. 42, 3869 (1965).

21) Ridley, B. A., Schulz, W. R. and LeRoy, D. J. J. Chem. Phys. 44, 3344 (1966).

22) Kuppermann, A. and White, J. M. J. Chem. Phys. 44, 4352 (1966).

23) Wittke, J. P. and Dicke, R. H. Phys. Rev. 103, 620 (1956).

24) Harteck, P. and Dondes, S. J. Chem. Phys. 23, 902 (1955).

25) Blake, A. R. and Hodgson, K. E. J. Chem. Soc. (A), 533 (1966).

26) von Weyssenhoff, H., Dondes, S., and Harteck, P. J. Am.

Chem. Soc. 84, 1526 (1962).

27) Bayes, K. D. J. Am. Chem. Soc. 83, 3712 (1962).

28) Bayes, K. D. Ibid. 84, 4077 (1962).

29) Bayes, K. D. Ibid. 85, 1730 (1963).

30) Smith, R. N., Smith, R. A., and Young, D. A. Inorg. Chem. 5, 145 (1966).

31) Bruns, R., Smith, D., and Devlin, P. J. Inorg. Chem. 6, 318 (1967).

32) Palmer, H. B. and Hirt, I. J. J. Am. Chem. Soc. 84, 113 (1962).

33) Smith, R. N., Young, D. A., Smith, E. N., and Carter, C. C. Inorg. Chem. 2, 826 (1963).

34) Blake, A. R., Eeles, W. T., and Jennings, P. P. Trans. Farad. Soc. 60, 691 (1964).

35) Harteck, P. Seminar, Pinawa, Manitoba, Canada. June, 1966.

36) Bell, S., Varadarajan, T. S., Walsh, A. D., and Warsop, P. A. J. Mol. Spectr. 21, 42 (1966).

37) Gesser, H. and Hussain, S. Nature 201, 290 (1964).

38) Stock, A. and Stoltzenburg, H. Ber. 50, 498 (1917).

39) Czubryt, J. J. M.Sc. Thesis, Univ. of Manitoba (1965).

40) Safrany, D. R. and Jaster, W. Pre-print, Atomic Energy of Canada, Pinawa, Manitoba.

41) Gesser, H., Mullhaupt, J. T., and Griffiths, J. E. J. Am. Chem. Soc. 79, 4834 (1957).

42) Willis, C. and Bayes, K. D. J. Am. Chem. Soc. 88, 3203 (1966).

43) Mui, J.Y.P. and Back, R. A. Can. J. Chem. 41, 826 (1963).

44) Linhard, M. Z. Anorg. Chem. 236, 200 (1938).

45) Herzberg, G. and Reid, C. Disc. Farad. Soc. 9, 22 (1950).

46) Back, R. A. Private Communication.

47) Koyano, I. and Tanaka, I. J. Chem. Phys. 40, 895 (1964).

48) "Solid Surfaces and the Gas-Solid Interface", No. 33 Advances in Chemistry Series, Am. Chem. Soc. (1961).

49) Bak, B. and Rastrup-Andersen, J. Acta Chem. Scand. 16, 111 (1962).

50) Wiles, D. M. and Winkler, C. A. J. Phys. Chem. 61, 620 (1957).

51) Shaw, T. M. General Electric Microwave Laboratory, Palo Alto, California, GEML Project #270-0401-119, August, 1958.

52) Schulz, W. R. Ph.D. Thesis, University of Toronto, May (1965).

53) Rony, P. R. Rev. Sci, Instr. 37, 235 (1966); (and references listed therein).

54) Harteck, P. and Roeder, E. Z. Phys. Chem. A 178, 380 (1937).

55) Smith, W. V. J. Chem. Phys. 11, 110 (1943).

56) Wood, B. J. and Wise, H., J. Phys. Chem. 65, 1976 (1961).

57) Thrush, B. A. Progress in Reaction Kinetics (Ed. by G. Porter) 3, 65 (1965).

58) Shuler, K. E. and Laidler, K. J. J. Chem. Phys. 17, 1212 (1949).

59) Bell, R. P. Proc. Roy. Soc. A 148, 241 (1935).

60) Bader, L. W. Private Communication.

61) Berg, H. C. and Kleppner, D. Rev. Sci, Instr. 33, 248 (1962).

62) Johnston, H. S. "Gas Phase Reaction Rate Theory", (Ronald Press, N. Y., 1966).

63) Laidler, K. J. and Polanyi, J. C. Prog. Reac. Kinet. (Ed. G. Porter), 3, 3 (1965).

64) Shavitt, I. J. Chem. Phys. 31, 1359 (1959).

65) Yasumori, I. and Ohno, S. Bull. Chem. Soc. of Japan 39, 1302 (1966).

66) Jamieson, J.W.S. Ph.D. Thesis (Appendix B), McGill University (1957).

67) Schulz, W. R. M.Sc. Thesis, Univ. of Toronto (1963).

68) Polanyi, J. C. J. Chem. Phys. 28, 1505 (1955).

69) Gorin, E., Kauzmann, W., Walter, J., and Eyring, H. J. Chem. Phys. 7, 633 (1939).

70) Hulett, J. R. Proc. Roy. Soc. A251, 274 (1959).

71) Glasstone, S., Laidler, K. J., and Eyring, H. "The Theory of Rate Processes" (McGraw-Hill, 1941).

72) Sullivan, J. H. J. Chem. Phys. 46, 73 (1967).

73) Jamieson, J.W.S. and Brown, G. R. Can. J. Chem. 42, 1638 (1964).

74) Eberhardt, W. H. A.C.C.C. Newsletter #8 (1967).

75) Bell, R. P. Trans. Farad. Soc. 55, 1 (1959).

76) Eckart, C. Phys. Rev. 35, 1303 (1930).

77) Billinge, B.H.M. and Gowenlock, B. G. Proc. Chem. Soc. 24 (1962).

78) Freeman, G. R. and Winkler, C. A. J. Phys. Chem. 59, 371 (1955).

79) Sugden, T. M. and Demerdache, A. Nature 195, 596 (1962).

80) Bunker, D. L. and Davidson, N. J. Am. Chem. Soc. 80, 5090 (1958).

81) Evans, H.G.V., Freeman, G. R. and Winkler, C. A. Can. J. Chem. 34, 1271 (1956).

82) Safrany, D. R. Private Communication.

83) Demchuk, N. and Gesser, H. Can. J. Chem. 42, 1 (1964).

84) Calvert, J. G. and Pitts, J. N. (Jr.) "Photochemistry" (Wiley and Sons, 1966).

85) Benson, S. W. ACCCS Resource Paper III, J. Chem. Ed. 42, 502 (1965).

86) Cottrell, T. L. "Strengths of Chemical Bonds" (2nd Ed., Butterworths, 1958).

87) Chupka, W. A., Meschi, D. J., and Berkowitz, J. Symposium on Chemical and Thermodynamic Properties at High Temperatures, XVIIIth International Congress of Pure and Applied Chemistry, Montreal, Canada (1961).

88) Willard, J. W. Nucleonics, October, 61 (1961).

89) Karplus, M., Porter, R. N., and Sharma, R. D. J. Chem. Phys. 43, 3259 (1965).

90) News Article, C. and E. News, November, 48, (1966).

APPENDIX I

Calculation of the galvanometer constant from the photolysis of ketene at 24.5° C.

e.g. Experiment #1:

V_{cell} (ill. part): 130 cc

V_{CO} : 4.43 cc-cm

time: 90.0 min

Room temp: 24.5° C

$$R_{CO}: \frac{(4.43)(6.02 \times 10^{23})}{(90)(60)(297.5)(82.06)(760)(130)} = 0.21 \times 10^{13} \text{ moles/cm}^3\text{/sec.}$$

Now, assuming $\phi_{CO} = 2.0$

$$I_a = \frac{R_{CO}}{2.0} = 0.11 \times 10^{13} \text{ quanta/cm}^3\text{/sec.}$$

And, since the average amount of light absorbed is 10.4% (see over)

$$I_o = \frac{100}{10.4} \times I_a = 1.06 \times 10^{13} \text{ quanta/cm}^3\text{/sec.}$$

Also, $i = i_R + i_G + i_{CDR}$

$$= \frac{i_g R_g}{CDR} + i_G + i_G R_G$$

$$= i_g \left(\frac{R_g}{CDR} + \frac{R_g}{R} + 1\right)$$

Now, CDR = 802 , R_g = 80 , gal. sens. = 0.0058×10^{-6} amp/div., and defl. was 95.0 div. for R = 24

Hence, $i = (95.0)(0.0058) \times 10^{-6} \left(1.1 + \frac{80}{24}\right) = 2.44 \times 10^{-6}$ amp.

And thus,

$$\beta = \frac{I_o}{i} = \frac{1.06 \times 10^{13}}{2.44 \times 10^{-6}} = 0.45 \times 10^{19} \text{ quanta/cm}^3\text{/sec/amp.}$$

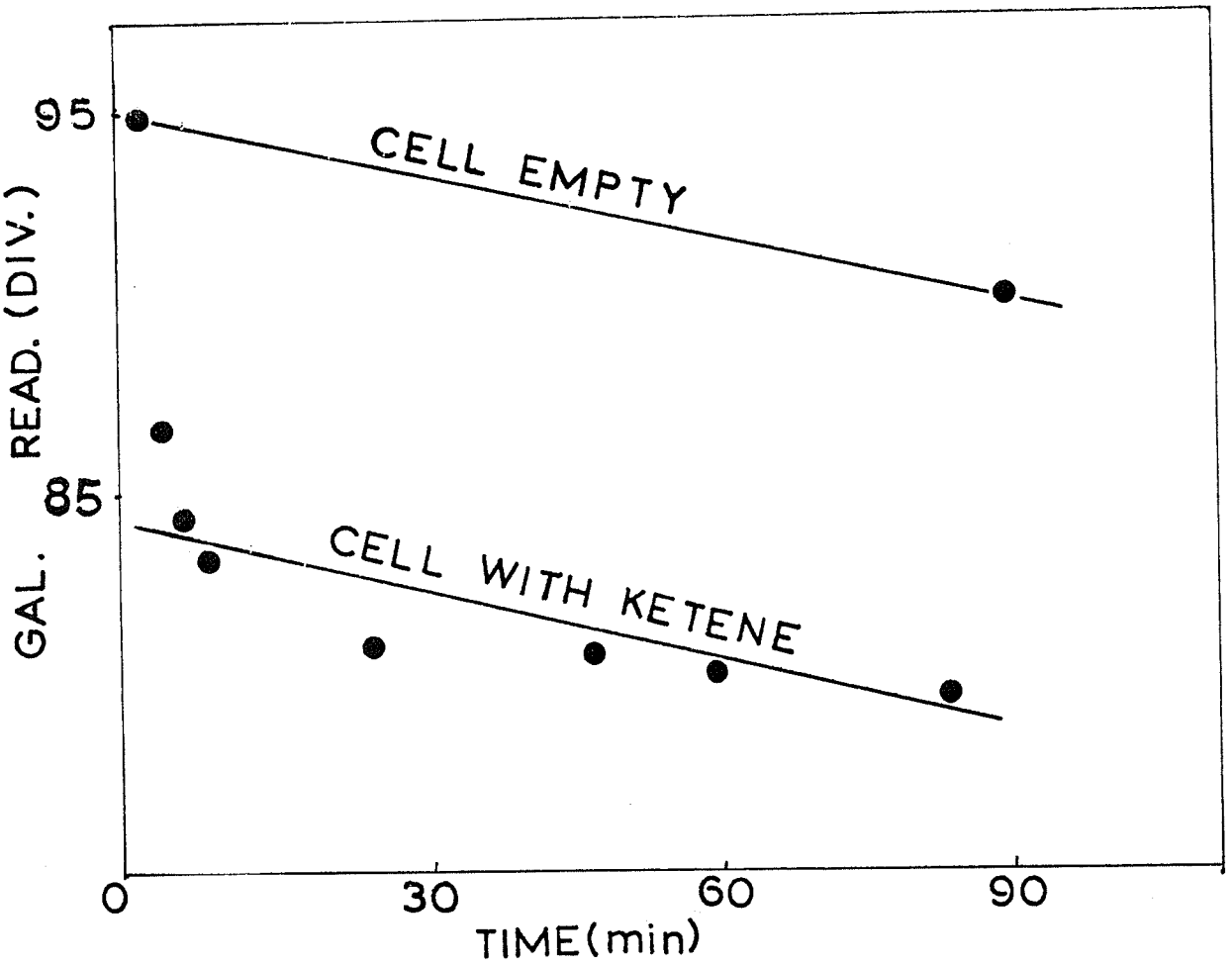

	galv. reading
shutter closed	0.00 (adjusted)
cell empty	95.0 (at 24 Ω for R)
time after ketene in	
1.0 (min)	86.5
4.0	84.5
8.0	83.5
25.0	81.5
47.0	81.5
60.0	80.0
84.0	79.5
90.0 (cell evac.)	90.0

cell empty: ave. galv. reading = $\frac{95.0 + 90.0}{2}$ = 92.5

cell with ketene: ave. galv. reading = $\frac{84.8 + 79.2}{2}$ = 82.1

Thus, % of light absorbed: 92.5 - 82.1 = 10.4.

APPENDIX II

Estimation of the atom concentration using a hot-wire scavenger

e.g. Experiment #1:

Temperature: 234^{o} C

Voltage across primary: 30

Let I = current in amps flowing through hot-wire

V = voltage across the wire

Discharge off: I_oV_o = 1.254 watts (bridge balanced)

Discharge on : I V = 1.165 watts (for bridge to be balanced)

Heat due to atom recombination: $I_oV_o - IV = 1.254 - 1.165$

$= 0.089$ watts.

Now, let x be the "moles" of atoms produced/min.

Then x/60 gives "moles" of atoms produced/sec.

And x/2(60) gives "moles" of H_2 produced/sec.

But 1 mole of H_2 gives off 103 kcal. of heat on recombination

Or 1 " " H_2 " " (103)(1000)(4.186) watts

Thus we have $\frac{x\,(103)(1000)(4.186)}{2(60)} = 0.089$

and $x = 24 \times 10^{-6}$ moles/min

$= 24$ micromoles/min.

APPENDIX III

The reaction of hydrogen atoms with CCl_4 at low temperatures

Using the apparatus described on page 70 it was decided to see whether the reaction of H-atoms with CCl_4 proceeds at low temperatures. Freeman and Winkler[78] report a rapid chain reaction of hydrogen atoms with ammonia at -67° C. It has been shown previously in this study[83] that ketene reacts with H-atoms at temperatures as low as -135° C. The preliminary results with CCl_4 at -78° C were as follows:

TABLE XXIV

Results from the reaction of H-atoms with CCl_4 at -78° C.

Exp. #	Atom conc. using hot-wire (moles x 10^6/min)	CCl_4 flow-rate (moles x 10^6/min)	HCl produced (moles x 10^6/min)
1	338	124	502
2	82	271	180

Note: These experiments were conducted in a pure H_2 system at a flow-rate of 2700 micromoles/min and a pressure of 1.03 mm Hg.

APPENDIX IV

Calculation of the "contact time" or reaction time, t:

e.g. Series A experiments:

Temperature = -78° C or 195° K

Pressure = 1.91 mm Hg

Helium flow-rate = 5430 moles x 10^{-6}/min

Volume of reaction vessel = 550 cc

Using equations (59) and (60) we have

$$t = \frac{PV}{RT\ r}$$

$$\text{or} = \frac{\frac{1.91}{760} \times 0.550}{\frac{5430}{60} \times 10^{-6} \times 0.082 \times 195}$$

$$= 0.96 \text{ sec.}$$

APPENDIX V

Typical calculation of D_2 consumption (or $\frac{\text{HD } \mu\text{moles/min}}{2}$)

e.g. Experiment A1

D_2 in: 36 cc-cm (Room temperature: 32° C)

Top portion: HD area = 221

D_2 area = 13200

% HD from formula (58):

$$\frac{2(221)}{2(221) + 13200} \times 100 = 3.24$$

HD_{abs}: 3.24 - 0.74 (ave. blank) = 2.50

2.50 x 36 (D_2 in) = 0.90 cc-cm

Bottom portion: repeat of the above procedure = 0.95 cc-cm

Ave. $HD_{abs.}$ = 0.93 cc-cm

or $HD_{abs.}$ = 0.93 x 0.52 μmoles

or $HD_{abs.} = \frac{0.93 \times 0.52}{7.0}$ μmoles/min

or $\frac{\text{HD } \mu\text{moles/min}}{2} : \frac{0.93 \times 0.52}{2 \times 7.0} = 0.035$

Conversion factor for cc-cm to μmoles:

$$PV = nRT$$

$$\text{cc-cm} \left(\frac{PV}{RT} \times 10^6\right) = \mu\text{moles}$$

$$\text{cc-cm} \left(\frac{1 \times 1000 \times 10^6}{76 \times 0.082 \times 305}\right) = \mu\text{moles}$$

$$\text{cc-cm} \left(\frac{10^6}{76 \times 82 \times 305}\right) = \mu\text{moles}$$

$$\text{cc-cm} \; (0.52) = \mu\text{moles}$$

APPENDIX VI

Olivetti Underwood Programma 101 program for the calculation of 2nd order rate constants

A) Turbulent flow (after Jamieson[66])

$$k_t = \frac{60\ V\ r\ 10^6}{t^2\ (p-r)\ (q-r)}$$

where r = flow-rate of product in μmoles/min

p = atom concentration in μmoles/min

q = reactant flow-rate in μmoles/min

V = volume of reaction vessel

See program #1

B) Streamlined flow (after Jamieson[66])

$$k_s = \frac{60\ V\ 10^6}{t^2\ (q-p)} \ln \frac{p(q-r)}{q(p-r)}$$

$$(\quad J \quad)\ (\quad K \quad)$$

where r = flow-rate of product in μmoles/min

p = atom concentration in μmoles/min

q = reactant concentration in μmoles/min

V = volume of reaction vessel

J = non-log. term

K = log. term in above expression

See program #2.

SYSTEM _____ APPLICATION Calculation of 2nd order Rate Constant on the basis of Turbulent Flow

DATE 5/1/64 PROG. NO. 1

PROG. BY N. Senchuk

DECIMAL SETTING 5

REMARKS

NO.	INSTRUCTIONS			M	A	R	b	B	c	C	d	D	e	E	f	F
1	A	V														
2		d	↓													
3		d	x													
4		e	↕													
5		D	↓													
6		F	X													
7		e	÷													
8		/	◇													
9	B	V														
10		S		enter	h,	(S) or	depress V as req'd									
11		b	↑													
12		S		enter	p ↓,	(S)										
13		b	-													
14		f	↕													
15		S		enter	q ↓,	(S)										
16		b	-													
17		f	X													
18		C	↕													
19		b	↓													
20		C	÷													
21		E	X													
22		A	◇	gives	$k_0/10^6$											
23	C	V														
24																

To start:

Depress GEN RESET key

Will pass PROG. RECORD ON (in) enter prog.

To use program:

Store constants

t into d↑

V into D↑

60 into F↑

depress V

enter variables as shown within instructions at left.

SYSTEM _____ APPLICATION Calculation of 2nd order Lofe Constant on the basis of Streamlined Flows. of 1

DATE 7/7/67 PROG. NO. 2

PROG. BY N. Senchuk

DECIMAL SETTING 5

REMARKS

NO.	Reg① INSTRUCTIONS			M	Reg② A	R	Reg④ b	B	c	C	d	D	e	E	f	F
1	A	V														
2		S	enter	constants(S)	A◇	prints J	e↓									
3		e	↓		E*		EX									
4		e	X		C*		e↕									
5		b	↕		b↓		e↓									
6		E	↓		d+		CX									
7		b	÷		b↕		b+									
8		B	↕		d−		b↕									
9	B	W			b÷		b−									
10		S	enter	variables(S)	b↕		A↕									
11		E	↓		d↓		/V									
12		b	−		e↕		b↓									
13		f	X		b↓		DX									
14		C	↕		bX		A◇	print K								
15		f	↓		E↕		C*									
16		b	−		b↓		S									
17		E	X		e↕		punch in J X and get				ks/10⁶					
18		C	÷		aV		depress C W or V as req'd									
19		b	↕		f↓											
20		f	↓		D+											
21		E	−		f↕											
22		C	↕		d↓											
23		B	↓		f÷											
24		C	÷		C*											

To start:

Depress GEN. RESET Key with PROG. RECORD ON (in) enter prog.

Constants:

t	e↑
60V	E↑
1	d↑
2	D↑

Variables

r	b↑
p	E↑
g	f↑

APPENDIX VII

Calculation of theoretical rate constant for H + D_2 using elementary collision theory along with Bell's equation (95) to include quantum mechanical effects.

A chemical reaction may be looked upon as a stream of particles approaching a barrier of a certain shape and thickness from one side. The appearance of particles on the other side of this barrier corresponds to the formation of products during the reaction. The total number of particles approaching the barrier per unit time, N_o, may be taken to correspond to a collision rate between unlike molecules of the reactants and can be easily estimated from elementary collision theory as shown below. To obtain the number of particles passing across the barrier in unit time, N_o must be multiplied by a factor q, which is a function of the distribution of energy among the particles and of the properties of the barrier. It is this factor which differs in the classical and quantum mechanical treatments of a chemical reaction rate. Classically, q is calculated from the Boltzmann distribution law and is given by $e^{-E_c/kT}$ where E_c is the classical activation energy for the reaction and T the

absolute temperature. This is just the exponential term of the well known Arrhenius rate law.

Quantum mechanically this is not quite true because the probability that a particle will cross the barrier varies continuously with its energy, and there is a finite probability that particles having an energy well below the barrier height could still cross the barrier and cause a reaction. This is commonly referred to as "tunnelling" by the particles and becomes significant for particles having a small mass (e.g. electron, proton, or hydrogen atom). Using a truncated parabola as the approximate shape of the energy barrier Bell[59] obtained an approximate expression for q by solving the Shrödinger wave equation as follows:

$$q = \frac{-1}{\beta - \alpha} (\beta e^{-\alpha} - \alpha e^{-\beta}) \qquad \ldots\ (95)$$

where $\alpha = \frac{E}{kT}$, and $\beta = \frac{2\pi^2 a\sqrt{2mE}}{h}$

in which E is now the true height of the barrier,

2a is its width at the base,

m is the mass of the approaching particle,

and the other terms have their usual connotation.

A number of improvements of the above expression have since been made and in 1958 Bell[75] derived a more exact equation for q, but Hulett[70] has shown that using it does not change the height of the barrier by more than 1%, nor its width by more than 5%. Other treatments using different barrier shapes have appeared. One of these is the so-called "Echart barrier"[76] which is the more or less accepted one in most text-books on physical Chemistry. However, the mathematical equations describing it are more complicated, and Bell[59] has shown that its shape near the top can be approximated fairly well by an inverted parabola providing the width at the base is taken to be 3a rather than 2a. (This of course holds only for reactions where the heat effect is close to or equal to zero). Thus to a first approximation, Bell's original equations are sufficient and will be the ones that are applied to the following work.

For purposes of calculation of theoretical rate constant equation (95) can be simplified as follows:

Case I: High temperature region

$$\text{if} \quad e^{-\alpha} >> e^{-\beta} \quad \text{or} \quad \beta >> \alpha$$

$$q = \frac{\beta e^{-\alpha}}{\beta - \alpha}$$

$$\text{or} \quad \ln q = \ln \left(\frac{\beta}{\beta - \alpha}\right) - \alpha \qquad \ldots\ldots (96)$$

$$\text{or} \quad \log q = \log \left(\frac{\beta}{\beta - \alpha}\right) - \frac{\alpha}{2.303}$$

Case II: Low temperature or tunnelling region

when $e^{-\alpha} \ll e^{-\beta}$ or $\beta \ll \alpha$

$$q = \frac{\alpha\, e^{-\beta}}{\alpha - \beta}$$

$$\text{or} \quad \ln q = \left(\frac{\alpha}{\alpha - \beta}\right) - \beta \qquad \ldots\ldots (97)$$

$$\text{or} \quad \log q = \left(\frac{\alpha}{\alpha - \beta}\right) - \frac{\beta}{2.303}$$

Case III: Intermediate case

when $e^{-\alpha} = e^{-\beta}$ or $\alpha = \beta$

then $q = (1 + \beta)e^{-\beta}$

$$\text{or} \quad \ln q = \ln (1 + \beta) - \beta \qquad \ldots\ldots (98)$$

$$\text{and} \quad \log q = \log (1 + \beta) - \frac{\beta}{2.303}$$

Now, in general, a second order rate expression is

$$\text{rate} = k\,[H][D_2]$$

where k is the second order rate constant expressed in units of cc-mole^{-1}-sec^{-1} from above discussion

Also, $\text{rate} = N_o q$

Thus $N_o q = k\,[H][D_2]$

or $$k = \frac{N_o q}{[H][D_2]}$$

But, from elementary collision theory

$$N_o = Z_{AB} = \left[\frac{8\pi RT}{\mu}\right]^{1/2} \sigma_{AB}^2\,[A][B]$$

$$= Z_{H\,D_2} = \left[\frac{8\pi RT}{\mu}\right]^{1/2} \sigma_{H,D_2}^2\,[H][D_2]$$

And thus

$$k = \left[\frac{8\pi RT}{\mu}\right]^{1/2} \sigma_{H,D_2}^2\; q$$

$$= \left[\frac{8\pi R}{\mu}\right]^{1/2} \sigma_{H\,D_2}^2\; T^{1/2}\, q$$

$$= \left[\frac{8 \times 3.14 \times 8.31 \times 10^8}{4/5}\right]^{1/2} 2.42 \times 10^{-8} \times 6.02 \times 10^{23}\, T^{1/2}\, q$$

$$\text{or} \quad k = 1.80 \times 10^{13}\, T^{1/2}\, q$$

$$\text{and} \quad \ln k = 2.303 \log (1.80 \times 10^{13}) + \tfrac{1}{2} \ln T + \ln q$$

$$= 2.303 \log (1.80 \times 10^{13}) + \tfrac{1}{2}(2.303 \log 100) + \tfrac{1}{2} \ln T/100 + \ln q$$

$$= 32.84 + \tfrac{1}{2} \ln T/100 + \ln q$$

$$\text{or} \quad \log k = \frac{32.84 + \tfrac{1}{2} \ln T/100 + \ln q}{2.303}$$

where lnq is estimated from equation (96), (97), or (98) as the case may be.

An Olivetti Underwood programma 101 program for the calculation of log k by the above equations is given on the following page, and some theoretical rate constants calculated in the above manner are given in Table XXV.

Note: Collision diameters used: H-atom : 2.10 Å

D_2 molecule: 2.74 Å

SYSTEM _____ APPLICATION Calculation of a theoretical rate constant using Bell's equations. of 1

DATE 10/7/67 PROG. NO. 3

PROG. BY N Wenclek

DECIMAL SETTING 5

NO.	Reg ① INSTRUCTIONS			M	Reg ② A	R	Reg Ⓔ b	B	c	C	d	D	e	E	f	F
1	A	V			b ↕		D÷									
2		S	enter	values (S)	e ↕		↕									
3		C	X		CW		d↓									
4		C	↕		aY		÷									
5		b	↓		b↕		C*									
6		C	÷		b÷		C ↕									
7		b	↕		B↕		b↓									
8		B	X		BV		Ex									
9		A	↓		BY		b↕									
10		↕	X		E*		b↓									
11		E	X		C*		Cx									
12		e	↕		B↓		B+									
13	B	W			d+		B↕									
14		b	↓		d-		B-									
15		e	-		B÷		A↕									
16		/	Y		d↓		/V									
17		A	↕		↕		S	start (S) or		e+						
18		/	Z		B↓		Dx			32.64+						
19		e	↓		Bx		e-			2.303÷	printout log k					
20		d	+		E↕		e↕			depress V						
21		B	↕		B↓		S	enter	T/100							
22	C	V			↕			into	B↑							
23	a	Z			aV			out	depress CY							
24		e	↕		↕											

NOTE: This program breaks down when $\alpha \neq \beta$ but not at exactly $\alpha = \beta$.

To start:

Depress GEN. RESET key with PROG. RECORD ON (in) enter prog.

Values to enter at S:

0.149 into E↑ [$\pi/66.5$ from $\frac{\pi}{4}$]

3.32 into B↑ [$2m \times 10^{2}$]

1.38 into C↑ [$k \times 10^{4}$]

T into ↓ (°K)

E into b↑ ($e_{xp} \times 10^{8}$)

2a into c↑ ($\times 10^{8}$)

1 into d↑

2 into D↑

Typical result:

T = 500

E = 6000

2a = 1.0

gives 11.06491 for $\log_{11} k$.

TABLE XXV

Log k computed from Bell's equations for different values of E_c and 2a:

Temp. (°K)	2a = 0.50	2a = 0.70	2a = 1.0	
a) $E_c = 0.50 \times 10^{-13}$ (5000 entry into program) or 6.5 kcal/mole				
150	10.40	8.87	7.00	
195	10.55	9.13	7.83*	See
273	10.87	10.46*	9.23	Fig.XXXVIII
323	11.19	10.27	10.03	for plot
373	12.30*	10.88	10.63	
443	11.86	11.44	11.27	
500	12.07	11.80	11.67	
b) $E_c = 0.60 \times 10^{-13}$ (6000 entry into program) or 7.8 kcal/mole				
150	9.98	8.26	5.78	
195	10.12	8.48	6.52	See
273	10.38	9.21	8.17	Fig. XXXIX
323	10.61	6.73	9.11	for plot
373	10.99	10.17	9.84	
443	11.50	10.80	10.59	
500	11.60	11.22	11.07	
c) $E_c = 0.70 \times 10^{-13}$ (7000 entry into program) or 9.1 kcal/mole				
150	9.59	7.72	4.97	
195	9.72	7.91	5.44	See
273	9.96	8.41	7.15	Fig. XXXX
323	10.14	9.60*	8.21	for plot
373	10.40	9.47	9.04	
443	11.74*	10.16	9.92	
500	11.17	10.65	10.46	

TABLE XXV (CONT'D)

Temp. (°K)	2a = 0.582
d) $E_c = 0.90 \times 10^{-13}$ (9000 entry into program) or 11.7 kcal/mole	
195	8.15
273	8.39
323	8.59
373	8.88
443	9.93*
500	9.83
700	11.05
1000	12.18

Note: *indicates that the value is erroneous due to the fact that $\alpha \sim \beta$ for this calculation; i.e. the approximation in Bell's equations breaks down. This was evidenced by a longer than usual time required for the computer to make the calculation.

FIGURE XXXVIII

Arrhenius law plots for H + D_2; present results compared with theoretical values generated by Bell's equations for E_c = 6.5 kcal/mole and different values for the width of the parabolic energy barrier, 2a.

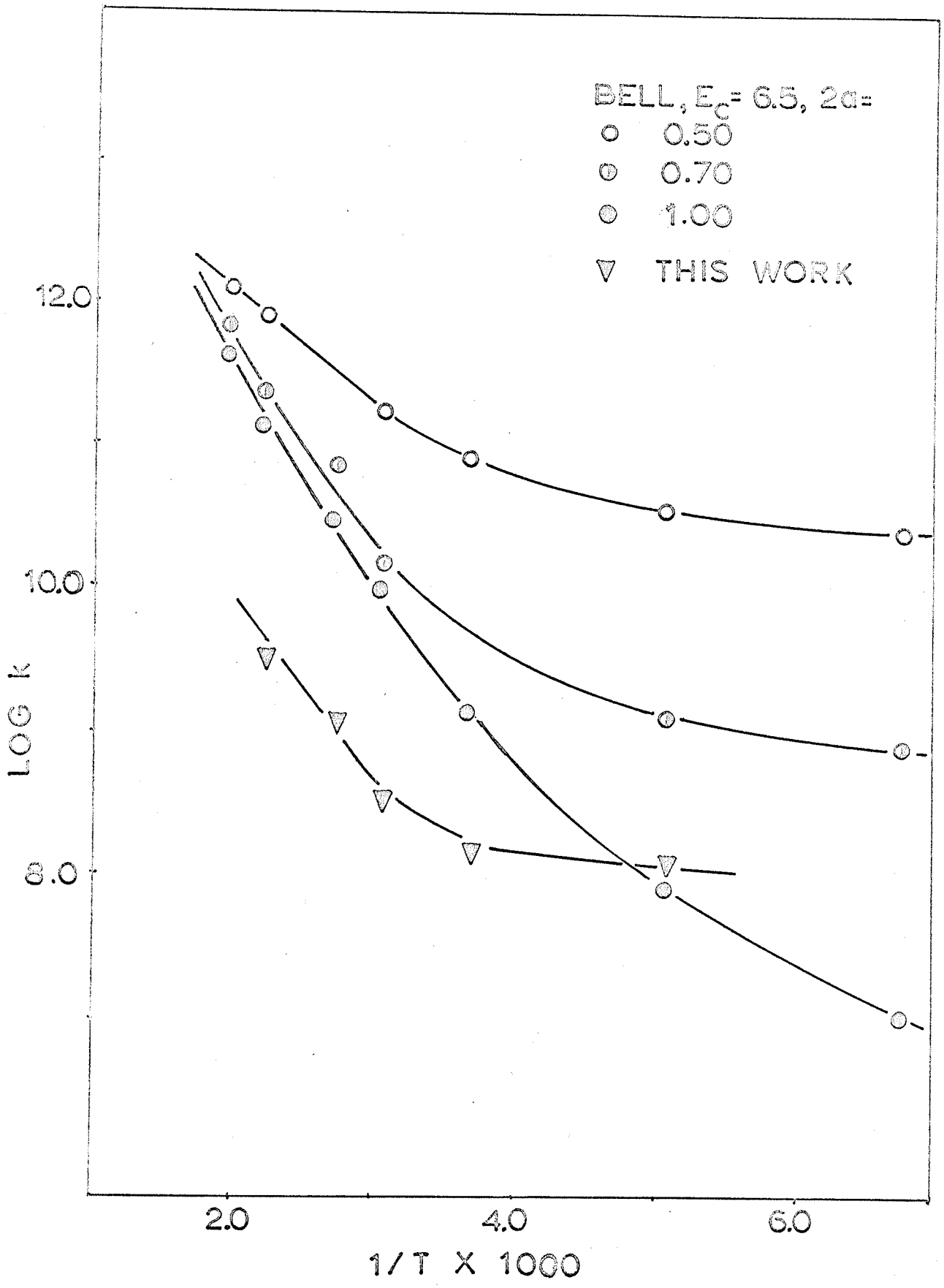
BELL, E_c= 6.5, 2a=
0.50
0.70
1.00
THIS WORK
12.0
10.0
8.0
LOG K
2.0
4.0
6.0
1/T X 1000

FIGURE XXXIX

Arrhenius law plots for H + D_2; present results compared with theoretical values generated by Bell's equations for E_c = 7.8 kcal/mole and different values for the width of the parabolic energy barrier, 2a.

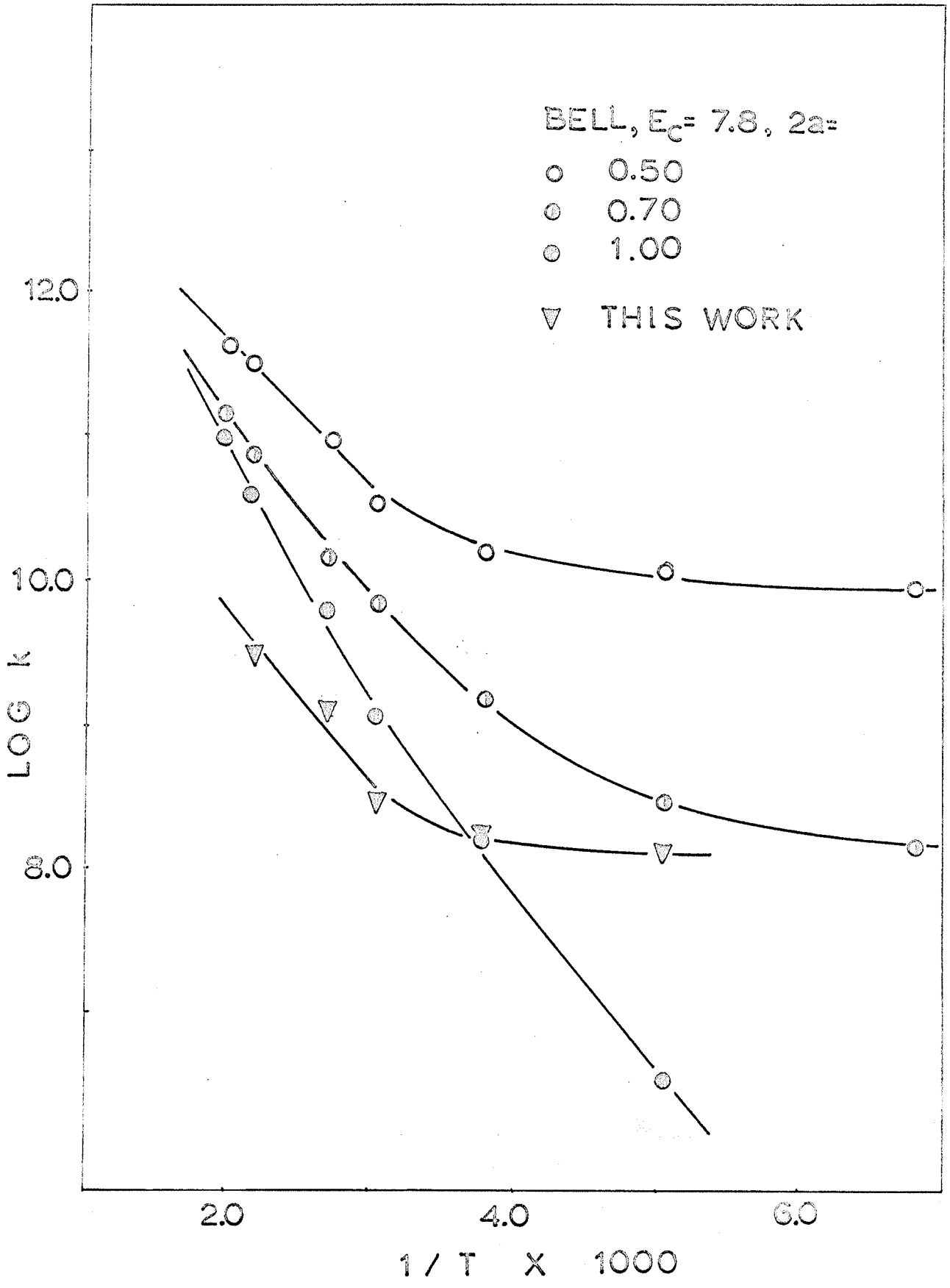
BELL, E_c= 7.8, 2a=
0.50
0.70
1.00
THIS WORK
12.0
10.0
8.0
LOG k
2.0
4.0
6.0
1 / T X 1000

FIGURE XXXX

Arrhenius law plots for H + D_2; present results compared with theoretical values generated by Bell's equations for E_c = 9.1 kcal/mole and different values for the width of the parabolic energy barrier, 2a.

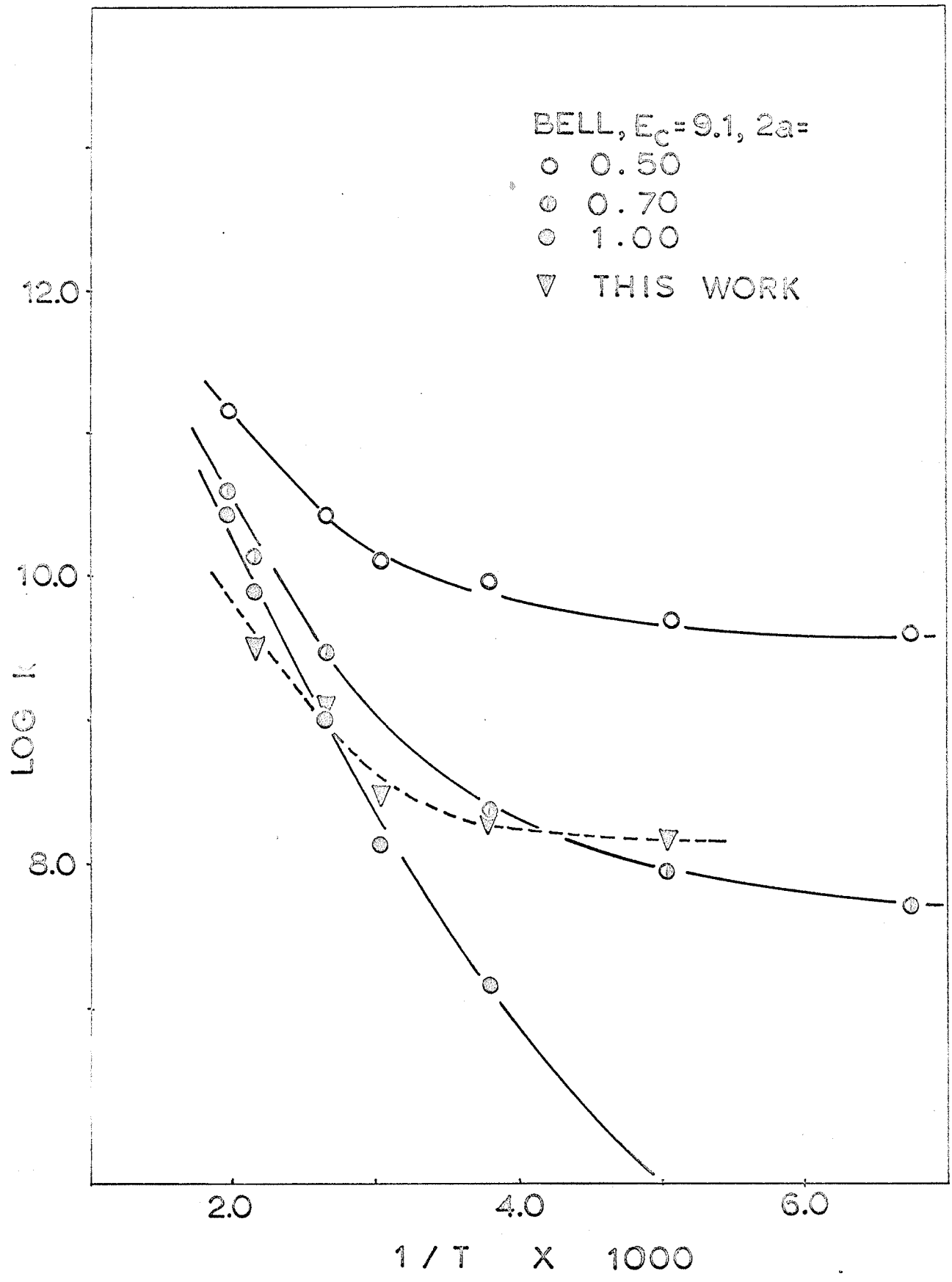
BELL, E_c = 9.1, 2a =
0.50
0.70
1.00
THIS WORK
12.0
10.0
8.0
LOG K
2.0
4.0
6.0
1 / T X 1000

APPENDIX VIII

The thermochemical data as calculated for some of the reactions in this thesis were either obtained directly from the heats of formation of the radicals or molecules involved as listed in Table XXVI or estimated approximately from bond dissociation energies as listed in Table XXVII. All values were taken directly from references 84, 85, 86, and 87.

TABLE XXVI

Pertinent heats of formation of radicals and molecules

Compound or free radical	ΔH_f° (298°K) kcal/mole
H	52.1
C	170.9
CH_2	85
CH_3	32
CH_4	-17.9
C_2H_4	12.50
C_2H_6	20.2
CH_2CO	-14.5
H_2CO	-27.7
HCO	2
CH_3CO	-4.3
CO	-26.4
C_3O_2	-8.3

TABLE XXVII

Pertinent bond dissociation energies

Bond	$\Delta H^{\circ}_{298^{\circ}K}$ kcal/mole
$H_2C=CH_2$	120
C-H	82
CH_3-CH_3	84
$CH_2=CO$	54
CH_3-CO	10
C-C (general)	83
H-H	1042
OC-H (aldehydes)	76

Note: All Δ H values calculated for the reactions are based on atoms, molecules, and radicals in their ground state.

APPENDIX IX

Hot-atom chemistry

The normal way of approaching a kinetic problem during the past fifty years has been to place the reactants into a fixed temperature environment and to determine the rate at which they disappear or the rate at which products form inferred from changes in composition. The results are then summarized by a differential equation relating the rate of disappearance of a reactant or the rate of appearance of a product species to the concentrations of reactants and products. From this expression the rate constant is calculated and by determining this rate constant over a temperature range an activation energy ΔE_o can be calculated from the well-known Arrhenius law:

$$k(T) = A \exp(-\Delta E_o/RT) \qquad (99)$$

where constants A and E_o were obtained from the slopes and intercepts of a log k versus 1/T plot. The constant A is related to the number of collisions in some fashion and the constant ΔE_o measures in some manner the height of the barrier over which the reactants must pass along a poorly defined path or "reaction co-ordinate".

A more recent approach to the problem has arisen as follows. Photolysis, and nuclear transformation experiments[88] have been able to produce atoms, in the gaseous phase (H, D, T, F, Br, I, C) within a reaction cell, having kinetic energies far above those of ordinary or thermal atoms. By varying the wavelength (or moderator in nuclear recoil studies) it has been possible to vary the energy (E) of these hot atoms and thereby obtain a relationship between their energy and the amount of product formed. A curve similar to that shown in Fig. XXXXIa is obtained. Extrapolating this curve back to zero products gives an "energy threshold" or the minimum amount of energy the atoms must have to form products on collision. This value roughly corresponds to the "activation energy" of the older approach. The first estimate of such a threshold experimentally has been for the D + H_2 reaction by Kuppermann and White (1966)[22] who photolyzed DI, and DBr at various wavelengths in the presence of H_2. Extrapolating back to zero product formation they obtained a value of 0.33 $\pm$ 0.02 ev. as the threshold for this reaction.

Using the above approach attempts have now been made at interpreting the rate constant in terms of expressions which are more meaningful when related to the collision process. A

"collision cross section" $\sigma(E)$ has been postulated which may be defined as the probability that two molecules (or rather particles) with relative energy E will react on collision. This can be estimated experimentally from the total number of collisions and the rate of formation of product. The overall rate constant for a reaction is then just an integral overall possible energies of the cross-section for one energy weighted by the Boltzmann factor and the relative energy:

$$K(T) = \int \sigma(E)\, E \exp(-E/RT)\, dE \qquad (100)$$

The most crucial part of the above expression is the determination of how the cross-section $\sigma(E)$ varies with energy (E) of the hot atom. Attempts have been made to calculate this by the thorough study of collision dynamics and reaction trajectories[89]. Using hot atom data it has now been verified that the curve looks like the dashed curve of Fig. XXXXIb[90]. At very low relative energies the molecules do not have sufficient energy to overcome the barrier to their reaction during a collision and behave essentially as elastic balls bouncing off each other. At very high relative energies, the molecules move past each other so rapidly that the

intermolecular forces have little time to cause significant change. Thus, only for intermediate energies will the cross-section be significant. The Boltzmann factor at the temperature of the reaction is a well-defined function and is shown by the dotted curve in Fig. XXXXIb. The product of the two curves or the integrand of the expression for the rate constant is the solid curve and the rate is proportional to the area under this curve. The relatively narrow peak of this curve is associated with the simple energy of activation of the Arrhenius law expression. In faster reactions with lower barriers, a more complex description may be required and no simple formula of the Arrhenius type need be expected. In this way it is hoped that rate constants may be interpreted in terms of the microscopic events taking place within a chemical reaction.

FIGURE XXXXI

Diagrams showing (a) threshold energy for a typical hot-atom reaction

(b) dependence on the relative kinetic energy of the two factors determining the rate constant for a bimolecular hot-atom reaction.

a.

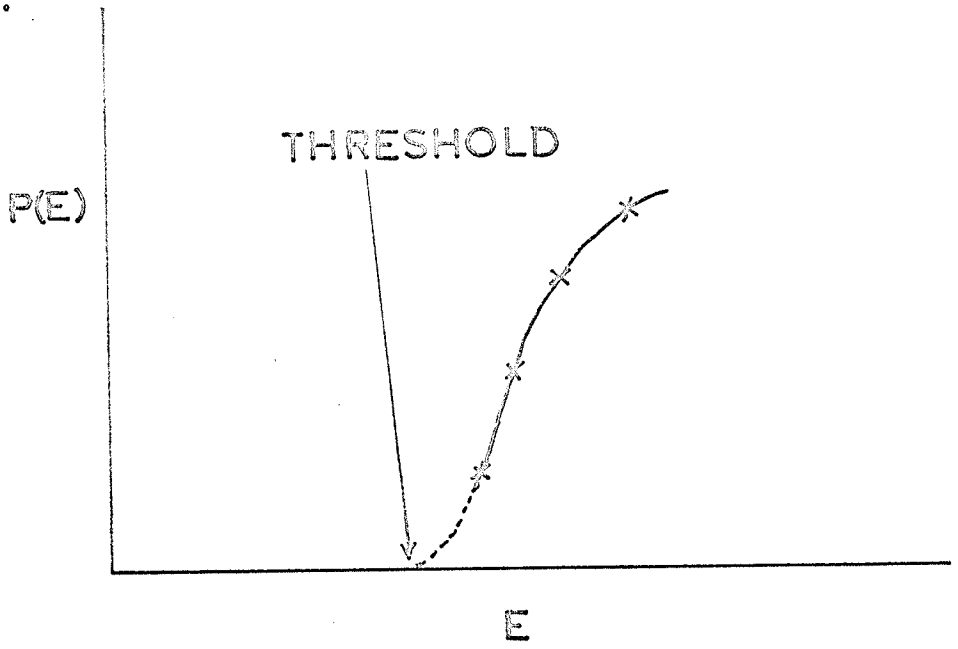

b.